

PDF hosted at the Radboud Repository of the Radboud University Nijmegen

The following full text is a publisher's version.

For additional information about this publication click this link.

<http://hdl.handle.net/2066/27024>

Please be advised that this information was generated on 2017-12-05 and may be subject to change.

Protein Tyrosine Phosphatase PTPRR isoforms
in cellular signaling and trafficking

ISBN – 10: 90919889X

ISBN – 13: 9789090198897

The research presented in this thesis was performed at the Department of Cell Biology, Nijmegen Center for Molecular Life Sciences, Radboud University Nijmegen Medical Centre, and was financed by the Radboud University Nijmegen Medical Centre (grant number V.089942). This research was also partly supported by grants from the European Research Community Fund (HPRN-CT-2000-00085), the Dutch Cancer Society (KUN 93-538), and the Dutch Organization for Scientific Research (NWO 901-01-191).

Protein Tyrosine Phosphatase PTPRR isoforms in cellular signaling and trafficking

Een wetenschappelijke proeve op het gebied van de Medische Wetenschappen

Proefschrift

ter verkrijging van de graad van doctor aan de Radboud Universiteit Nijmegen,
op gezag van de Rector Magnificus Prof. Dr. C.W.P.M. Blom,
volgens besluit van het College van Decanen
in het openbaar te verdedigen op donderdag 24 november 2005
des namiddags om 1.30 uur precies

door

Gönül Dilaver
geboren op 7 april 1973
te Doetinchem

Promotor:

Prof. Dr. B. Wieringa

Copromotores:

Dr. J. A. M. Fransen

Dr. W. J. A. J. Hendriks

Manuscriptcommissie:

Prof. Dr. R. J. M. Bindels (voorzitter)

Prof. Dr. G. J. M. Martens

Dr. P. van der Sluijs, Universiteit Utrecht

Annemin ve Babamin Sevgisiyle

Table of Contents

| | | |
|------------------|---|-----|
| Chapter 1 | General introduction | 9 |
| Chapter 2 | Colocalization of the protein tyrosine phosphatases PTP-SL and PTPBR7 with β 4-adaptin in neuronal cells | 25 |
| Chapter 3 | Characterization of multiple transcripts and isoforms derived from the mouse protein tyrosine phosphatase gene <i>Ptprr</i> | 53 |
| Chapter 4 | Proteolytic shedding of the brain-specific receptor-type protein tyrosine phosphatase PTPBR7 | 83 |
| Chapter 5 | Differential localization of the protein tyrosine phosphatases PTPBR7 and PTP-SL in early endocytic compartments | 117 |
| Chapter 6 | General discussion | 141 |
| | Abbreviations | 155 |
| | Summary in Dutch | 159 |
| | Acknowledgements | 163 |
| | Curriculum Vitae | 165 |
| | Publications | 167 |
| | Color Illustrations | 169 |

Chapter 1

General Introduction

Introduction

Eucaryotic cells contain a diverse range of membrane-bound compartments, organelles, each with distinct composition and cellular function. To maintain this compartmental organization, the cell selectively transports cargo molecules through an elaborate network of vesicle trafficking pathways to the appropriate target organelle. Extracellular communication, steering this network, is mediated by hormones, neurotransmitters, and growth factors, through signal transduction events involving receptors. The study of signal transduction pathways and membrane trafficking were once considered unrelated disciplines in cell biology. It is becoming evident, however, that membrane trafficking and signal transduction events are intimately intertwined (1,2). The temporal and spatial delivery of signals and their receptors to different intracellular compartments has been shown to be critical in many cellular processes. Furthermore, proteins involved in signaling pathways can also interact with and regulate components of the membrane trafficking machinery itself (3). Therefore intracellular transport is nowadays considered to be a choreographed program of secretory, biosynthetic and endocytic protein traffic that serves the cell's internal physiological needs, propagates its internal organization and allows communication with the environment.

It is intriguing how this complicated network of communication, in which signaling and trafficking molecules have to cooperate, is regulated. One of the fundamental processes governing signal transduction events is reversible phosphorylation. The level of protein phosphorylation is tightly regulated by the concerted action of kinases and phosphatases. Some of these kinases and phosphatases are found specifically at organelles and are now implicated in localized signaling and membrane trafficking events. To shed light on this complex system of cellular regulation, it is important to identify and understand the behaviour of all players involved.

Prior to the start of this PhD thesis study a signaling molecule, protein tyrosine phosphatase PTP-SL, was identified by members of our group. PTP-SL resides on vesicular structures that partly belong to the endosomal compartments (4). Subsequently, it was revealed that PTP-SL is a member of the PTPRR protein tyrosine phosphatase subfamily that is implicated in various MAPK (mitogen-activated protein kinase) signaling pathways (5-7). In addition, PTP-SL was found to interact in the yeast two-hybrid system with the β 4-adaptin of the AP-4 complex, an important component of the vesicular transport machinery. These

findings are suggestive of a role for PTP-SL in localized signaling and/or trafficking. In this thesis research the PTPRR phosphatase subfamily was investigated in great detail, with special emphasis on their (sub)cellular localization and isoform diversity. Before presenting the outline and scope of this work I will first provide some general information relevant for the studies described in the following chapters.

Vesicle transport

In vesicle transport three essential steps can be discerned: vesicle formation, vesicle transport, and vesicle fusion. These carefully orchestrated processes require the complex interplay of many components (8). There are three known coat complexes; clathrin, coatamer protein I (COPI) and COPII (9). Clathrin functions at the plasma membrane and in transport between late endosomes and the Golgi-apparatus (Fig. 1) by introducing a membrane curvature. Intracellular transport between the endoplasmic reticulum and Golgi-apparatus compartments is mediated by the coat protein complexes COPI and COPII that form transport vesicles and collect the specified set of cargo (10).

Adaptor proteins bind the cytoplasmic domains of transmembrane proteins and recruit coat proteins to membranes. By providing a link between cargo concentration and vesicle formation, they have a crucial role in the sorting of membrane proteins (11-13). One specific class of adaptors is that of the adaptor protein (AP) heterotetrameric complexes (14). AP complexes interact with short peptide sequences found in the cytosolic tails of cargo transmembrane proteins, referred to as “sorting signals”. These motifs determine which vesicular traffic pathway is used to transport a particular molecule and hence determine its final destination (12,15). AP-1 is involved in trafficking between the *trans*-Golgi network (TGN) and endosomes, AP-2 functions with clathrin at the plasma membrane, and AP-3 is involved in the formation of specialized lysosome-related compartments (for example melanosomes). The AP-4 complex is localized to the Golgi-apparatus and late endocytic vesicles (16). The precise role of AP-4 is unknown at present, but data suggest that it mediates sorting processes at the TGN and/or endosomal membranes (17,18). In addition to the AP family, the GGA (Golgi-localized, γ -ear containing, ARF-binding protein) family also functions in membrane-protein trafficking by linking cargo proteins to transport vesicles (19).

The pinching off of the clathrin-coated membrane requires further the action of several accessory proteins (20). These include, but are not limited to, epsins, endophilins (proteins that are thought to induce the bending of the membrane that is required for vesicle budding), dynamin (a protein required for the fission of a vesicle from a donor membrane), and amphiphysin (which binds endophilin).

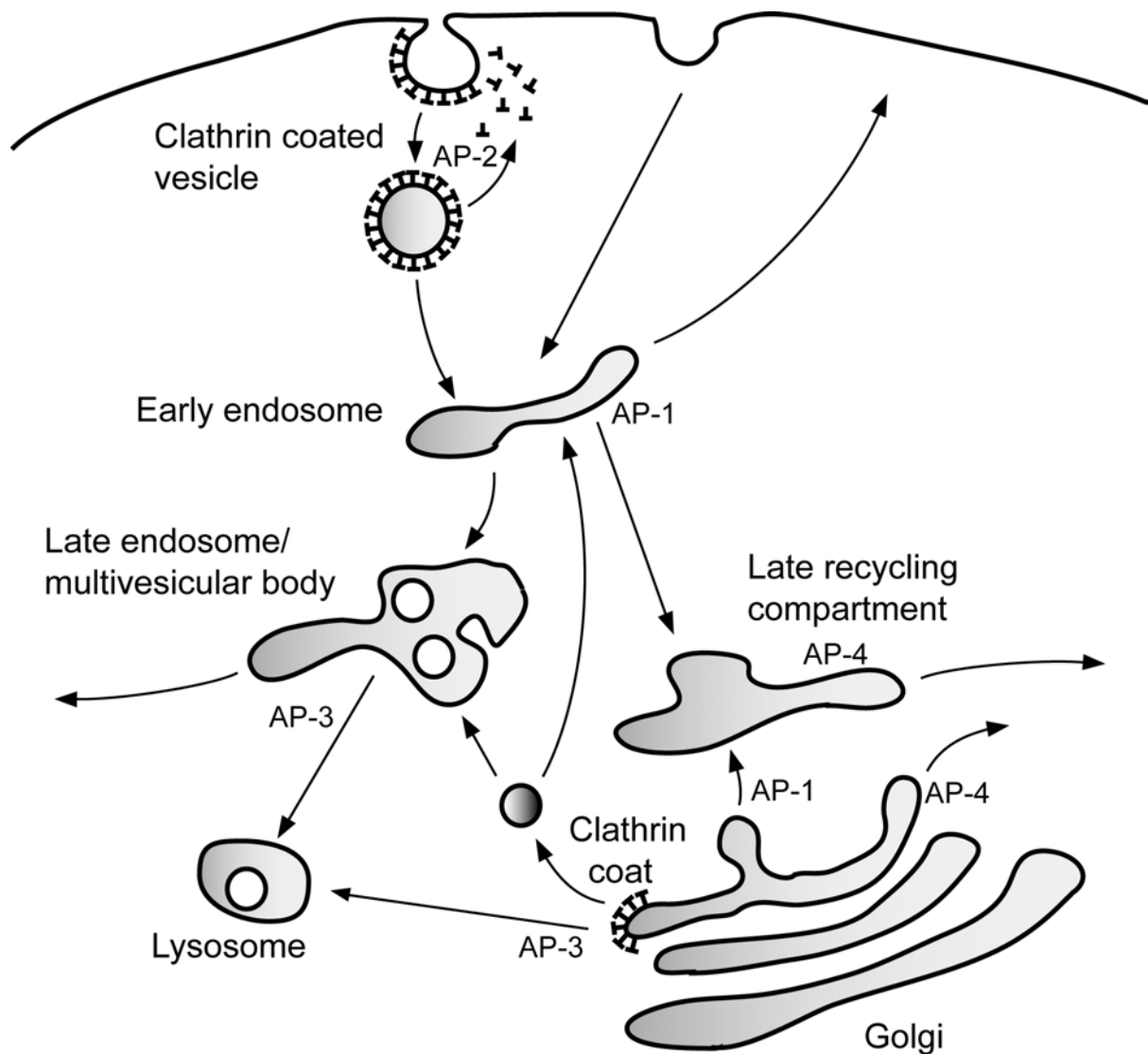


Figure 1. The major membrane traffic pathways in endocytosis.

The different adaptor complexes (AP-1 till 4) involved in specific transport routes are depicted.

Adapted from ref. 2.

Vesicles then have to be sorted and transported to various intracellular destinations for which the small GTPases of the Rab family are essential (21). For almost every vesicular transport step specific (or combinations of) Rab proteins are required and they function through the recruitment of specific effector proteins to the membrane on which they are localized (22).

Membrane fusion, the final step in vesicular trafficking events, is in part also mediated by Rab proteins and furthermore requires proteins such as SNAREs. SNARE proteins function in cognate pairs, with one set of the pair being localized to the vesicle and the other to the target membrane (23). Membrane fusion of vesicles is crucial for the transfer of proteins and lipids between different compartments, and for exo- and endocytotic traffic of signaling molecules and receptors (24).

Endocytosis and Signaling

Endocytosis is defined as the uptake of material into a cell by an invagination of the plasma membrane, ultimately resulting in its internalization in a membrane-bound vesicle. An outline of the endocytic pathway is depicted in Figure 1. In mammalian cells, cargo can be endocytosed in three ways: via clathrin-coated pits, through a clathrin independent pathway and by means of caveolae (25). Clathrin-dependent endocytosis involves the formation of vesicles using a clathrin coat; clathrin triskelions assemble at the membrane and form a polyhedral lattice. Internalization via the clathrin-independent pathway is poorly understood, but evidence for its existence is gradually accumulating (26). Endocytosis via caveolae involves the formation of small, flask-shaped membrane invaginations enriched in cholesterol, sphingolipids, and caveolin proteins (25).

After internalization, endocytosed material is delivered to early endosomes, where efficient sorting occurs. From early endosomes cargo is either recycled back to the plasma membrane, sorted to the late recycling compartment or delivered to the late endosomes. This can occur either by means of carrier vesicles or through a “maturation” process, a change in biochemical composition and morphology (27). Likewise, late endosomes either mature into lysosomes or transfer cargo to lysosomes through vesicular intermediates. It is difficult to distinguish between early and late endosomes and the boundary between late endosomes and

lysosomes is even more elusive, but based on their lipid composition, six different stages have been distinguished in the journey from the cell surface to lysosomes (28,29). Transport routes also connect the biosynthetic and endocytic pathways, and can send or receive cargo from the TGN (Fig. 1).

Traditionally, endocytosis of cell surface receptors has been considered as a mechanism to down-regulate signal transduction by desensitising the cell's response to signaling molecules. However, endocytosis may also increase signaling by associating the internalized receptors with their signaling targets on the endosomes and only later on decrease signaling by sorting receptors to the lysosomes for degradation. Indeed it has become evident that endocytosis can regulate signaling through multiple mechanisms, and nowadays the process is viewed as a powerful means to regulate the distribution of signaling molecules over distinct organelles thereby creating compartmentalization of signaling events (30).

Subcellular compartmentalization in signaling is well documented for the MAPK cascades, that relay extracellular stimuli from the plasma membrane to crucial cellular targets distant from the membrane (1-3,31,32). For example, in epidermal growth factor receptor (EGFR) signaling, on and off switches are spatially separated. Following specific stimuli, EGFR is endocytosed from the cell surface and the resulting endosomes migrate close to the endoplasmic reticulum (ER), where the protein tyrosine phosphatase 1B resides, subsequent dephosphorylation of EGFR takes place (33). Another example of compartmentalized regulation is provided by the human Sef (acronym for similar expression to *fgf* genes) protein (34). Sef resides on the Golgi-apparatus and specifically binds extracellular regulated kinase (ERK), thereby blocking ERK nuclear translocation without inhibiting its activity in the cytoplasm. Hence, this protein acts as a spatial regulator for ERK signaling (34).

Recent data even indicate the importance of so-called 'signaling endosomes' for the initiation of downstream signaling events (35). Nerve growth factor (NGF) signaling, for example, occurs over long distances from the cell periphery to the cell body and involves the retrograde transport of endocytic vesicles containing activated receptors (trkA and p75). These signaling endosomes actually facilitate the trkA and p75 signaling events that are temporally and spatially distinct (36,37). Likewise, the activated and phosphorylated EGFR associates with its downstream targets, such as Shc, Grb2, PI3K and Ras signaling molecules, on the endosome (30,38,39), which then are expected to further relay the signaling cascade.

Regulation of membrane trafficking by phosphorylation

From the preceding section it is clear that vesicle trafficking is a crucial regulator of cell signaling but the opposite mechanism, i.e. that signaling events determine vesicular transport, is equally true. Protein phosphorylation, being a signal-induced rapid and reversible post-translational modification, is apparently an ideal mechanism for controlling trafficking events since the activity of many proteins that are implicated in endocytosis, including dynamin 1, amphiphysins, synaptojanin 1, epsin, Eps15 and AP-180, is regulated in this way (40-43). These proteins are e.g. found in the phosphorylated state in resting nerve terminals, and are dephosphorylated when a depolarization stimulation evokes a burst of clathrin coated vesicle formation (42). It was further shown that phosphorylation of dynamin 1 and synaptojanin 1 inhibits their binding to amphiphysin, while phosphorylated amphiphysin has an impaired affinity for the earlier discussed adaptor protein AP-2 and for clathrin (44). *In vivo* serine and threonine phosphorylation of the different subunits of AP-2 complex has also been reported (43). Phosphorylation of the μ 2 subunit of AP-2 significantly increases the affinity of AP-2 for cargo internalization signals *in vitro* (45) and *in vivo* (46,47), whereas phosphorylation of the α and β 2 subunit of the AP-2 complex is inhibitory for clathrin coated vesicle formation.

There is also increasing data pointing to the importance of tyrosine-specific phosphorylation in the regulation of intracellular traffic. Upon ligand-induced EGFR endocytosis, for example, the β 2 subunit of the clathrin adaptor complex AP-2 becomes phosphorylated on tyrosine and this appears to be important in the regulation of EGFR turnover (48). Moreover, EGFR endocytosis itself requires tyrosine phosphorylation of Eps15, an endocytic protein, by EGFR (49). Much of the work on the regulation of vesicular transport by phosphorylation has been focused on protein tyrosine kinase signaling, but recent findings now underscore the importance of protein tyrosine phosphatases in these processes as well. For example, PTP-MEG2 is localized to the membrane of secretory vesicles and it can dephosphorylate and thereby activate the N-ethylmaleimide-sensitive factor (NSF), a key regulator of secretory vesicle fusion (50). And inhibition of the tyrosine phosphatase activity of PTP-1B, which is located at secretory vesicles of glucagon-producing cells, was found to be associated with a strong stimulation of glucagon secretion (51). It is therefore to be expected that protein tyrosine phosphatases, being the counteractors of the protein tyrosine kinases, will play an equally important role in vesicle traffic.

Protein tyrosine phosphatases

The protein tyrosine phosphatase (PTP) superfamily is a large group of enzymes showing extensive diversity in structure and biological function (52-55). Tyrosine phosphatases are classified into three groups: receptor-type (I), non-transmembrane (II) and dual-specificity phosphatases (III) (56). A schematic representation of different types of family members is shown in Figure 2. The first group has a transmembrane domain, a receptor-like extracellular region and one but mostly two catalytic PTP domains. The second group is cytoplasmic in location, and can in turn be subdivided in membrane-associated and true cytosolic PTPs. In contrast to these tyrosine-specific PTPs, the third group consists of promiscuous enzymes that can dephosphorylate phosphoserine, phosphothreonine as well as phosphotyrosine residues. The non-transmembrane PTPs and dual-specificity phosphatases contain one single catalytic PTP domain. The approximately 250 residues long PTP domain is highly conserved, and contains an essential cysteine residue within its active site that is used in a cyteinyI-phosphate enzyme intermediate during dephosphorylation.

The regulation of PTPs is not completely understood, but includes alternative mRNA splicing, modulation of steady state levels, posttranslational modification, dimerization and/or subcellular confinement (52). These mechanisms contribute to the diversity of “the phosphatome” and add to the complexity of cellular signaling programs. Often, the non-catalytic regions of PTPs contain domains that target the enzymes to their appropriate subcellular locations and interacting proteins, including substrates. These non-catalytic regions may even participate in the regulation of phosphatase activity by intra-molecular folding mechanisms. As with other signaling molecules, complex formation and regulation of enzymatic activity are highly dynamic and tightly regulated in space and time. In addition, many PTPs can be phosphorylated on serine, threonine or tyrosine residues, which adds a further layer of complexity regarding their regulation.

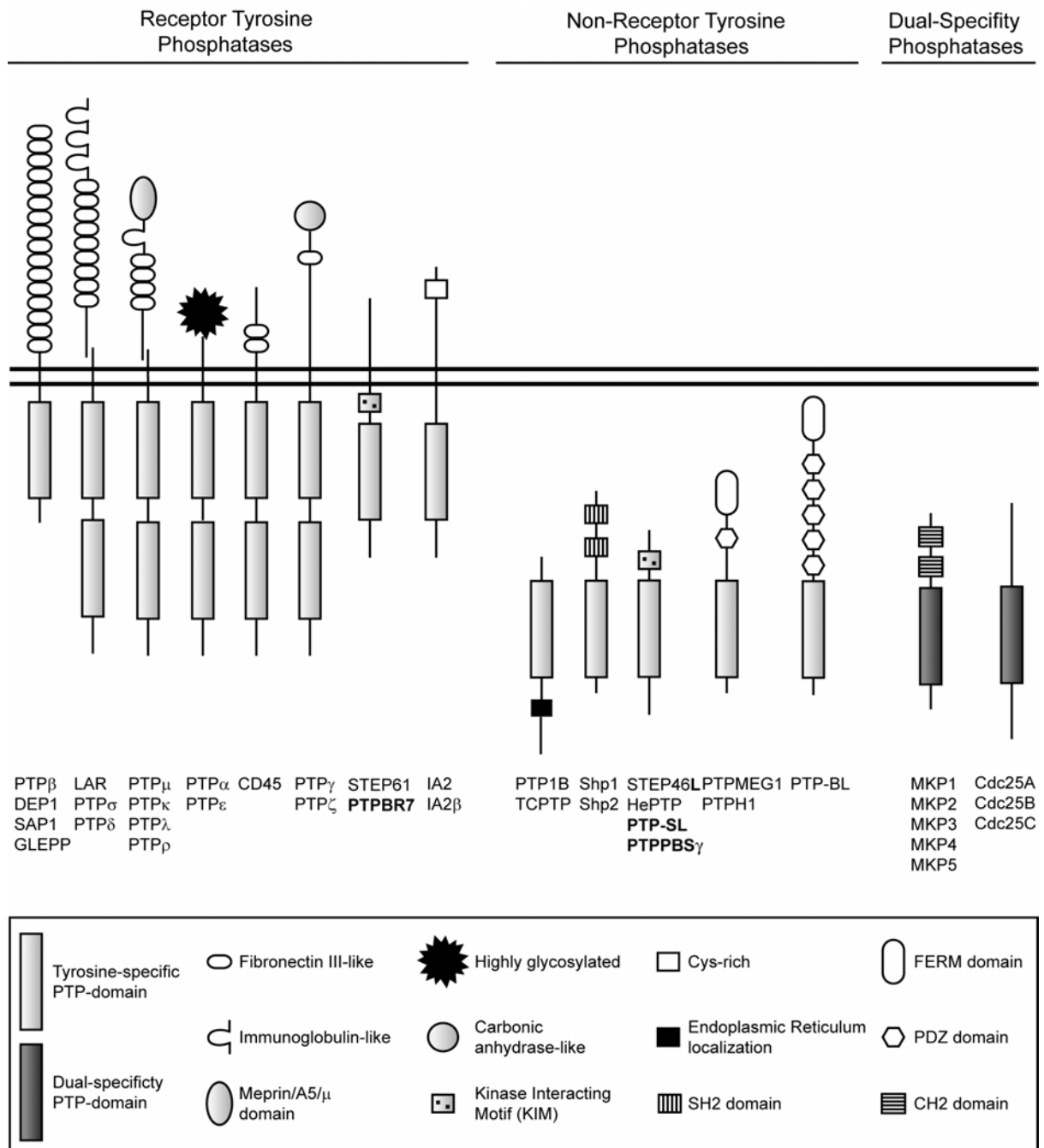


Figure 2. Schematic representation of the different types of family members of receptor PTPs, non-receptor PTPs and dual specificity PTPs. Structural characteristics of PTP regulatory domains are shown in the boxed inset. Adapted from refs. 52 and 54.

PTPRR protein tyrosine phosphatase isoforms

A decade ago our group cloned the mouse protein tyrosine phosphatase PTP-SL, a product of the *Ptprr* gene (4,57). During the studies described in this thesis it was established that the mouse gene *Ptprr* not only codes for PTP-SL but actually gives rise to multiple neuronal protein tyrosine phosphatases through the use of distinct promoters and differential translation starts (57-61). The resulting PTPRR protein family consists of the isoforms PTPBR7, PTP-SL, PTPPBS γ -42 and PTPPBS γ -37 that differ in their N-terminal part (Fig. 2) and have molecular weights of 72, 60, 42 and 37 kDa, respectively (described in Chapter 3 of this thesis).

PTPBR7 and PTP-SL are expressed through developmentally regulated use of alternative promoters (4). PTPBR7 is expressed during early embryogenesis in spinal ganglia as well as in the developing Purkinje cells. Postnatally, PTPBR7 is expressed in various regions of the adult mouse brain, but expression in Purkinje cells then ceases and is replaced by the PTP-SL transcript (4). PTPPBS γ mRNAs are found in the hippocampal region, cerebellar granular layer and in the gastrointestinal tract (59). In rat, a comparable situation exists: a short messenger, encoding PCPTP1-Ce, is exclusively found in adult cerebellar Purkinje cells whereas the longer form, PCPTP1, is more generally expressed albeit at lower levels (62,63). The human PTPRR family includes PTPPBS α , PTPPBS β and PTPPBS γ , which are the orthologues of mouse PTPBR7, PTP-SL and PTPPBS γ , respectively (58,59). However, the human family is even larger and in addition includes PTPPBS δ .

The mammalian MAP kinase cascades in signal transduction pathways are initiated by a wide variety of extracellular stimuli as illustrated in Figure 3A. All PTPRR isoforms have an identical C-terminal part that contains the catalytic PTP domain and a so-called kinase interaction motif (KIM) that enables binding to the MAP kinases ERK1, ERK2, ERK5 and p38 (5-7). Binding of these MAP kinases to PTP-SL results in the inactivation of the MAPK through dephosphorylation and the blocking of nuclear translocation (6) (Fig. 3B). But before it can do so, PTP-SL first serves as a substrate for the MAPK, resulting in its phosphorylation on Thr²³⁹. Following proper stimuli, PTP-SL itself can become phosphorylated on Ser²¹⁷ within its KIM motif by the cyclic-AMP-dependent protein kinase, PKA, which results in the dissociation of PTP-SL and MAPK and translocation to the

nucleus of the latter (64). A region termed kinase-specificity sequence (KIS), that is responsible for the differential recognition of ERK and p38 as substrates, has been identified adjacent to the KIM sequence in PTP-SL (65).

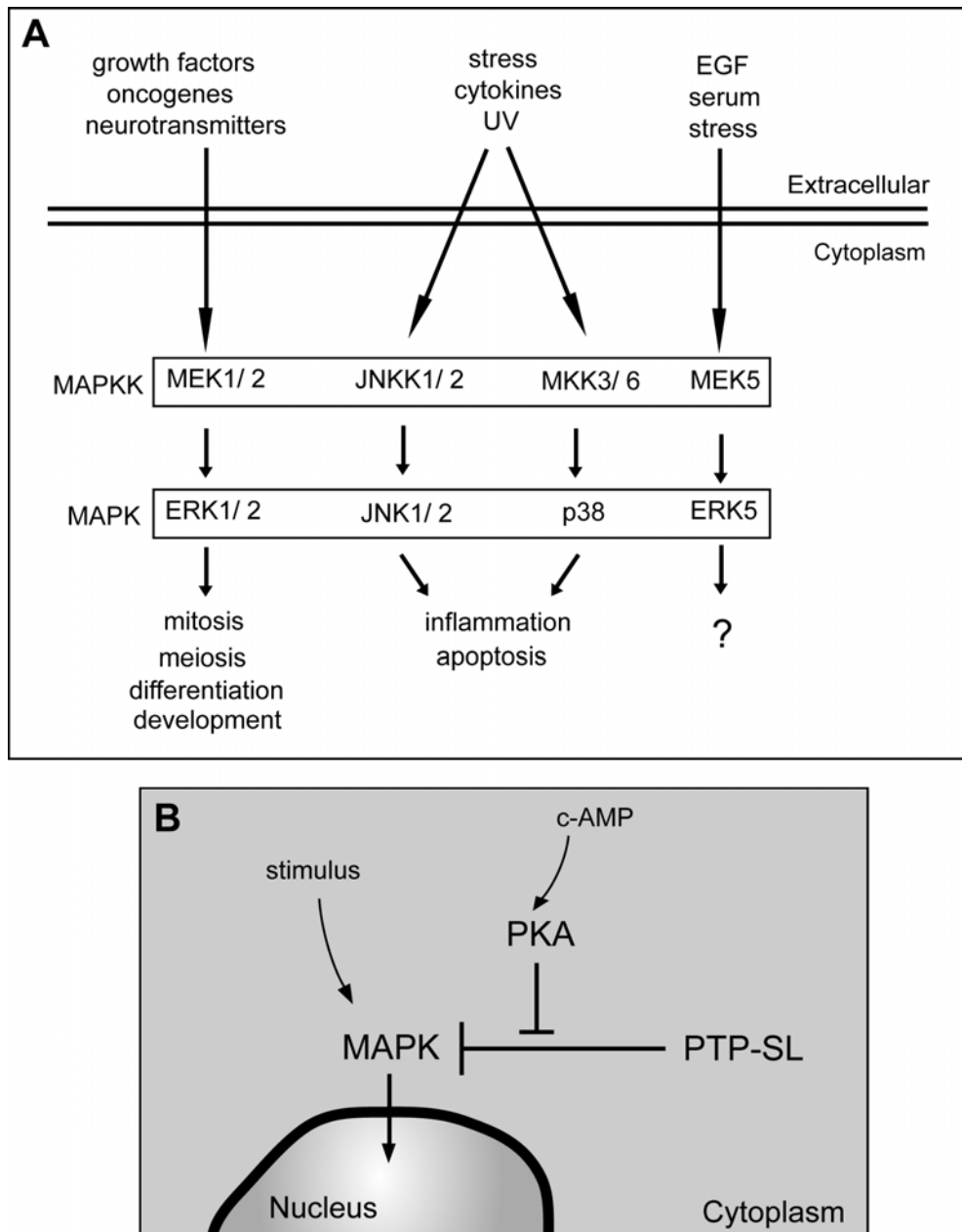


Figure 3. A, Schematic representation of mammalian MAP kinase signal transduction pathways. B, Model of MAP kinase regulation by PKA and PTP-SL. Adapted from ref.7.

The PTPRR subfamily has the closest homology with the STEP (striatum enriched phosphatase) and HePTP/LC-PTP (haematopoietic and leukocyte PTPs) phosphatases (66-68). The STEP family comprises cytosolic and membrane bound PTP isoforms that are preferentially expressed in striatum, hippocampus cortex and other related brain structures in primates and rodents (66,69). The human HePTP/LC-PTP is a cytosolic protein and mainly expressed in lymphoid tissues. Also these two related PTP families contain a conserved KIM sequence just N-terminal of their catalytic domains and serve as substrates for MAPKs (5,7,70,71).

The catalytic PTP domain of the PTPRR isoforms has been crystallized and the structure indicates a monomeric PTP domain with an unhindered catalytic site (72). In addition to the characteristic PTP-core structure, there is an extending N-terminal helix that may possibly orient the KIM motif upon interaction with target MAPKs. Within the PTP-core, structure the so-called mobile WPD loop was found to adopt an open conformation in the absence of the substrate. Upon binding of substrate, the WPD loop undergoes an extensive conformational change to adopt the closed state, but it appeared much less flexible as for example in PTP-1B. Based on the crystal structure, a docking model for the interaction with ERK2 was suggested, in which the phosphorylation of the phosphatase should be accomplished first. The subsequent dephosphorylation of ERK2 will only be possible after a conformational rearrangement of the two interacting partners has taken place (72).

Interestingly, the different PTPRR isoforms display distinct subcellular localization patterns: PTPBR7 is a true type I plasma membrane protein, and additionally localizes to the Golgi apparatus and vesicles, PTP-SL appears membrane-associated at the Golgi complex and at vesicles that are in part from endocytic origin (4,73), whereas the PTPBS γ isoforms are true cytosolic proteins (61).

Outline of this thesis

The presence of PTP-SL on endosomal structures is intriguing and prompted for further research. To gain more insight into the possible role of this protein tyrosine phosphatase and its subfamily members in localized signaling and/or trafficking, we studied both the localization and the biochemistry of PTPRR isoforms. First, the molecular environment of PTPBR7 and PTP-SL was explored and a marked overlap in localization of these PTPs and β 4-adaptin was found (**Chapter 2**). Previous work had predicted that multiple isoforms could originate from the PTP-SL-encoding gene *Ptprr* in mouse (4,58,59). We therefore performed a careful annotation of transcript and protein products derived from the mouse gene *Ptprr*, and investigated protein expression both *in situ* and at the subcellular level (**Chapter 3**). These experiments revealed that *Ptprr* encodes four isoforms through the use of distinct promoters, alternative splicing and differential translation starts. Furthermore, these studies as well as literature data (5,6,64,74) pointed to the occurrence of posttranslational modifications. In **Chapter 4**, we have analyzed the posttranslational modifications imposed upon the PTPRR protein isoforms in great detail. We could show that the PTPBR7 isoform is proteolytically cleaved at a furin-like convertase consensus site within its N-terminal extracellular segment. Since PTPBR7 and PTP-SL display a great deal of overlap in their localization patterns in neuronal cells, we analyzed the subcellular (co-)occurrence of these isoforms using confocal laser scanning and electron microscopy (**Chapter 5**). PTPBR7 and PTP-SL were found to co-localize on late endocytic compartments, but PTPBR7 shows an additional localization at early endosomes. The implications of the above findings, as described in the various Chapters, are then discussed in **Chapter 6**.

References

1. Kholodenko, B. N. (2002) *Trends Cell Biol.* **12**, 173-177
2. Sorkin, A., and von Zastrow, M. (2002) *Nat. Rev. Mol. Cell. Biol.* **3**, 600-614
3. Gonzalez-Gaitan. (2003) *Nat. Rev. Mol. Cell. Biol.* **4**, 213-224
4. van den Maagdenberg, A. M. J. M., Bachner, D., Schepens, J. T. G., Peters, W., Franssen, J. A. M., Wieringa, B., and Hendriks, W. J. A. J. (1999) *Eur. J. Neurosci.* **11**, 3832-3844
5. Pulido, R., Zuñiga, A., and Ullrich, A. (1998) *EMBO J.* **17**, 7337-7350
6. Zuñiga, A., Torres, J., Ubeda, J., and Pulido, R. (1999) *J. Biol. Chem.* **274**, 21900-21907
7. Buschbeck, M., Eickhoff, J., Sommer, M. N., and Ullrich, A. (2002) *J. Biol. Chem.* **277**, 29503-29509
8. Evans, P. R., and Owen, D. J. (2002) *Curr. Opin. Struct. Biol.* **12**, 814-821
9. Kirchhausen, T. (2000) *Nat. Rev. Mol. Cell Biol.* **1**, 187-198
10. Barlowe, C. (2000) *Traffic* **1**, 371-377
11. Kirchhausen, T., Bonifacino, J. S., and Riezman, H. (1997) *Curr. Opin. Cell Biol.* **9**, 488-495
12. Kirchhausen, T. (2002) *Cell* **109**, 413-416
13. Boehms, M., and Bonifacino, J. S. (2002) *Gene* **286**, 175-186
14. Hirst, J., and Robinson, M. (1998) *Biochim. Biophys. Acta* **1404**, 173-193
15. Sorkin, A. (2004) *Curr. Opin. Cell Biol.* **16**, 392-399
16. Barois, N., and Bakke, O. (2005) *Biochem. J.* **385**, 503-510
17. Dell'Angelica, E. C., Mullins, C., and Bonifacino, J. S. (1999) *J. Biol. Chem.* **274**, 7278-7285
18. Hirst, J., Bright, N. A., Rous, B., and Robinson, M. S. (1999) *Mol. Biol. Cell* **10**, 2787-2802
19. Bonifacino, J. S. (2004) *Nat. Rev. Mol. Cell Biol.* **5**, 23-32
20. Slepnev, V. I., and De Camilli, P. (2000) *Nat. Rev. Neurosci.* **1**, 161-172
21. Zerial, M., and McBride, H. (2001) *Nat. Rev. Mol. Cell Biol.* **2**, 107-117
22. de Renzis, S., Sonnichsen, B., and Zerial, M. (2002) *Nat. Cell Biol.* **4**, 124-133
23. Chen, Y. A., and Scheller, R. H. (2001) *Nat. Rev. Mol. Cell Biol.* **2**, 98-106
24. Mayer, A. (2002) *Annu. Rev. Cell Dev. Biol.* **18**, 289-314
25. Maxfield, F. R., and McGraw, T. E. (2004) *Nat. Rev. Mol. Cell Biol.* **5**, 121-132
26. Cavalli, V., Corti, M., and Gruenberg, J. (2001) *FEBS lett.* **498**, 190-196
27. Dunn, K. W., McGraw, T. E., and Maxfield, F. R. (1989) *J. Cell Biol.* **109**, 3303-3314
28. Gruenberg, J. (2001) *Mol. Cell Biol.* **2**, 721-730
29. Möbius, W., van Donselaar, E., Ohno-Iwashita, Y., Shimada, Y., Heijnen, H. F. G., Slot, J. W., and Geuze, H. J. (2003) *Traffic* **4**, 222-231
30. Seto, E. S., Bellen, H. J., and Lloyd, T. E. (2002) *Genes Dev.* **16**, 1314-1336
31. Philips, M. R. (2004) *Mol. Cell* **23**, 168-169
32. Gonzales-Gaitan. (2003) *Nat. Reviews* **4**, 213-224
33. Haj, F. G., Verveer, P. J., Squire, A., Neel, B. G., and Bastiaens, P. I. H. (2002) *Science* **295**, 1708-1711

34. Torii, S., Kusakabe, M., Yamamoto, T., Maekawa, M., and Nishida, E. (2004) *Dev. Cell* **7**, 33-44
35. Paolo Di Fiore, P., and De Camilli, P. (2001) *Cell* **106**, 1-4
36. Kuruvilla, R., Ye, H., and Ginty, D. D. (2000) *Neuron* **27**, 499-512
37. Bronfman, F. C., Tcherpakov, M., Jovin, T. M., and Fainzilber, M. (2003) *J. Neurosci.* **23**, 3209-3220
38. DiGuglielmo, G. M., Baass, P. C., Ou, W. J., Posner, B. I., and Bergeron, J. J. (1994) *EMBO J.* **13**, 4269-4277
39. Oskvold, M. P., Skarpen, E., Lineman, B., Roos, N., and Huitfeldt, H. S. (2000) *J. Histochem. Cytochem.* **48**, 21-33
40. Robinson, P. J., Sontag, J. M., Liu, J. P., Fyske, E. M., Slaughter, C., McMahon, H., and Sudhof, T. C. (1993) *Nature* **365**, 163-166
41. Bar-Zvi, D., Mosley, S. T., and Branton, D. (1988) *J. Biol. Chem.* **263**, 4408-4415
42. Cousin, M. A., Tan, T. C., and Robinson, P. J. (2001) *J. Neurochem.* **76**, 105-116
43. Wilde, A., and Brodsky, F. M. (1996) *J. Cell Biol.* **135**, 635-645
44. Slepnev, V. I., Ochoa, G., Butler, M. H., Grabs, D., and De Camilli, P. (1998) *Science* **281**, 821-824
45. Ricotta, D., Conner, S. D., Schmid, S. L., von Figura, K., and Honing, S. (2002) *J. Cell Biol.* **156**, 791-795
46. Conner, S. D., and Schmid, S. L. (2002) *J. Cell Biol.* **156**, 921-929
47. Korolchuk, V., and Banting, G. (2002) *Traffic* **3**, 428-439
48. Huang, F., Jiang, X., and Sorkin, A. (2003) *J. Biol. Chem.* **278**, 43411-43417
49. Confalonieri, S., Salcini, A. E., Puri, C., Tacchetti, C., and Di Fiore, P. P. (2000) *J. Cell Biol.* **150**, 905-912
50. Huynh, H., Bottini, N., Williams, N., Cherepanov, V., Musimeci, L., Saito, K., Bruckner, S., Vachon, E., Wang, X., Kruger, J., Chow, C., Pellecchia, M., Monosov, E., Greer, P. A., Trimble, W., Downy, G. P., and Mustelin, T. (2004) *Nat. Cell Biol.* **6**, 831-839
51. Wimmer, M., Tag, C., Schreiner, D., and Hofer, H. W. (2004) *J. Endocr.* **181**, 437-447
52. Alonso, A., Sasin, J., Bottini, N., Friedberg, I., Osterman, A., Godzik, A., Hunter, T., Dixon, J. E., and Mustelin, T. (2004) *Cell* **117**, 699-711
53. Tonks, N. K., and Neel, B. G. (2001) *Curr. Opin. Cell Biol.* **13**, 182-195
54. Zhang, Z. (2001) *Curr. Opin. Chem. Biol.* **5**, 416-423
55. Paul, S., and Lombroso, P. J. (2003) *Cell. Mol. Life Sci.* **60**, 2465-2482
56. Andersen, J. N., Mortensen, O. H., Peters, G. H., Drake, P. G., Iversen, L. F., Olsen, O. H., Jansen, P. G., Andersen, H. S., Tonks, N. K., and Moller, N. P. (2001) *Mol. Cell Biol.* **21**, 7117-7136
57. Hendriks, W., Schepens, J., Brugman, C., Zeeuwen, P., and Wieringa, B. (1995) *Biochem. J.* **305**, 499-504
58. Augustine, K. A., Rossi, R. M., Silbiger, S. M., Bucay, N., Duryea, D., Marshall, W. S., and Medlock, E. S. (2000) *Int. J. Dev. Biol.* **44**, 361-371
59. Augustine, K. A., Silbiger, S. M., Bucay, N., Ulias, L., Boynton, A., Trebasky, L. D., and Medlock, E. S. (2000) *Anat. Rec.* **258**, 221-234

Chapter 1

60. Ogata, M., Sawada, M., Fujino, Y., and Hamaoka, T. (1995) *J. Biol. Chem.* **270**, 2337-2343
61. Chirivi, R., Dilaver, G., van de Vorstenbosch, R. A., Schepens, J., Croes, H. J. E., Wanschers, J., Fransen, J., and Hendriks, W. (2004) *Genes Cells* **9**, 919-933
62. Watanabe, Y., Shiozuka, K., Ikeda, T., Hoshi, N., Suzuki, T., Hashimoto, S., and Kawashima, H. (1998) *Mol. Brain Res.* **58**, 83-94
63. Shiozuka, K., Wanatanabe, Y., Ikeda, T., Hashimoto, S., and Kawashima, H. (1995) *Gene* **162**, 279-284
64. Blanco-Aparicio, C., Torres, J., and Pulido, R. (1999) *J. Cell Biol.* **147**, 1129-1136
65. Munoz, J. J., Tarrega, C., Blanco-Aparicio, C., and Pulido, R. (2003) *Biochem. J.* **372**, 193-201
66. Lombroso, P. J., Murdoch, G., and Lerner, M. (1991) *Proc. Natl. Acad. Sci. USA* **88**, 7242-7246
67. Zanke, B. (1992) *Eur. J. Immunol.* **22**, 235-239
68. Adachi, M., Sekiya, M., Kumura, Y., Ogita, Z., Hinoda, Y., Imai, K., and Yachi, A. (1992) *Biochem. Biophys. Res. Commun.* **188**, 1607-1617
69. Boulanger, L. M., Lombroso, P. J., Raghunathan, A., During, M. J., Wahle, P., and Naegle, J. R. (1995) *J. Neurosci.* **15**, 1532-1544
70. Saxena, M., Williams, S., Tasken, K., and Mustelin, T. (1999) *Nat. Cell Biol.* **1**, 305-311
71. Petifford, S. M., and Herbst, R. (2000) *Oncogene* **19**, 858-869
72. Szedlaczek, S. E., Aricescu, A. R., Fulga, T., Renault, L., and Scheidig, A. J. (2001) *J. Mol. Biol.* **311**, 557-568
73. Dilaver, G., Schepens, J., van den Maagdenberg, A., Wijers, M., Pepers, B., Fransen, J., and Hendriks, W. (2003) *Histochem. Cell Biol.* **119**, 1-13
74. Ogata, M., Oh-hora, M., Kosugi, A., and Hamaoka, T. (1999) *Biochem. Biophys. Res. Commun.* **256**, 52-56

Chapter 2

Colocalization of the protein tyrosine phosphatases PTP-SL and PTPBR7 with β 4-adaptin in neuronal cells

Gönül Dilaver, Jan Schepens, Arn van den Maagdenberg, Mietske Wijers,
Barry Pepers, Jack Fransen and Wiljan Hendriks

Histochem. Cell Biol. 119: 1-13, 2003

Summary

The mouse gene *Ptprr* encodes the neuronal protein tyrosine phosphatases PTP-SL and PTPBR7. These proteins differ in their N-terminal domains, with PTP-SL being a cytosolic, membrane-associated phosphatase and PTPBR7 a type I transmembrane protein. In this study, we further explored the nature of the PTP-SL associated vesicles in neuronal cells using a panel of organelle markers and noted a comparable subcellular distribution for PTP-SL and the β 4-adaptin subunit of the AP4 complex. PTP-SL, PTPBR7 and β 4-adaptin are localized at the Golgi apparatus and at vesicles throughout the cytoplasm. Immunohistochemical analysis demonstrated that PTP-SL, PTPBR7 and β 4-adaptin are all endogenously expressed in brain. Interestingly, co-expression of PTP-SL and β 4-adaptin leads to an altered subcellular localization for PTP-SL. Instead of the Golgi and vesicle-type staining pattern, still observable for β 4-adaptin, PTP-SL is now distributed throughout the cytoplasm. Although β 4-adaptin was found to interact with the phosphatase domain of PTP-SL and PTPBR7 in the yeast two-hybrid system, it failed to do so in transfected neuronal cells. Our data suggest that the tyrosine phosphatases PTP-SL and PTPBR7 may be involved in the formation and transport of AP4 coated vesicles or in the dephosphorylation of their transmembrane cargo molecules at or near the Golgi apparatus.

Introduction

Protein tyrosine phosphorylation is one of the important mechanisms that modulate the functional properties of neurons in processes like cell migration, axonal guidance and synapse formation during development. The level of protein tyrosine phosphorylation is tightly regulated by the concerted action of protein tyrosine kinases and protein tyrosine phosphatases (PTPs). Several PTPs, most notably the cell adhesion molecule-like receptor-type PTP LAR, PTP δ and PTP σ , have been shown to be crucial for proper development and function of the nervous system. Their homologues in *Drosophila* are important players in motor neuron axonal guidance (1,2). In mice, targeted inactivation of PTP LAR results in basal forebrain cholinergic neuron abnormalities and a reduced cholinergic innervation of the hippocampal dentate gyrus (3,4). PTP δ deficient mice showed impaired learning with enhanced hippocampal long-term potentiation (5), whereas PTP σ deficient mice display a much more dramatic neuronal phenotype, including neuroendocrine dysplasia (6,7). For many other PTPs their specific neuronal expression pattern in combination with the sometimes complex regional-specific generation of isoforms by means of alternative splicing, has been viewed as highly suggestive for an important regulatory role in the nervous system (8).

In previous studies, we have cloned a cDNA encoding PTP-SL (9), which is highly expressed in brain and is homologous to the rat STEP (striatal enriched phosphatases) family. This STEP family of PTPs is comprised of both transmembrane and cytosolic isoforms that originate from a single gene by the use of alternative splicing (10-12). Interestingly, the mouse gene *Ptprr*, encoding PTP-SL, also produces an additional isoform, but in this case through the use of developmentally regulated alternative promoters (13). The second isoform, termed PTPBR7 (14), is identical to PTP-SL in its C-terminal 535 amino acids but has N-terminally 121 additional residues. PTPBR7 is expressed in brain, especially in the habenula and the hippocampal region (14). Although PTPBR7 is initially expressed during Purkinje cell development, PTP-SL expression takes over postnatally and remains high in adult Purkinje cells (13). In rat, a comparable situation is encountered: a short messenger, encoding PCPTP1-Ce, is exclusively found in cerebellar Purkinje cells whereas the long form is more generally expressed albeit at lower levels (15). This rat orthologue of PTPBR7, named

PCPTP1 (16) or PC12-PTP, is also expressed in PC12 cells and is transiently increased nine-fold upon treatment with nerve growth factor (10).

Recently, Augustine et al. presented evidence that PTP-SL and PTPBR7 are members of an even larger family of PTP isoforms, called PTPPBS, that includes two additional members, PTPPBS γ and PTPPBS δ (17). The closest homologue to the STEP and PTPPBS phosphatases is HePTP (or LC-PTP), which is mainly expressed in lymphoid tissues (18,19). All three PTP types have in common that they can interact with the extracellular regulated kinase (ERK) family (20) via a conserved 16 amino acids kinase interacting motif (21) just proximal of the PTP domain, causing retention of the MAP kinases in the cytoplasm through tyrosine dephosphorylation (22,23). Following proper stimuli, PTP-SL itself can be phosphorylated by the c-AMP-dependent protein kinase PKA on Ser²³¹ residue, resulting in the dissociation of PTP-SL and MAP kinase and translocation of the latter (24).

In previous investigations it was shown that in COS-1 cells ectopically expressed PTPBR7 is a transmembrane PTP (14), whereas PTP-SL is localized on intracellular vesicles partly belonging to the endocytic compartment (13). Here we describe further studies addressing the nature of the intracellular transport vesicles containing PTPRR isoforms in neuronal cells. We show that PTP-SL is localized at the Golgi and at vesicles that are in part late endosomal structures. In addition, we noted that a conspicuous overlap in the subcellular localization of PTP-SL and β 4-adaptin, the β -adaptin subunit of the AP4 complex. Upon co-expression of PTP-SL and β 4-adaptin in transfected Neuro-2a cells, however, the subcellular localization for PTP-SL is dramatically altered. Instead of the Golgi and vesicle-type staining pattern, still observable for β 4-adaptin, PTP-SL is now distributed throughout the cytoplasm. A possible direct interaction between the PTPRR gene products and β 4-adaptin was found using yeast two-hybrid, however could not be detected in mammalian cell system. Furthermore, PTP-SL, PTPBR7 and β 4-adaptin are all endogenously expressed in brain. Since we observe a clear overlap in localization our data suggest that PTPRR tyrosine phosphatases may be involved in the formation and transport of AP4 coated vesicles or in the dephosphorylation of transmembrane cargo molecules at or near the Golgi apparatus.

Material & Methods

Expression plasmid constructions

To create the plasmids pPTP-SL-EGFP and pPTPBR7-EGFP first a plasmid pPTP-EGFP was constructed by excising the PTP domain from mPTP13-6 (9) using BamHI (nucleotide 993) and BglII (nucleotide 1700) and cloning it into the BamHI site of pEGFP-N3. Then the N-terminal part of the phosphatases PTP-SL and PTPBR7, cDNA fragments 1- 993 and 1-1567, respectively, were acquired by BamHI digestion of the plasmids pSG8/PTP-SL-FL-VSV and pSG5/PTPBR7-FL (13) and cloned into the BamHI site of pPTP-EGFP.

To obtain the plasmid pSG8/PTP-SL_{cyt}-VSV; encoding non-hydrophobic region of PTP-SL (142-550 aa), first a PCR was performed on mPTP13-6 with the following primers: pEG5SL position 534 (5' GAAGATCTAGGTTAAAAGAAAGGT-3') and pEG3SL position 1779 (5' CCGCTCGAGCTCTGGTAAATCTTCGG-3'). The 1245-bp PCR product was digested with BglII and XhoI and cloned into a modified pSG8-VSV tagged vector (25).

A construct, p β 4-adaptin-EGFP, for the expression of an EGFP tagged version of mouse β 4-adaptin was generated as follows. First a PCR on pBluescript- β 4-adaptin was performed with the general T3 sequencing primer and a specific primer, 5NotKGFP (5'-ATAAGAATGCGGCCGCTAAAGATTTTATGTCTCCAA-3'); the last 16 nucleotides correspond to position 2201-2216 of the mouse β 4-adaptin sequence (Acc. No. AF155157). The 2.5 kb PCR product was digested with NotI and cloned into pSG8 Δ b/Not-EGFP-his plasmid. This vector is a modified pSG5 in which in between the multiple cloning site a sequence has been inserted that introduces a NotI site immediately preceding the startcodon and open reading frame of an EGFP variant that C-terminally contains the hexahis tag (details available upon request). The resulting p β 4-adaptin-EGFP thus encodes the mouse β 4-adaptin protein which is C-terminally tagged with EGFP and the hexahis sequence.

pMyc-2 is a pEGFP-N3-derived vector in which in between the BglII and ApaI site of the multiple cloning site a synthetic DNA fragment was introduced that entails an initiator AUG codon followed by the cMyc-epitope tag and EcoRI and Xho site respectively. ERK2 (Acc. no. M84489) and β 4-adaptin (aa region 627- 739 of Acc. no. AF 092094) coding sequence were both excised from the pJG4-5 prey vector using the restriction enzymes EcoRI

and XhoI and cloned into the pMyc-2 vector resulting in the pMyc-ERK2 and pMyc- β 4-adaptin plasmids.

The plasmids Rab6B-VSV (26), pSG8/PTP-SL-FL-VSV (13) and pNAEGFP which encodes a EGFP cDNA placed downstream of sequences encoding the cytoplasmic, transmembrane, and stalk region of human N-acetylglucosaminyltransferase I (27) have been described elsewhere.

All constructs were checked by sequence analysis.

Cell lines and antibodies

COS-1 (ATCC nr: CRL-1650) and Neuro-2a (ATCC nr: CCL-131) cells were cultured in DMEM/10% Fetal Calf Serum (FCS) and DMEM/5% FCS, respectively. The generation of the antisera α -SL (13), anti-EGFP (28), anti- β glucocerebrosidase (29), anti-cMyc hybridoma 9E10 (30), and the anti-LBPA (lysobisphosphatidic acid) antibody (31) have been described elsewhere. To generate polyclonal antiserum against β 4-adaptin, a BamHI restriction fragment encoding amino acids 94-548 of human AP4 β -subunit was cloned in BamHI-digested pGEX-2T. The resulting plasmid was introduced in DH5 α strain and GST-fusion proteins were induced and isolated as described (32). Purified fusion-protein was used to immunize rabbits following established protocols.

Immunofluorescence microscopy

Neuro-2a cells, cultured on glass cover slips that were coated overnight with 0.5 mg/ml poly-L-lysine, were transiently transfected with pPTP-SL-EGFP, pPTPBR7-EGFP, p β 4-adaptin-EGFP or pNAEGFP DNA using Lipofectamine-Plus according to the manufacturer. After 24 h the cells were washed with PBS (phosphate buffered saline), fixed for 10 min in 1% paraformaldehyde in 0.1M Phosphate buffer, washed three times with PBS and mounted on glass slides using mowiol containing 2.5 % sodium azide. Some of the coverslips containing transfected cells were treated with 10 μ g/ml Nocodazole for 3 hours prior to washing and fixational mounting. Images were collected using a Bio-Rad MRC-1024 confocal laser scanning microscope (CLSM). When cells were co-transfected with either p β 4-adaptin-EGFP and pSG8/PTP-SL-FL-VSV or p β 4-adaptin-EGFP and Rab6B-VSV, fixation was followed by three wash steps with PBST (PBS, 0.05% Tween-20, 20 mM Glycine) and blocked with

1% cold-water-fish-skin-gelatin in PBS. Subsequently, cells were incubated for 1 hour with anti-VSV monoclonal antibody P5D4 (ascites, 1: 1000 dilution in PBST (PBS, 0.05% Tween-20)). Unbound antibodies were removed by washing with PBST and cells were then incubated with Texas Red-conjugated goat-anti-mouse IgG (1: 100 dilution in PBST) for 1 hour at room temperature. Finally, after three PBST washes coverslips were mounted on glass slides using Mowiol containing 2.5 % sodium azide. All immunofluorescence microscopy was performed on a Biorad MRC 1024 confocal laser scanning microscope.

For the transferrin uptake experiments, Neuro-2a cells were transfected with pPTP-SL-EGFP and 24 hours later cells were washed twice with serum-free medium and subsequently incubated with serum-free medium for 30 min at 37 °C. Then 5 μ g/ml of Alexa-549-labeled transferrin was added and cells were incubated for various time periods at 37 °C. After the incubation the cells were put on ice, washed with ice-cold PBS for three times and fixed and mounted as described above.

Immunoelectron microscopy

Ultrastructural localization studies were performed on Neuro-2a cells transfected with either p β 4-adaptin-EGFP, pPTP-SL-EGFP or pPTPBR7-EGFP. After 24 hours the transfected cells were sorted by fluorescence activated cell sorting (FACS) for their EGFP content. These sorted cells were cultured for an additional 24 hours before fixation in 1% paraformaldehyde (PFA) in 0.1M phosphate buffer for 2 hours at room temperature. Fixed cells were stored until use in 1% PFA. Before sectioning, cells were pelleted in 10% gelatin and post-fixed in 1% PFA for 24 hours. Ultrathin cryosectioning was performed as described before (33,34). Sections were incubated with an antiserum against EGFP at a 1: 100 dilution (28) followed by protein A complexed with 10 nm gold (33). Electron microscopy was performed using a JEOL 1010 electron microscope operating at 80 kV.

Yeast two-hybrid interaction trap

Plasmid DNAs, pEG202-1 and human foetal brain cDNA library in pJG4-5, and the yeast strain used for the interaction trap assay were kindly provided by Drs. Finley and Brent (Massachusetts General Hospital, Boston, MA) and used as described (35). The PTP-SL cytoplasmic region (amino acid 142-550) was cloned in the pEG202-1 vector by performing a PCR with the primers pEG5SL position-534 (5'-GAAGATCTAGGTTAAAAGAAAGGT-

3') and pEG3SL position-1779 (5'-CCGCTCGAGCTCTGGTAAATCTTCGG-3') using mPTP13-6 (9) as a template. The PCR product was digested with BglIII and XhoI and cloned in the BamHI - XhoI site of pEG202-1. Following library screening, positively interacting clones were retested in a second round to exclude false positives. Comparison of cDNA sequences of interacting clones with database entries were done using the BLAST program (36).

Selected clone inserts were radioactively labelled by random priming (37), and used to screen a mouse brain cDNA λ -ZAPII phage library. Hybridisation conditions were according to Church and Gilbert (38). In brief, membranes were preincubated in hybridisation buffer (7% SDS, 0.5M sodium phosphate buffer (pH 7.4), 1 mM EDTA) for 10-60 min at 65 °C. After probe denaturation and addition, membranes were hybridised overnight at 65 °C. Washing at high stringency (0.1% SDS, 0.04 M sodium phosphate buffer (pH 7.4), 1 mM EDTA) was performed three times at 65° C for 20 min. Autoradiography was performed using Kodak X-Omat S1 films at -70 °C for 1-2 days using Dupont Cronex intensifying screens. Positive phages were plaque-purified and inserts were rescued as pBlueScript SK plasmids according to the manufacturer's protocols. Nucleotide sequences were determined by the chain termination method on an ALF express sequence apparatus according to established protocols.

Immunoprecipitation

COS-1 cells cultured on 9-cm dishes were used at 60 % confluency. The cells were washed with Optimem and submerged with 6 ml transfection medium (5.7 ml Optimem, 300 μ l 1 mg/ml DEAE-Dextran chloride form (Sigma), 5 μ l 100 mM Chloroquine), containing the DNA of interest: pPSG8PTP-SLcyt-VSV, pMyc-ERK2, and/or pMyc- β 4-adaptin. After an incubation of 2 hours at 37 °C the transfection medium was removed and replaced by 6 ml of 10% DMSO in PBS. After 3 min, the DMSO shock medium was replaced by normal culture medium containing 10% FCS. Twenty-four hours after transfection cells were washed with PBS and lysed on the plate with 50 mM Tris-HCl (pH 8.0), 150 mM NaCl, 5 mM EDTA, 1% (v/v) Triton-X-100, 1 mM PMSF, 1 mM Na₃VO₄, 50 mM NaF, and 5 mM sodium pyrophosphate. Cell lysates were used for immunoprecipitation with protein A-sepharose CL-4B preloaded with α -SL antiserum, for 3 hours as described (39). The samples were

subjected to 10% polyacrylamide gels and transferred to nitrocellulose membranes by Western blotting. Blots were blocked using 3% non-fat dry milk in 10 mM Tris-HCl (pH= 8.0), 150 mM NaCl, and 0.05% Tween 20 (TBST). The blots were then incubated overnight at room temperature with a 1: 1000 dilution of the monoclonal anti-Myc antibody 9E10 culture supernatant. The blots were then washed 3 times with TBST and incubated for 1 hour with a 1: 10,000 dilution of peroxidase-conjugated Goat anti-Mouse IgG. Subsequent washes were done with TBST and followed by a final rinse with PBS. Immunoreactive bands were visualised using freshly prepared chemiluminescent substrate (100mM Tris-HCl, pH8.5, 1.25 mM p-coumaric acid, 0.2 mM luminol, and 0.009% H₂O₂) and exposure to Kodak X-omat autoradiography films.

Immunohistochemistry

Brains were removed from C57BL/6 mice anaesthetised with pentobarbital. Ten μ m cryosections of unfixed frozen tissue were cut and mounted on Superfrost/Plus slides. The sections were fixed for 5 min in PBS containing 3% paraformaldehyde. Reactive aldehyde groups were blocked by incubating the slides for 60 min in PBST containing 1% normal swine serum. Tissue section were incubated with polyclonal antiserum α -AP4 (1: 100 dilution in PBST) or α -SL (1: 500 dilution in PBST) for 2 h at RT and then washed three times for 5 min in PBST. Subsequently, sections were incubated with biotinylated Donkey-anti-Rabbit IgG (1: 250 dilution in PBST), washed three times in PBS and visualised using the Vecta Staining kit according to the manufacturer's instruction. Samples were mounted in Kaisers gelatin and images were collected on a Dialux 20 microscope. For immunofluorescence microscopy, fluorescein-conjugated Swine-anti-Rabbit IgG 1: 100 was used as a second antibody. After three successive PBS washes, sections were mounted in mowiol and images were collected on a Zeiss Axioskop microscope with epifluorescent illumination.

Results

Previous investigations showed that PTP-SL RNA is expressed in the Purkinje cells of the cerebellum, whereas PTPBR7 mRNA is found in the cortex, hippocampus and striatum (13). To study the subcellular localization of PTPRR isoforms in neuronal cells, we transiently transfected Neuro-2a mouse neuroblastoma cells with constructs encoding enhanced green fluorescent protein (EGFP)-tagged PTP-SL (Fig. 1A) or PTPBR7 (Fig. 1B). Transfected cells were studied by CLSM, exploiting the endogenous fluorescence of the EGFP tag. As in overexpressing COS-1 cells (13) PTP-SL displays a Golgi apparatus-like pattern and in addition shows a vesicular localization. This specific localization is also observed without fixation in living cells. In addition to these sites, PTPBR7 is detected at the plasma membrane. The Golgi association of PTP-SL and PTPBR7 is in line with the observation that the fluorescence pattern is dispersed in the transfected Neuro-2a cells upon treatment with Nocodazol (Fig. 1C and 1D) and Brefeldin A (data not shown), drugs known to disrupt the Golgi apparatus.

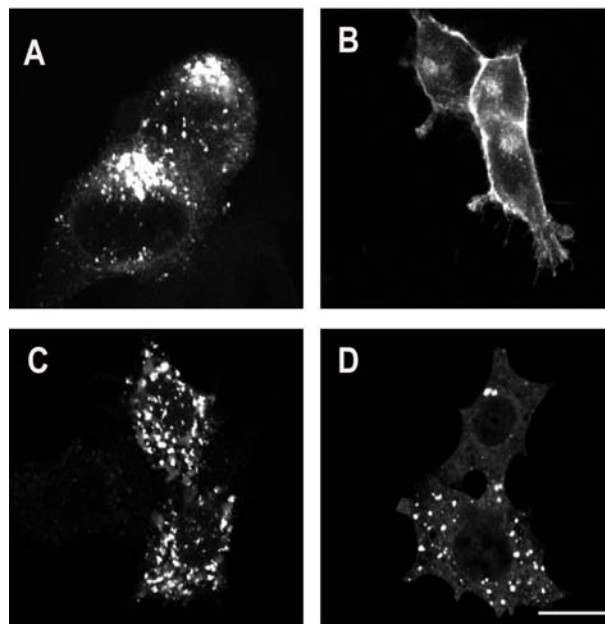


Fig. 1 PTP-SL and PTPBR7 are located at perinuclear vesicular structures.

Analysis of the expression patterns of EGFP fusion protein following transient transfection of mouse Neuro-2a cells with constructs encoding PTP-SL-EGFP (A), PTPBR7-EGFP (B). Nocodazole treatment of PTP-SL-EGFP (C) and PTPBR7-EGFP (D) transfected Neuro-2a cells leads to fragmentation of the EGFP signal. Confocal sections of the EGFP signals were detected by confocal laser scanning microscope. Bar indicates 10 μ m.

To reveal the nature of the PTPRR-containing vesicles in Neuro-2a cells, immunostaining using antibodies against established cell organelle markers was performed. Cells, transfected with EGFP-tagged PTPRR expression constructs, were incubated with the anti-LBPA specific antibody (31) to determine co-localization with multi vesicular bodies (MVB). Lysosomes were detected using an antiserum directed against β -glucocerebrosidase (29). Fig. 2 (panels A-F) shows that the vesicles decorated by EGFP-tagged PTP-SL are distinct from MVBs and lysosomes. Similar results were obtained using cells transfected with an EGFP-tagged PTPBR7 expression plasmid (data not shown). To study whether PTP-SL-decorated vesicles represent endosomal structures, transferrin uptake experiments using PTP-SL-transfected Neuro-2a cells were performed. No colocalization was found after 5 min of transferrin uptake (Fig. 2G-I), whereas after 10 min late endosomal structures containing both PTP-SL and transferrin are apparent (Fig. 2J-L).

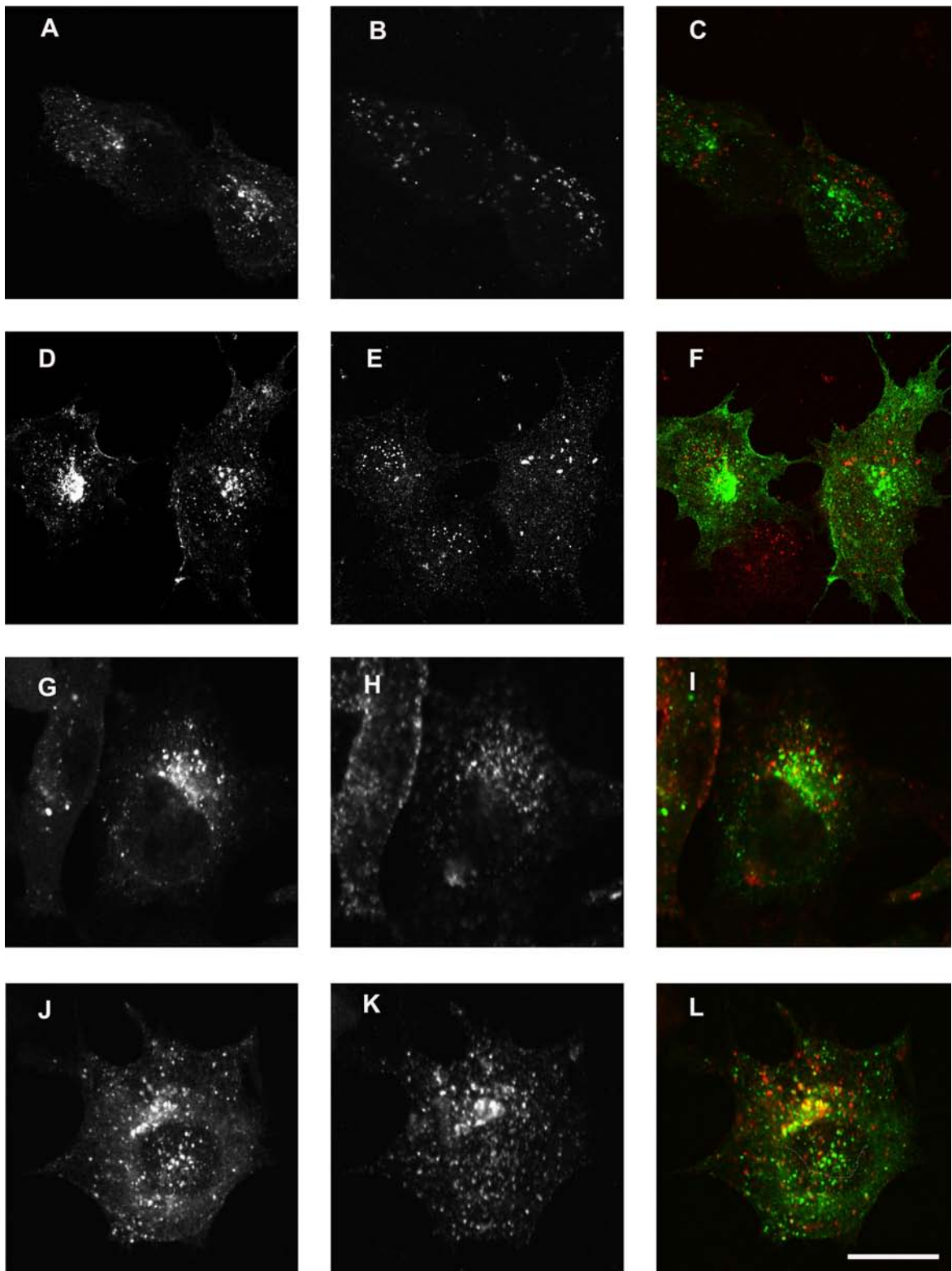
Subsequently, double transfections with the EGFP-tagged Golgi marker Rab6B (26) (Fig. 3A-C) and the trans-Golgi network protein β 1,2 N-acetylglucosaminyl transferase (NAGT) (27) (Fig. 3D-F) with untagged PTP-SL or PTPBR7 gene constructs were performed. Immunohistochemistry was done using polyvalent rabbit antiserum against the phosphatase moiety of PTP-SL (amino acid residues 241-535) (α -SL), and consequently also immunoreactive towards PTPBR7 (13). The PTPRR isoforms co-localize with the TGN to a large extent. Especially in the case of PTP-SL, however, quite some α -SL reactive vesicles were negative for the TGN markers (compare Fig. 3A, D with B, E). Since the AP4 complex has been shown to be present at the Golgi apparatus and at putative late endosomal vesicular structures (27), cells were transfected with an expression construct encoding EGFP-tagged β 4-adaptin (Fig. 3H, K). Remarkably, the localization patterns for EGFP-tagged PTP-SL (Fig. 3A, D, J) and β 4-adaptin (Fig. 3H, K) are very similar in cells expressing either the PTP-SL or the β 4-adaptin-EGFP construct, including both the Golgi apparatus and additional vesicle-like structures in the cell.

Intriguingly, we noted that co-expression of PTP-SL and β 4-adaptin in one and the same Neuro-2a cell (Fig. 3G- I) resulted in a completely distorted localization pattern, in which the β 4-adaptin protein remained at the Golgi (Fig. 3H), but PTP-SL was redistributed throughout the cytoplasm (Fig. 3G). This abnormal distribution was not observed in cells where PTP-SL was expressed simultaneously with the other Golgi proteins (Fig. 3A-F).

Similarly, when β 4-adaptin was co-transfected with Rab6B (Fig. 3L), or with NAGT (data not shown), the distribution of the proteins remained unaltered as compared to the single transfected situation. This demonstrates that the Golgi exclusion effect seen for PTP-SL upon co-transfection with β 4-adaptin is specific. A redistribution of one of the two proteins was not seen when PTPBR7 was co-transfected with β 4-adaptin (data not shown).

Fig. 2 PTP-SL containing vesicles partly colocalize with late endosomes but not with MVB and Lysosomes ►

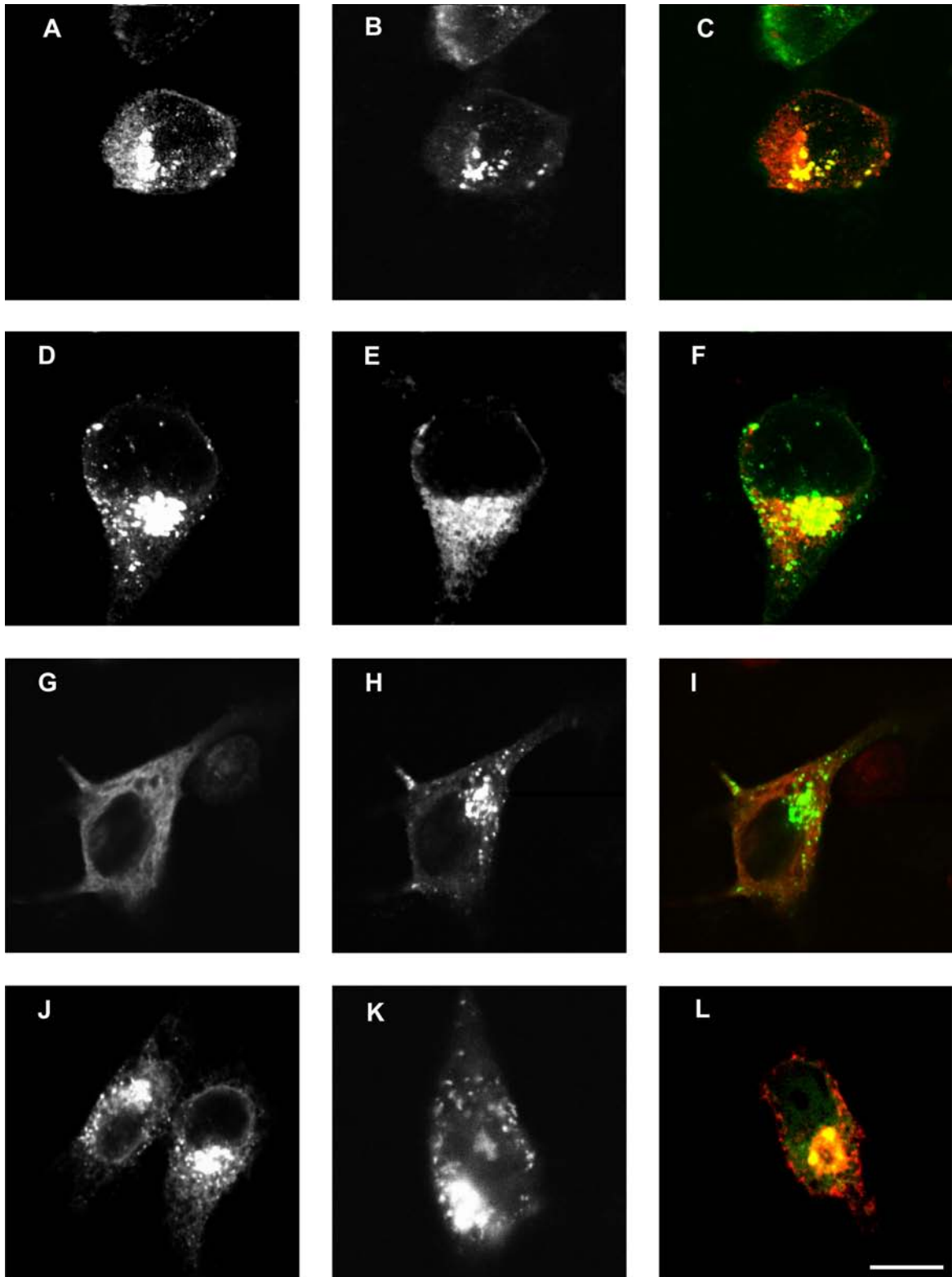
Neuro-2a cells were transiently transfected with a construct encoding EGFP-tagged PTP-SL (A, D, G, J). Expression of PTP-SL-GFP was found at the Golgi area and at vesicles that are distinct from multi vesicular bodies (B) or lysosomes (E). MVBs were detected immunohistochemically using an antibody directed against LBPA (31). Lysosomes were stained with an antiserum against β -glucocerebrosidase (29). GFP fluorescence was recorded directly. After 5 min of Alexa-549-labeled transferrin uptake (H) no colocalization with PTP-SL-containing vesicles (G) is observed. After 10 min of transferrin uptake (K), suggestive for late endosomes, overlapping structures start to appear (L). Merged images are shown on the right (C, F, I, L), with PTP-SL-GFP fluorescence patterns in green and LBPA (C), β -glucocerebrosidase (F) or transferrin (I, L) signals in red. Experiments using GFP-tagged PTPBR7 essentially led to the same conclusion (data not shown). Confocal sections of the fluorescence signals were collected by CLSM. Bar indicates 10 μ m.



Ultimately, we performed immuno-electron microscopy to investigate the precise localization of PTP-SL to compare it with the ultrastructural localization of β 4-adaptin. Unfortunately, our polyvalent rabbit antisera against PTP-SL and β 4-adaptin were not performing well under the conditions required for this technique, precluding the analysis on endogenous proteins. Therefore, we made use of Neuro-2a cells that were transiently transfected with constructs encoding GFP-tagged proteins that could be detected with a GFP-directed antiserum that has demonstrated to be compatible with immunoelectron microscopy (28). Figure 4 shows that PTP-SL, PTPBR7 and β 4-adaptin are localized to coated structures resembling Golgi cisternae and vesicles. However, the architecture of the Golgi is clearly affected due to overexpression of PTP-SL, β 4-adaptin or, although to a lesser extent, PTPBR7 (Fig. 4A- C). This feature was not apparent in the light microscopic studies (Fig. 3) and was not observed when other Golgi proteins were overexpressed like NAEGFP (Fig. 4D) or Rab6B (data not shown), indicating that the poor morphology observed is specifically due to overexpression of these proteins.

Fig. 3 Co-transfection of PTP-SL and β 4-adaptin results in an altered localization for PTP-SL. ►

Analysis of localization patterns in mouse Neuro-2a cells co-transfected with constructs encoding PTP-SL and EGFP-Rab6B (A-C), PTP-SL and EGFP-NAGT (D-F), PTP-SL and EGFP- β 4-adaptin (G-I), and β 4-adaptin and EGFP-Rab6B (L). Panels J and K show single transfectants for PTP-SL and β 4-adaptin, respectively. Untagged PTP-SL and β 4-adaptin proteins were detected immunohistochemically using the antisera anti-SL and anti- β 4-adaptin, respectively. Note the cytoplasmic distribution for PTP-SL (G) upon co-transfection with β 4-adaptin construct (H) as opposed to the vesicle-associated appearance in single transfected cells (J) and in cells co-expressing Rab6B or NAGT (A, D). Merged pictures are shown on the right (C, F, I, L) with PTP-SL (A, D, G) or β 4-adaptin (L) immunofluorescence in red and GFP-fusion protein signals (B, E, H, L) in green. Confocal sections of the fluorescence signals were detected by confocal laser scanning microscopy. Bar indicates 10 μ m.



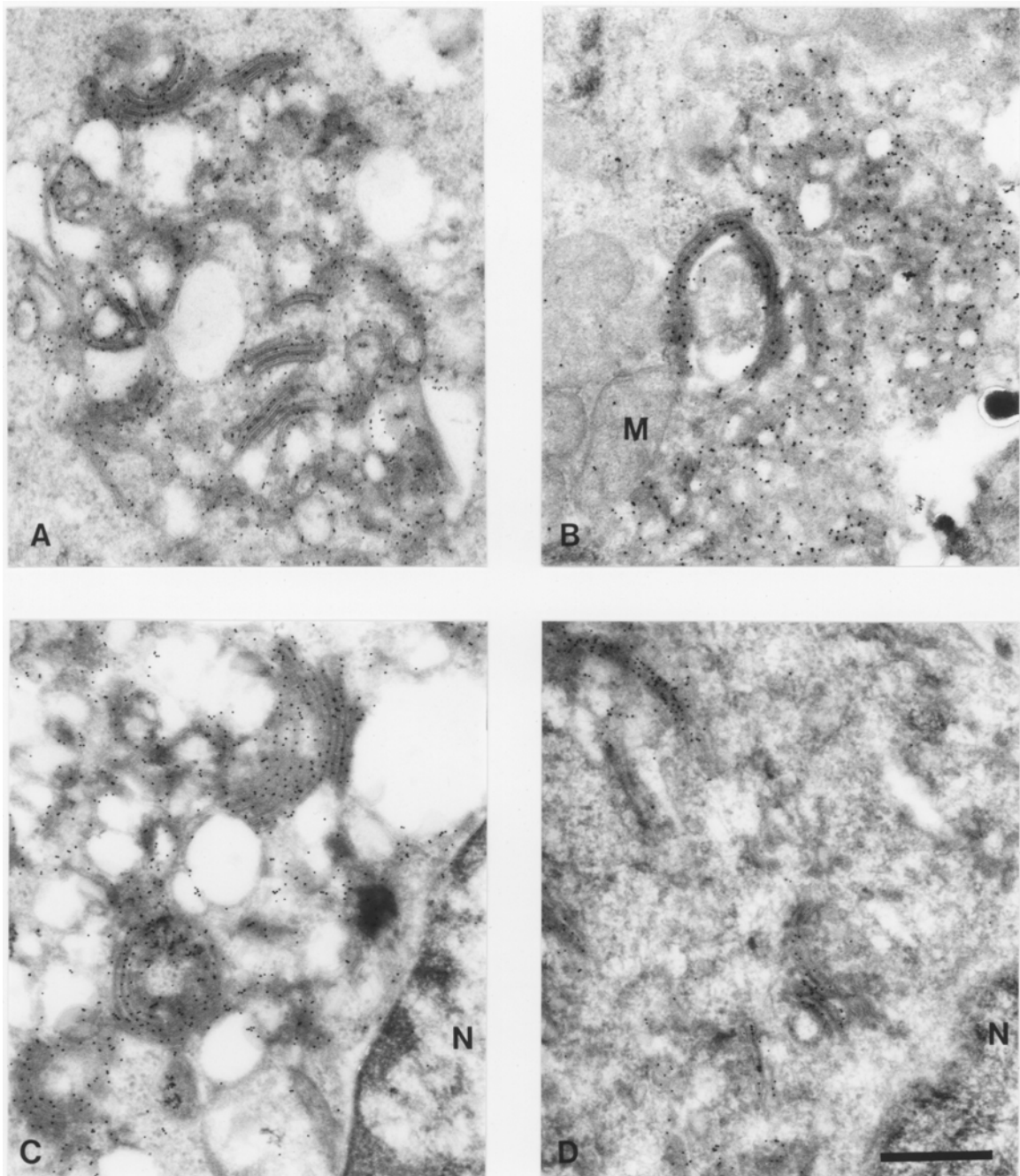


Fig.4 PTP-SL, PTPBR7 and β 4-adaptin localize at coated structures belonging to the Golgi network.

Immuno electron microscopy analysis of transfected Neuro-2a cells expressing PTP-SL-EGFP (A), β 4-adaptin-EGFP (B), PTPBR7-EGFP (C) or NAEGFP (D) showing immunogold staining at the TGN. Ultrastructural immunolocalization revealed strong labelling by the anti-EGFP antibody of coated structures resembling Golgi cisternae and vesicles. M; mitochondria, N; nucleus, Bar indicates 0.5 μ m

The distortion of PTP-SL localization upon co-expression with β 4-adaptin as noted above (Fig. 3G, I) prompted us to investigate whether there might be a direct interaction of PTP-SL and β 4-adaptin. Therefore, a yeast two-hybrid interaction trap screening was performed using the non-hydrophobic carboxyl-terminal part of the protein (amino acid residues 142-550, including the PTP domain) as bait. Screening of a human brain cDNA prey library indeed yielded two clones encoding β 4-adaptin fragments of different length (Table 1). In addition, specifically interacting clones representing the MAP kinases ERK2 and p38 were obtained, confirming data described before in a different experimental set-up (20). The specificity of the PTP-SL interaction with β 4-adaptin was verified using another adaptin protein, human β 3B-adaptin, as a prey. No interaction was found in the yeast two hybrid interaction assay using this neuron-specific adaptin. The interactions were subsequently investigated by co-immuno-precipitation experiments on lysates from transfected COS-1 cells. An expression vector containing the non-hydrophobic region of PTP-SL (residues 142-550) was introduced into COS-1 cells with or without constructs encoding Myc-tagged ERK2 or Myc-tagged carboxyl-terminal part of β 4-adaptin (residues 627-739).

Cell lysates were prepared and PTP-SL-containing protein complexes were precipitated using α -SL antiserum and subjected to SDS-PAGE. Following Western blotting, co-immunoprecipitating proteins were detected using monoclonal antibody 9E10 against the Myc epitope tag (Fig. 5). As expected (20), the MAP kinases were specifically co-precipitated by the α -SL antiserum. In contrast, the β 4-adaptin could not be precipitated, although the protein was readily detectable in the lysate. This may well reflect the exclusion phenomenon observed upon simultaneous over-expression of both proteins described above. We therefore also tested for an interaction by means of a pull-down assay (data not shown) using soluble GST-PTP-SL loaded beads (9). In line with the co-immunoprecipitation data (Fig. 5), cMyc-tagged ERK2 could be unambiguously identified by Western blot analysis of the isolated fractions. β 4-adaptin, however, was undetectable under the conditions used.

Table 1: PTPRR phosphatase moiety interacts with β 4-adaptin in the yeast two-hybrid system.

Baits (top row) and preys (left column) expression plasmids in various combinations were transfected into the EGY48 yeast strain containing appropriate reporter constructs. The relative strength of the bait-prey interaction was scored on the basis of the β -galactosidase activity-dependent blue colouring in combination with growth selection on medium lacking leucine. +++++: very strong interaction (blue colonies < 3 days); ++++: strong interaction (blue colonies \geq 3 days); ++: (blue colonies > 3 days); -: no interaction (no blue colonies after 7 days). Amino acid positions that indicate the PTP-SL (Acc. No. Z30313), h β 4-adaptin (Acc. No. AF092094), h β 3B-adaptin (Acc. No. AF022152), ERK2 (Acc. No. M84489), p38 Map kinase (Acc. No. L35263) and PTP-IA2 (Acc. no U 11812) protein portions used are indicated between brackets. Empty vectors were included as negative controls. n.d., not determined.

| Bait | PTP-SL (aa 142-550) | PTP IA-2 aa 601-979 | vector control (pEG202) |
|------------------------------------|---------------------|------------------------|--------------------------|
| Prey | | | |
| vector control (pJG4-5) | - | - | - |
| h β 4-adaptin (aa 549-739) | +++ | - | - |
| h β 4-adaptin (aa 293-739) | + | - | - |
| h β 3B-adaptin (aa 669-1082) | - | n.d. | - |
| ERK2 Map kinase (aa 8-360) | ++++ | - | - |
| p38 Map kinase (aa2-360) | +++ | - | - |

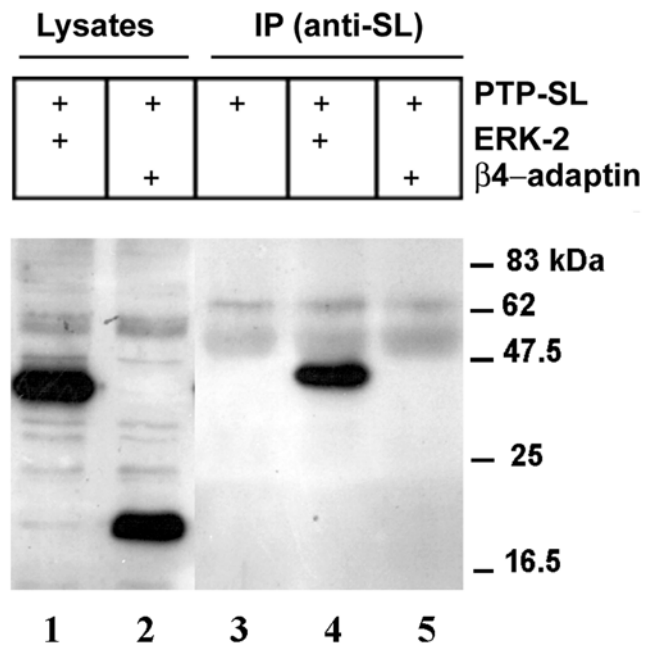


Fig.5 The ERK2 MAP-kinase, but not β 4-adaptin, co-purifies with PTP-SL from transfected COS-1 cell lysates. Transfected COS-1 cells expressing PTP-SL (aa 142-550) and either cMyc-tagged ERK2 MAP kinase (aa 1-360) or β 4-adaptin (aa 627-739) parts were lysed. Production of the Myc-tagged proteins was verified by Western blotting using monoclonal antibody 9E10 (lanes 1, 2). Immuno-precipitation using α -SL antiserum led to the detection ERK2 MAP kinase (lane 4), but not β 4-adaptin lane by Western blotting using mAb 9E10. Precipitation from COS-1 lysates lacking PTP-SL was negative for all constructs. Molecular mass standards in kDa are shown on the right.

The exclusion effect as seen in cells co-transfected with PTP-SL and β 4-adaptin expression constructs thus must be due to indirect effects. To be physiologically relevant, endogenous PTPRR isoforms and β 4-adaptin should be co-expressed in at least some cells and tissues. Northern blot analysis of total RNA isolated from various mouse tissues demonstrates that the 3kb mature transcript encoding β 4-adaptin is rather ubiquitously expressed (40). The level of expression, however, differs between tissues and is high in brain the tissue where PTPRR isoforms reside.

To study endogenous β 4-adaptin and PTP-SL/BR7 proteins at the tissue level, immunohistochemistry was performed using polyvalent anti- β 4-adaptin (against the N-terminal domain of human β 4-adaptin) and α -SL (13) rabbit antiserum. Immunoreactivity towards β 4-adaptin was detected in all tissues tested and was high in brain (Fig. 6), tubuli of the kidney, epithelial cells of the epididymis and the parietal cells of the stomach (data not shown). Since PTP-SL and PTPBR7 are expressed exclusively in brain, we examined in detail the localization of β 4-adaptin in neuronal tissues. In adult mouse brain we observed β 4-adaptin staining in the cortex, striatum and ependym, all regions known to contain considerable levels of PTPBR7 mRNA (13,14). Specific and strong labelling of β 4-adaptin was also observed in individual neurons of the hippocampus (Fig. 6). Importantly, the typical subcellular pattern of the signal is in line with its Golgi localization. Sequential cryosections of brain regions were also incubated with α -SL. Using this anti-PTPRR serum, again individual neurons of the hippocampus stained positive, indicating that PTPBR7 and β 4-adaptin are endogenously expressed in the same types of neurons (Fig. 6C, D). Both PTPBR7 and β 4-adaptin are also co-expressed in neurons of the cortex (Fig. 6A, B). PTP-SL is exclusively expressed in the Purkinje cells of the cerebellum (13). Also these large neurons were found to be positive for β 4-adaptin (Fig. 6E, F), albeit weakly and staining was more uniformly distributed throughout the cell body.

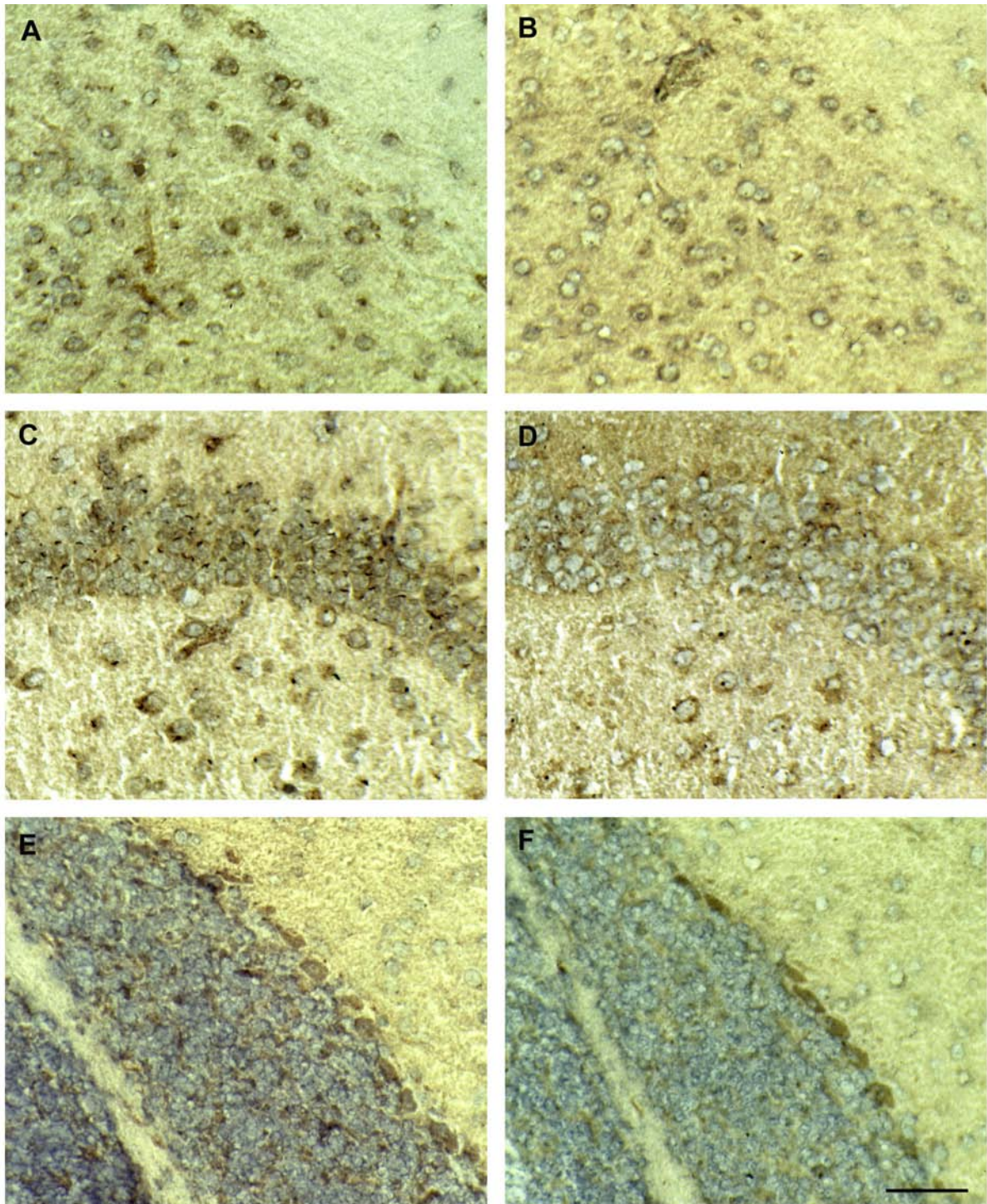


Fig. 6 β 4 adaptin and PTP-SL/PTPBR7 immunoreactivity in neurons of several brain regions.

Immunohistochemical staining of sequential sections with antibodies against β 4-adaptin (A, C, E), and PTP-SL (B, D, F). Colocalization is shown for mouse brain cortex (A, B), pyramidal cells of the hippocampus (C, D), and cerebellum (E, F). Bar indicates 100 μ m.

Discussion

We have previously shown that the mouse gene *Ptprr* encodes two neuronal PTPs, one of which is a cytosolic membrane-associated form of approximately 60 kDa in size, PTP-SL, whereas the other, PTPBR7, is a type I transmembrane protein of 74 kDa (13). Here we reported on further studies addressing the subcellular localization of the PTPRR gene products. PTP-SL is localized to the Golgi and at vesicles throughout the cytoplasm (Fig. 1A). PTPBR7 is localized to Golgi and vesicles as well, but predominantly in the cell membrane (Fig. 1B). Double labeling experiments revealed that the nature of PTP-SL containing vesicles is in part late endosomal. We observed a comparable distribution for PTP-SL and the β 4-adaptin subunit of the AP4 adaptor complex, using immunofluorescence (Fig.3) and immuno-electron (Fig. 4) microscopy. Immunohistochemical analysis demonstrated further that PTPRR isoforms and β 4-adaptin are endogenously expressed in the same cells in brain (Fig. 6).

Adaptins are subunits of adaptors (APs), which are heterotetrameric complexes, consisting of two distinct high-molecular-weight subunits of ~100 kDa (α , β or γ adaptins), a medium size subunit of ~47 kDa (μ adaptins), and a small subunit of ~17 kDa (σ adaptins) (41). Different adaptors are involved in the formation of clathrin-coated vesicles for different transport pathways (for a review see (42-44)). The $\alpha\beta\gamma$ -type subunits contain a hinge and an ear domain. The hinge region is thought to be the flexible part of the subunit, and the protease-sensitive C-terminal ear domain is thought to mediate association to other proteins (41,45,46).

The precise role of the AP4 complex in subcellular transport routes is still subject of investigation, but current data suggest that it mediates sorting processes at the TGN and/or endosomal membranes (40,47). Interestingly, both mouse and human β 4-adaptin contain a rather short carboxyl-terminal ear segment (about 150 residues) as compared to other $\alpha\beta\gamma$ -type adaptin subunits (over 400 residues). Only one other subunit, the γ_2 -adaptin isoform, contains such a truncated ear domain (48) and it is tempting to speculate that this structural feature of some of the $\alpha\beta\gamma$ -type adaptins reflects a functional difference. Phylogenetic analysis revealed that both the C-terminal ear domain and the intermediate hinge region are the most variable region within the adaptin subfamily (49), strengthening possible functional

divergence in these parts of the protein. In line with this, β -adaptins, but not α and γ types, have been shown to interact with clathrin through their hinge/ear domain (50). This raises the interesting question whether the short-eared β 4-adaptin will be capable of mediating a similar interaction with clathrins.

RNA transcripts of both PTP-SL and PTPBR7 are restricted to the nervous system. β 4-adaptin, on the contrary, seems rather ubiquitously expressed. Immunohistochemistry shows that PTP-SL/PTPBR7 and β 4-adaptin proteins are co-expressed in many neurons, including neurons of the hippocampal area. In addition, the subcellular localization of PTP-SL/PTPBR7 and β 4-adaptin, as revealed by transient transfection studies using neuroblastoma cells, are very similar. This overlap in localization of PTP-SL/PTPBR7 and β 4-adaptin was even confirmed by immuno-electron microscopy. A surprising observation was made when β 4-adaptin and PTP-SL were transiently co-expressed in neuroblastoma cells. Double-transfected cells, as opposed to single positive cells, all show a markedly disturbed localization pattern of the PTP-SL protein. The majority of the PTP-SL signal was not localized to the Golgi anymore, but instead was found in the cytoplasm, whereas the β 4-adaptin localization did not change. This change in localization pattern was consistently observed in multiple independent transfections using different DNA preparations, and was not observed when either PTP-SL or β 4-adaptin was co-expressed with Rab6B (26) or NAEGFP (27), which have been described to accommodate also at the Golgi in neurons. Additionally, when an unrelated cytosolic PTP, PTP-BL (51), was co-transfected with β 4-adaptin, these abnormalities were also not observed. The above findings suggest a functional connection between PTP-SL and β 4-adaptin.

Despite a consistent and significant interaction in yeast, a clearly overlapping subcellular localization and an intriguing effect following co-expression of β 4-adaptin and PTP-SL, we were unable to demonstrate a direct interaction for these proteins using co-immuno-precipitation or GST pull-down experiments in mammalian cell system (Fig. 5). This leaves the possibility that the association is of short duration, perhaps occurring only at specific stages during vesicle transport. It is also possible that other factors are necessary for interaction, which are not abundantly present in overexpression studies. Finally, the co-transfection experiments revealed that both proteins might perhaps compete for the same subcellular localization, since PTP-SL is specifically redistributed by β 4-adaptin. Clearly,

these effects are not observed in yeast ectopically expressing PTP-SL and β 4-adaptin fusion proteins.

Could there be a role for PTP-SL and/or PTPBR7 in regulating formation and/or transport of AP4 containing vesicles? Several reports present evidence that reversible phosphorylation of clathrin coat components can regulate endocytosis/exocytosis either directly or indirectly (52-56). For example, the β 2-adaptin of the AP2 complex is phosphorylated by a staurosporine sensitive kinase and de-phosphorylated by protein phosphatase PP2A (57) or Synaptojanin 1, thereby regulating adaptor protein dynamics (58). Evidence is accumulating that vesicle trafficking is regulated by tyrosine-specific phosphorylation as well. For example, Nucifora et al. reported that rapid endocytosis is controlled by tyrosine phosphorylation (59). Also, the endocytosis of the ROMK1 potassium channel is regulated by tyrosine phosphorylation (60). Thus, one may expect that tyrosine-specific phosphatases will influence the vesicle transport process as well. An alternative explanation for the presence of PTP family members, such as PTP-SL, at specific organelles within the cell relates to the phenomenon observed by Haj et al (61). They found that after internalization of receptor tyrosine kinases (RTKs) from the cell surface, the vesicles travel close to the endoplasmic reticulum where the protein tyrosine phosphatase PTP1B resides. This enzyme dephosphorylates specific tyrosine residues in the autophosphorylated cytoplasmic domains of endocytosed RTKs, which then travel on to the lysosomes. Depending on the different destinations of transmembrane cargo proteins, dephosphorylation of endocytosed proteins may be organized at other meeting points as well e.g. at the endocytotic vesicles or sorting endosomes themselves. It is thus possible that the phosphatases PTPSL and PTPBR7 are involved in dephosphorylating cargo proteins of AP4-containing vesicles at a region in or near the Golgi apparatus. Future research will be aimed at investigating these possibilities.

Acknowledgments

We thank Huib Croes and Rinske van de Vorstenbosch for excellent technical assistance, Bas Wanschers for help with the double labeling experiments, and Ineke van der Zee for help and advice. We also thank Jean Gruenberg for providing anti-LBPA antibody, Hans Aerts for the anti- β glucocerebrosidase antibody and Mary Robinson for human β 3B-adaptin cDNA. This work was supported in part by a grant from the Dutch Cancer Society to W. H.

References

1. Krueger, N. X., Van-Vactor, D., Wan., W. M., Goodman, C. S., and Saito, H. (1996) *Cell* **84**, 611-622
2. Desai, C. J., Sun, Q., and Zinn, K. (1997) *Curr. Opin. Neurobiol.* **7**, 70-74
3. Yeo, T. T., Yang, T., Massa, S. M., Zhang, J., Honkaniemi, J., Butcher, L. L., and Longo, F. M. (1997) *J. Neurosci. Res.* **47**, 348-360
4. van Lieshout, E. M. M., van der Heijden, I., Hendriks, W. J. A. J., and Van der Zee, C. E. E. M. (2001) *Neurosci.* **102**, 833-841
5. Uetani, N., Kato, K., Ogura, H., Mizuno, K., Kawano, K., Mikoshiba, K., Yakura, H., Asano, M., and Iwakura, Y. (2000) *EMBO J.* **19**, 2775-2785
6. Elchebly, M., Wagner, J., Kennedy, T. E., Lanctot, C., Michalyszyn, E., Itie, A., Drouin, J., and Tremblay, M. L. (1999) *Nature Genet.* **21**, 330-333
7. Wallace, M. J., Fladd, C., Batt, J., and Rotin, D. (1998) *Mol. Cell Biol.* **18**, 2608-2616
8. Stoker, A., and Dutta, R. (1998) *BioEssays* **20**, 463-472
9. Hendriks, W., Schepens, J., Brugman, C., Zeeuwen, P., and Wieringa, B. (1995) *Biochem. J.* **305**, 499-504
10. Sharma, E., and Lombroso, P. J. (1995) *J. Biol. Chem.* **270**, 49-53
11. Boulanger, L. M., Lombroso, P. J., Raghunathan, A., During, M. J., Wahle, P., and Naegle, J. R. (1995) *J. Neurosci.* **15**, 1532-1544
12. Bult, A., Zhao, F., Dirx Jr, R., Sharma, E., Lukacsi, E., Solimena, M., Naegele, J. R., and Lombroso, P. J. (1996) *J. Neurosci.* **16**, 7821-7831
13. van den Maagdenberg, A. M. J. M., Bachner, D., Schepens, J. T. G., Peters, W., Fransen, J. A. M., Wieringa, B., and Hendriks, W. J. A. J. (1999) *Eur. J. Neurosci.* **11**, 3832-3844
14. Ogata, M., Sawada, M., Fujino, Y., and Hamaoka, T. (1995) *J. Biol. Chem.* **270**, 2337-2343
15. Watanabe, Y., Shiozuka, K., Ikeda, T., Hoshi, N., Suzuki, T., Hashimoto, S., and Kawashima, H. (1998) *Mol. Brain Res.* **58**, 83-94
16. Shiozuka, K., Wanatanabe, Y., Ikeda, T., Hashimoto, S., and Kawashima, H. (1995) *Gene* **162**, 279-284
17. Augustine, K. A., Silbiger, S. M., Bucay, N., Ulias, L., Boynton, A., Trebasky, L. D., and Medlock, E. S. (2000) *Anat. Rec.* **258**, 221-234
18. Zanke, B. (1992) *Eur. J. Immunol.* **22**, 235-239
19. Adachi, M., Sekiya, M., Kumura, Y., Ogita, Z., Hinoda, Y., Imai, K., and Yachi, A. (1992) *Biochem. Biophys. Res. Commun.* **188**, 1607-1617
20. Pulido, R., Zuñiga, A., and Ullrich, A. (1998) *EMBO J.* **17**, 7337-7350
21. Kim, W. T., Chang, S., Daniell, L., Cremona, O., Di Paolo, G., and De Camilli, P. (2002) *Proc. Natl. Acad. Sci. USA* **99**, 17143-17184
22. Saxena, M., Williams, S., Tasken, K., and Mustelin, T. (1999) *Nat. Cell Biol.* **1**, 305-311
23. Zuñiga, A., Torres, J., Ubeda, J., and Pulido, R. (1999) *J. Biol. Chem.* **274**, 21900-21907

24. Blanco-Aparicio, C., Torres, J., and Pulido, R. (1999) *J. Cell Biol.* **147**, 1129-1136
25. Cuppen, E., Gerrits, H., Pepers, B., Wieringa, B., and Hendriks, W. (1998) *Mol. Biol. Cell* **9**, 671-683
26. Opdam, F. J. M., Echard, A., Croes, H. J. E., van den Hurk, J. A. J. M., van de Vorstenbosch, R. A., Ginsel, L. A., Goud, B., and Fransen, J. A. M. (2000) *J. Cell Sci.* **113**, 2725-2735
27. Shima, D. T., Haldar, K., Pepperkok, R., Watson, R., and Warren, G. (1997) *J. Cell Biol.* **137**, 1211-1228
28. Cuppen, E., Wijers, M., Schepens, J., Fransen, J., Wieringa, B., and Hendriks, W. (1999) *J. Cell Sci.* **112**, 3299-3308
29. Willemsen, R., Brunken, R., Sorber, C. W. J., Hoogeveen, A. T., Wisselaar, H. A., Vandongen, J. M., and Reuser, A. J. J. (1991) *Histochem. J.* **23**, 2044-2047
30. Kari, B., Lussenhop, N., Goertz, R., Wabuke-Bunoti, M., Radeke, R., and Gehrz, R. (1986) *J. Virol.* **60**, 345-352
31. Kobayashi, T., Stang, E., Fang, K. S., de Moerloose, P., Parton, R. G., and Gruenberg, J. (1998) *Nature* **392**, 193-197
32. Frangioni, J. V., and Neel, B. G. (1993) *Anal. Biochem.* **210**, 179-187
33. Fransen, J. A., Ginsel, L. A., Hauri, H. P., Sterchi, E., and Blok, J. (1985) *Eur. J. Cell Biol.* **38**, 6-15
34. Schweizer, A., Fransen, J. A., Bachi, T., Ginsel, L., and Hauri, H. P. (1988) *J. Cell Biol.* **107**, 1643-1653
35. Gyuris, J., Golemis, E., Chertkov, H., and Brent, R. (1993) *Cell* **75**, 791-803
36. Altschul, S. F., Gish, W., Myers, E. W., and Lipman, D. J. (1990) *J. Mol. Biol.* **215**, 403-410
37. Feinberg, A. P., and Vogelstein, B. (1983) *Anal. Biochem.* **132**, 6-13
38. Church, G. M., and Gilbert, W. (1984) *Proc. Natl. Acad. Sci. USA* **81**, 1991-1995
39. Ogata, M., Oh-hora, M., Kosugi, A., and Hamaoka, T. (1999) *Biochem. Biophys. Res. Commun.* **256**, 52-56
40. Hirst, J., Bright, N. A., Rous, B., and Robinson, M. S. (1999) *Mol. Biol. Cell* **10**, 2787-2802
41. Traub, L. M. (1997) *Trends Cell Biol.* **7**, 43-47
42. Brodsky, F. M. (1997) *Trends Cell Biol.* **7**, 175-179
43. Robinson, M. S. (1997) *Trends Cell Biol.* **7**, 99-102
44. Boehms, M., and Bonifacino, J. S. (2001) *Mol. Biol. Cell* **12**, 2907-2920
45. Page, L. J., and Robinson, M. S. (1995) *J. Cell Biol.* **131**, 619-630
46. Robinson, M. S., Watts, C., and Zerial, M. (1996) *Cell* **84**, 13-21
47. Dell'Angelica, E. C., Mullins, C., and Bonifacino, J. S. (1999) *J. Biol. Chem.* **274**, 7278-7285
48. Lewin, D. A., Sheff, D., Eng Ooi, C., Whitney, J. A., Yamamoto, E., Chicione, L. M., Webster, P., Bonifacino, J. S., and Mellman, I. (1998) *FEBS Lett.* **435**, 263-268
49. Schledzewski, K., Brinkmann, H., and Mendel, R. R. (1999) *J. Mol. Evol.* **48**, 770-778
50. Clairmont, K. B., Boll, W., Ericsson, M., and Kirchhausen, T. (1997) *Cell. Mol. Life Sci.* **53**, 611-619
51. Hendriks, W., Schepens, J., Bachner, D., Rijss, J., Zeeuwen, P., Zechner, U., Hameister, H., and Wieringa, B. (1995) *J. Cell. Biochem.* **59**, 418-430

Chapter 2

52. Wilde, A., and Brodsky, F. M. (1996) *J. Cell Biol.* **135**, 635-645
53. Slepnev, V. I., Ochoa, G., Butler, M. H., Grabs, D., and De Camilli, P. (1998) *Science* **281**, 821-824
54. Freedman, S. D., Katz, M. H., Parker, E. M., and Geldrud, A. (1999) *Am. J. Physiol.* **45**, C306-C311
55. Wilde, A., Beattie, E. C., Lem, L., Riethof, D. A., Liu, S. H., Mobley, W. C., Soriano, P., and Brodsky, M. (1999) *Cell* **96**, 677-687
56. Reese, E. L., and Haimo, L. T. (2000) *J. Cell Biol.* **151**, 155-165
57. Lauritsen, J. P. H., Menne, C., Kastrup, J., Dietrich, J., Odum, N., and Geisler, C. (2000) *Biochim. Biophys. Acta*, 297-307
58. Haffner, C., Di Paolo, G., Rosenthal, J. A., and De Camilli, P. (2000) *Curr. Biol.* **10**, 471-474
59. Nucifora, P. G. P., and Fox, A. P. (1990) *J. Neurosci.* **19**, 9739-9746
60. Sterling, H., Lin, D., Gu, R., Dong, K., Heberts, S. C., and Wang, W. (2002) *J. Biol. Chem.* **277**, 4317-4323
61. Haj, F. G., Verveer, P. J., Squire, A., Neel, B. G., and Bastiaens, P. I. H. (2002) *Science* **295**, 1708-1711

Chapter 3

Characterization of multiple transcripts and isoforms derived
from the mouse protein tyrosine phosphatase gene *Ptprp*

Renato G.S. Chirivi[‡], Gönül Dilaver[‡], Rinske van de Vorstenbosch, Bas
Wanschers, Jan Schepens, Huib Croes, Jack Fransen and Wiljan Hendriks

[‡] These authors contributed equally to this work

Genes Cells **9**: 919-933, 2004

Summary

The use of alternative splice sites, promoters and translation start sites considerably adds to the complexity of organisms. Four mouse cDNAs (PTPBR7, PTP-SL, PTPPBS γ ⁺ and PTPPBS γ ⁻) have been cloned that contain different 5' parts but encode identical protein tyrosine phosphatase PTPRR catalytic domains. We investigated the genomic origin and coding potential of these transcripts to elucidate their interrelationship. Mouse gene *Ptprr* exons were identified within a 260 kbp segment on chromosome 10, revealing PTP-SL- and PTPPBS γ -specific transcription start sites within introns two and four, respectively, relative to the fourteen PTPBR7 exons. Northern and RT-PCR analyses demonstrated differential expression patterns for these promoters. Furthermore, transfection studies and AUG codon mutagenesis demonstrated that in PTP-SL and PTPPBS γ messengers multiple translation initiation sites are being used. Resulting 72, 60, 42 and 37 kDa PTPRR protein isoforms differ not only in the length of their N-terminal part but also in their subcellular localization, covering all major PTP subtypes; receptor-like, membrane associated and cytosolic. In summary, mouse gene *Ptprr* gives rise to multiple isoforms through the use of distinct promoters, alternative splicing and differential translation starts. These results set the stage for further investigations on the physiological roles of PTPRR proteins.

Introduction

Reversible phosphorylation of specific tyrosine residues within proteins is an essential intracellular signal transduction mechanism. Cellular responses like differentiation, proliferation, survival, metabolic activity, and more specifically for neuronal cells, migration, axonal guidance, synapse formation and activity are all regulated by modulating the phosphorylation state of target proteins (1-3). Protein tyrosine kinases and protein tyrosine phosphatases (PTPs) are the enzymes that are instrumental in determining the spatial and temporal balance between the tyrosine phosphorylated and non-phosphorylated targets, and thus coordinately regulate these cellular responses to extracellular cues.

PTPs have been categorized into two distinct subgroups (4). The first group possesses a transmembrane domain that follows a receptor-like extracellular region; the second group is cytoplasmic in location, and can in turn be subdivided in membrane-associated and true cytosolic PTPs. Interestingly, some PTP genes encode multiple isoforms that belong to several of these PTP subgroups. For instance, the STEP subfamily of PTPs consists of multiple transmembrane and cytosolic isoforms that are suggested to result from alternative splicing (5,6). Likewise, transmembrane, cytosolic and membrane-associated PTP ϵ isoforms exist, but these result from the use of alternative promoters, proteolytic processing and differential initiation of translation (7). It is commonly believed that the generation of multiple isoforms from a single PTP gene through (a combination of) such mechanisms warrants fine-tuning of cellular signaling programs, both in time and space dimensions, thus adding to the organismal complexity of higher eukaryotes. Consequently, when studying the functional potential of a given gene, it is imperative to delineate its catalogue of transcripts and the exact nature of the corresponding protein products.

Several mouse cDNA clones, encoding PTPBR7, PTP-SL and PTPPBS γ , respectively, have been reported that contain an identical, PTP-encoding 3' segment but differ completely in their 5' parts (8-11). We have recently proposed that the messengers that gave rise to the PTPBR7 and PTP-SL cDNAs are derived from a single mouse gene, *Ptprr*, through the use of developmentally regulated alternative promoters (12). The origin of two other transcript variants, both encoding PTPPBS γ (8), is as yet undefined. Moreover, uncertainties as to the translation initiation sites used in PTP-SL and PTPPBS γ -encoding mRNAs has led to confusion and, occasionally, discrepancies in amino acid residue numberings (12,13).

To clarify the above issues we performed a careful annotation of transcript and protein products for mouse gene *Ptprr*, and investigated protein expression both *in situ* and at the subcellular level. Results reveal a unique gene system in which alternative use of promoters and AUG start codons accounts for the generation of distinct protein isoforms. These PTPRR proteins differ in their subcellular localization and represent all major PTP subtypes; receptor-like, membrane-associated and cytosolic. This work gives important insight in the *Ptprr* gene structure and sets the stage for further investigations on the physiological role of the three mouse PTPRR protein isoforms, PTPBR7, PTP-SL and PTPPBS γ .

Material & Methods

Expression plasmid constructs and site directed mutagenesis

Plasmids pSG5/PTP-SL-FL and pSG5/PTPBR7-FL have been described elsewhere (12). To obtain a full-length mouse PTPPBS γ expression construct (pSG5/PTPPBS γ -FL) PCR was performed on mouse genomic DNA using oligonucleotides 5'-GGACTAGTCCGTGAACCAGGTAGTTTCCAG-3' (*SpeI* restriction site is underlined) and 5'-TCCTTCTTTGCTCCAGAT-3', which resulted in a 362-bp fragment encompassing the nucleotides (pos. 1-292) that are unique for PTPPBS γ + cDNA. The PCR product was cloned into the pGEM-T vector (Promega, Madison, WI, USA) and analyzed by sequencing to verify absence of mutations. The resulting plasmid was treated with endonucleases *Bg/III* and *SpeI*, and the obtained fragment was inserted into pSG5/PTP-SL-FL that had been first partially digested with *Bg/III* (position 441 in the PTP-SL cDNA) and digested to completion with *SpeI*.

AUG mutants of pSG5/PTPBR7-FL, pSG5/PTP-SL-FL and pSG5/PTPPBS γ plasmids were generated using the QuickChange Mutagenesis protocol according to manufacturers specifications (Stratagene Inc., La Jolla, CA, USA). In Table 1 the primers and nomenclature used is listed. Obtained mutant constructs were checked by sequence analysis.

The bacterial expression plasmid pGEX-SL has been described before (10). Deletion mutants pGEX-2T-SL1060, pGEX-2T-SL1213, and pGEX-2T-SL1582 were created by PCR using specific primers (sequences available upon request) and mPTP13-6 (10) as template. Resulting PCR products were cloned into the *BamHI* site of pGEX-2T. To enable production of His-tagged PTP-SL recombinant protein, an *NcoI-XhoI* cDNA fragment was excised from mPTP13-6 (10), blunted with Klenow and cloned into *XhoI*-digested and Klenow-treated pET-15b vector, rendering pET-15b-PTP-SL.

Table 1. Mutant nomenclature and primers used for site directed mutagenesis

| mutant | 5' primer | 3' primer |
|-----------------------|--|--|
| BR7-356 | caatgcacacactat c agagcggctc | cgaccgctctcctgatagtggtgcatg |
| BR7-719 | ccgacactgcaa a tcgatataaccaagctg | cagcttgggtatata c gatttgcagtgtcgg |
| SL-103 | gatggaagtcggatccatcgcaacactc | gagtgttgcgatg g atccgacttccatc |
| SL145 | ccgacactgcaa a tcgatataaccaagctg | cagcttgggtatata c gatttgcagtgtcgg |
| SL-643/759 | gaccacagcat c gtccagccgatc cttctcccttcagaat ca agcccataggactc | gatcgggctggac g atgctgtgggtc gagtcctatgggctt g attctgaagggagaag |
| PBS γ -401 | catagtaacctgtttgat c attatttacagg | cctgtaaataat g atcaaacaggttactatg |
| PBS γ -530 | gaccacagcat c gtccagccgatc | gatcgggctggac g atgctgtgggtc |
| PBS γ -647 | cttctcccttcagaat ca agcccataggactc | gagtcctatgggctt g attctgaagggagaag |
| PBS γ -704 | cttacgctggacat c agtagcctgggcag | ctgccaggctact g atgtccagcgtaa |
| PBS γ -530/647 | gaccacagcat c gtccagccgatc cttctcccttcagaat ca agcccataggactc | gatcgggctggac g atgctgtgggtc gagtcctatgggctt g attctgaagggagaag |

Several AUG start codons of PTPBR7 (Acc.no.: D31898), PTP-SL (Acc.no.: BN000437) and PTPPBS γ (Acc.no.: BN000438) were mutated into AUC using the primers above, and thereby mutating Methionines into Isoleucines. Numbers correspond to the position of the first nucleotide of the start codon. The mutated nucleotide is indicated in bold. Two numbers indicate mutations of two start codons.

Antibodies

Rabbit polyclonal antiserum against the PTP-containing part of PTP-SL (α -SL) has been described (12). In some experiments STEP-absorbed α -SL was used. Briefly, STEP cross-reactivity was removed from the polyvalent α -SL serum by passing it over glutathion-sepharose-bound GST-STEP fusion protein (13). To generate monoclonal antibodies against PTPRR protein isoforms, the pGEX-SL construct was used for bacterial production of GST-SL fusion protein as described previously (12). Immunization with purified GST-SL protein and later on fusion of mouse spleen B-cells with myeloma line Sp2/0-Ag14 was performed according to established protocols. Resulting hybridomas were screened by ELISA using 96-well plates coated with His-tagged PTP-SL protein. The latter was obtained essentially as described (14). Eight clones (6A6, 1E3, 3E11, 8F10, 5E4, 6H11, 11H8, and 6D6) were selected on the basis of their immunoreactivity and grown for antibody production and further analyses.

Bacterial expression plasmids pGEX-PTP-SL, pGEX-2T-SL1060, pGEX-2T-SL1213, and pGEX-2T-SL1582 were used for epitope mapping. In brief, expression of the various GST-PTP-SL fusion proteins was induced using 1 mM IPTG applied to DH5 α bacterial cells containing the respective pGEX-based plasmid. Protein lysates were analyzed by Western blot analysis essentially as described below.

Protein isolation, immunoprecipitation and Western blotting

Neuro-2a cells (ATCC nr. CCL-131) were cultured in 9-cm dishes using DMEM supplemented with 5% Fetal Calf Serum. Upon reaching 60% confluency cells were washed with OptiMEM (Gibco/BRL, Gaithersburg, MD, USA) and transiently transfected with appropriate plasmid DNA using Lipofectamine-Plus (Invitrogen Life Technologies, Breda, the Netherlands). Twenty-four hours after transfection, cells were washed with phosphate buffered saline (PBS) and taken up in lysis buffer (100mM Na₂HPO₄, 1% Triton-X-100, 0.2% BSA, pH 8.0), containing a complete protease inhibitor cocktail (Roche Diagnostics GmbH, Mannheim, Germany).

For immunoprecipitation purposes, 30 μ l mono α -SL (6A6) together with 30 μ l of protein A-Sepharose CL-4B (Amersham Pharmacia Biotech AB, Uppsala, Sweden) was added to 500 μ l cell lysate and incubated by overnight rotation at 4°C. The Sepharose beads with immunobound proteins were subsequently washed four times in lysis buffer, once in 0.1 M Na₂HPO₄, pH 8.1, and twice in 0.01 M M Na₂HPO₄. 2x sample buffer (100mM Tris-HCl, pH 6.8, 200mM dithiothreitol, 4%SDS, 0.2% bromophenol blue, 20% glycerol) was added to the beads, and proteins were subjected to 10% SDS-PAGE.

Mouse C57BL/6 tissue lysates were made by mechanical disintegration of whole brain or separate brain regions (olfactory bulb, hippocampus, midbrain, brainstem, cerebellum and cortex) in 1.5 ml lysis buffer. The lysates were incubated for 1h at 4°C and insoluble components were pelleted by centrifugation (14,000 rpm) for 30 min at 4°C. Protein concentration in the resulting supernatant was determined according to Lowry (15).

Protein samples were subjected to 10% SDS-PAGE gels and transferred to nitrocellulose membranes by Western blotting or alternatively first immunoprecipitated with mono α -SL (6A6) together with protein A-Sepharose CL-4B as described for cell lysates and then subjected to 10% SDS-page gel and Western blotting. Resulting membranes were blocked for 30 min using 3% non-fat dry milk in TBST (10 mM Tris-HCl (pH 8.0), 150 mM

NaCl, and 0.05% Tween 20) and incubated overnight at room temperature with a 1:1000 dilution of rabbit α -GST-SL in TBST. Blots were washed 3 times with TBST and incubated for 1h with a 1:10,000 dilution of peroxidase-conjugated Goat anti-Rabbit IgG (Pierce Biotechnology Inc., Rockford, IL, USA) in TBST. Subsequent washes were done with TBST, followed by a final rinse with PBS. For the epitope mapping purposes, blots were incubated with diluted hybridoma culture supernatant (1:2000) and peroxidase-conjugated Goat anti-mouse IgG (1:20.000) (Pierce) as first and second antibody, respectively. Immunoreactive bands were visualized using freshly prepared chemiluminescent substrate (100mM Tris-HCl, pH 8.5, 1.25 mM p-coumaric acid (Sigma Chemical Co., St. Louis, MO, USA), 0.2 mM luminol (Sigma), and 0.009% H₂O₂) and exposed to Kodak X-Omat autoradiography films (Eastman Kodak Company, Rochester, NY, USA).

RNA expression analyses

Total RNA from different brain regions (olfactory bulb, hippocampus, midbrain, brainstem, cerebellum and cortex) was purified using RNazol B (Campro Scientific, Veenendaal, The Netherlands). Ten μ g of RNA was loaded on a 1% formamide agarose gel and after electrophoretical size separation, the RNA was transferred onto nylon membrane (Amersham Pharmacia Biotech BA, Uppsala, Sweden) according to standard procedures (16). The pSG5/PTPBR7-FL construct was ³²P-labeled and used as a probe. Hybridization was carried out overnight at 65°C (17), and blots were washed several times with 40 mM phosphate buffer containing 0.2% SDS at 65°C and exposed to Kodak X-Omat S1 films. Probes specific for PTPBR7 (Acc. No. D31898: pos. 414-709), PTP-SL (TPA Acc. No. BN000437: bp1-135) and PTPPBS γ (TPA Acc. No. BN000438: bp 1-346) were obtained by PCR on mouse genomic DNA, radioactively labeled, and used for hybridization as described above.

For RT-PCR analyses cDNA was synthesized from 2 μ g total RNA by random hexamer priming using SuperScriptTM II RNase H⁻ Reverse Transcriptase (Invitrogen Life Technologies, Breda, the Netherlands). PTPBR7, PTP-SL, PTPPBS γ and β -actin cDNA fragments were amplified by PCR using the following specific primers: BR7-forward, 5'-CCTCAATGCACACTATGAGG-3'; BR7-reverse, 5'-TCCTTCTTTGCTCCAGAT-3'; SL-forward, 5'-TCCAGGTGACTAAACGAGG-3'; SL-reverse, 5'-TCCTTCTTTGCTCCAGAT-3'; PBS γ -forward, 5'-GTGAACCAGGTAGTTCCAG-3';

PBS γ -reverse, 5'-AGGGTCCACAACCACGTTCA-3'; β -actin-forward, 5'-GCTAGAGCTGCCTGACGG-3'; β -actin-reverse, 5'-GAGGCCAGGATGGAGCC-3'. Resulting products were analyzed by electrophoresis using a 2% agarose gel for size-separation and ethidium bromide for fluorescent detection.

Immunohistochemistry

C57BL/6 mice were anaesthetized with hypnorm/dormicum and perfused with 15 ml 0.9% NaCl (saline). Brain tissue was removed, snap-frozen in liquid nitrogen and stored at -80°C until further use. Brains were either horizontally or coronally cryo-sectioned in 8 μ m slices and mounted on Superfrost/Plus glass slides (Menzel-Gläser, Braunschweig, Germany). Selected slides that were representative for the different brain regions were used for immunohistochemical analysis. Sections were treated for 10 min with ice-cold acetone, dried, pre-incubated in horse serum for 10 min, and subsequently incubated for 60 min with a mixture of three α -PTPRR monoclonal antibodies (diluted culture supernatant of hybridoma clones 1E3 (1:4), 3E11 (1:4) and 6A6 (1:8)) or with α -PTPRR monoclonal antibody 5E4 (1:16) in PBS with 0.1% BSA. Similar sections were also incubated with STEP-absorbed α -SL serum. After several washes with PBS and incubation for 30 min with biotin-conjugated secondary antibody (Pierce) (1:250 in PBS), immunoreactivity was visualized using the Vectastain protocol (Vector laboratories, Burlingame, CA, USA). 3,3'-diaminobenzidine tetrahydrochloride (brown stain; Fig. 6, panels A-B) or 3-amino-9-ethyl-carbazole (red stain; Fig. 6, panels C-F) were used as substrate. Subsequently, sections were rinsed with water, incubated in 0.9% NaCl and 0.5% CuSO₄ for 5 min, and counterstained with haematoxylin for 3 min. Finally, sections were dehydrated with ethanol and xylene, embedded in Eukitt (Electron Microscopy Sciences, Fort Washington, PA, USA) and examined by light microscopy.

Immunofluorescence assay

Neuro-2a cells cultured on glass coverslips were transiently transfected with appropriate plasmid constructs as described above. After 24 hours the cells were washed with PBS, fixed for 10 min with 1% paraformaldehyde in PHEM buffer (60 mM Pipes, 25 mM Hepes, 10 mM EGTA, 2 mM MgCl₂, pH 6.9), and permeabilized using 0.1% saponin and 20 mM Glycine in PBS for 30 min. Subsequently, cells were incubated for 1h with a 1:200 dilution of α -SL

antiserum in SPBS (PBS + 0.1% saponine) at room temperature. Following three washes with SPBS, cells were incubated with FITC-conjugated goat-anti-rabbit IgG (10mg/ml; Jackson ImmunoResearch Laboratories, Inc., West Grove, PA, USA) (1:100 dilution in SPBS) at room temperature for 1h. Finally, after three washes with SPBS and methanol dehydration, cells were mounted on glass slides using Mowiol (Sigma) containing 2.5% sodium azide as anti-fading reagent. Images were examined and collected using confocal laser scanning microscopy (MRC 1024, Bio-Rad).

Results

Genomic structure of Ptprr

In order to make a full annotation of exonic sequences contained within the mouse gene *Ptprr*, we performed Blast searches using the PTPBR7, PTP-SL and PTPPBS γ cDNA entries as queries (Fig. 1). Gene contigs were encountered in commercial (Celera) and public databases. In the EnSEMBL Mouse Genome database (release 20.32b.1; mouse species C57BL/6J) a single 257251 bp stretch was identified that comprised the full annotation of all fourteen PTPBR7 exon sequences (Gene ID number ENSMUSG00000020151; Unigene cluster Mm.3771). Searches using PTP-SL and PTPPBS γ transcripts exclusively yielded hits within this very same genomic region, underscoring that the above transcripts all originate from the single-copy gene *Ptprr*. As proposed earlier (12), there is a single PTP-SL-specific exon in between PTPBR7 exons two and three, defining the PTP-SL-specific promoter to reside within the largest intron, intron 2, of *Ptprr*. For generating the PTP-SL specific transcript, this first PTP-SL exon is joined to PTPBR7 sequences in exons 3 to 14 through splicing. Thus, PTP-SL transcripts differ from PTPBR7 mRNAs in that sequences contained within *Ptprr* exons 1 and 2 (709 bases in total) are replaced by the 135 nucleotide PTP-SL-specific exon-derived sequence.

The unique 5' segment in the PTPPBS γ cDNAs (8) could be mapped in a 292 bp sequence stretch immediately upstream of *Ptprr* exon 5. Thus, *Ptprr* intron 4 also harbors an alternative promoter, this time giving rise to either PTPPBS γ ⁺ or PTPPBS γ ⁻ mRNAs depending on whether a small (117 nucleotide) intron is excised from the unique PTPPBS γ ⁺ leader sequence. To generate PTPPBS γ ⁻ transcripts, therefore, 175 nucleotides, derived from exonic sequences unique for both PTPPBS γ mRNA variants, are joined through splicing to sequences delivered by *Ptprr* exons 5 to 14. The complete *Ptprr* gene structure (schematically depicted in Fig. 1A) is summarized in Table 2, where reference is made to positions in the four different cDNAs. This gene annotation has also been deposited to the mouse genome database under TPA accession numbers BN000439 to BN000454.

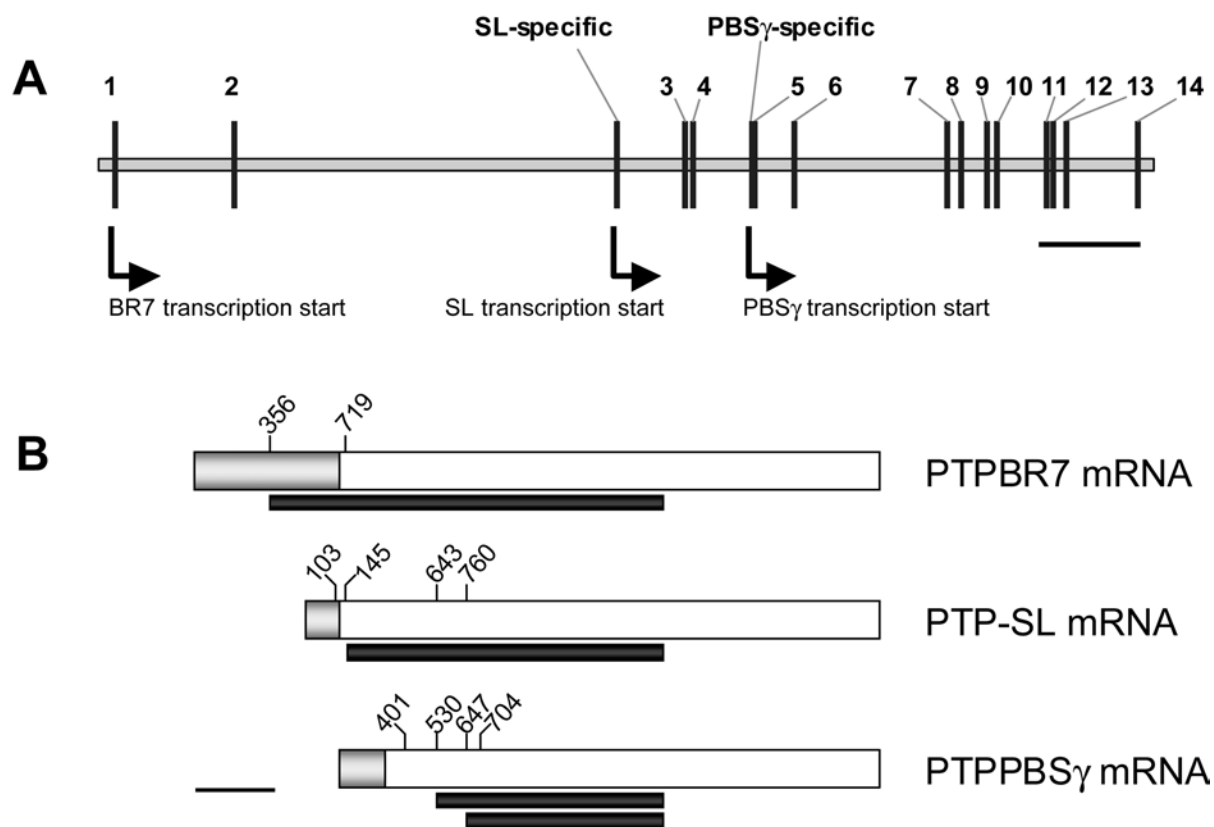


Fig. 1 Schematic representation of the *Ptprr* exon-intron structure and its major mRNA products.

In panel **A**, mouse genomic DNA is represented by the gray horizontal bar. Exons are depicted as vertical bars with exon number or name indicated above. Arrows symbolize the relative positions of the three distinct transcription start sites. The black horizontal bar, depicted on the right, indicates 25 kbp of DNA. Resulting *Ptprr* transcripts are depicted in panel **B** as thick horizontal boxes, with mRNA names indicated on the right. Transcript specific nucleotide sequences are indicated in light gray at the left end of the transcript. ORFs are depicted as dark gray horizontal bars. The numbers indicate the first nucleotide of potential start codons that were included in mutational analyses experiments (Fig. 4). Nucleotide numbers are based on PTPBR7, PTP-SL and PTPPBS γ + cDNA sequences (Acc.no's. D31898, BN000437 and BN000438, respectively). Bar on the left indicates 500 bp.

Table 2. *Ptprr* exon-intron boundaries

| Exon | Length (bp) | Starting position in cDNA | | | Acceptor splice site ^a | Donor splice site ^a |
|--------------------------|----------------|------------------------------|--------|-------------------|-----------------------------------|--------------------------------|
| | | PTPBR7 | PTP-SL | PTPPBS γ + | | |
| 1 | 413 | | | | TGCTGCAG/gttatgtcttgcgggg | |
| 2 | 296 | 414 | | | gattcctgtctctgtag/GTTGTTTT | |
| SL specific | 135 | | | | CCACACCG/gtaagagagcccatgg | |
| 3 | 114 | 710 | 136 | | ttcctctgtttccag/ACACTGCA | |
| 4 | 156 | 824 | 250 | | ggtgtgttctcactag/GAAAAGAA | |
| PBS γ specific | 292 | | | | GGCTCATT/gtaagagtttgcttt | |
| 5 | 111 | 980 | 406 | 293 | GGCTGAG/gtatgtccttgcatgc | |
| 6 | 269 | 1091 | 517 | 404 | GTTTGATG/gtaagtttgcttcttt | |
| 7 | 187 | 1360 | 786 | 673 | GTTTGATG/gtaagtttgcttcttt | |
| 8 | 85 | 1547 | 973 | 860 | CAGGACCG/gtaagagcctcaactg | |
| 9 | 80 | 1632 | 1058 | 945 | AATTCATG/gtgagcccgcctcttc | |
| 10 | 138 | 1712 | 1138 | 1025 | TTTGCAA/gtaagtttctcgagac | |
| 11 | 111 | 1850 | 1276 | 1163 | ATATTCGG/gtaagtaactatacat | |
| 12 | 158 | 1961 | 1387 | 1274 | AAAATGAG/gtatggagcttatccc | |
| 13 | 114 | 2119 | 1545 | 1432 | TCTTAAAG/gtaagatcgtgagctg | |
| 14 | 1197 | 2233 | 1659 | 1546 | CACTGCAG/gtaaggcggaaccga | |
| | | | | | GTAGACAG/gtacgtggaccggggg | |
| | | | | | aatctcttccatgcag/GGGTGGTA | |

^a The exonic and intronic sequences are indicated in uppercase and lowercase respectively.

Ptprr transcript expression patterns

Data supporting the differential use of the three distinct transcription start sites within mouse *Ptprr* have been obtained mainly by RNA *in situ* hybridization studies. The use of transcript-specific probes has revealed that PTPBR7 messengers appear during early embryogenesis in spinal ganglia and developing Purkinje cells. Postnatally, PTPBR7 is expressed throughout the brain but expression gradually ceases in maturing Purkinje cells and PTP-SL type transcripts take over (12). PTPPBS γ RNAs are quite prominent in the hippocampal region, cerebellar granular layer and in the gastrointestinal tract (9). Furthermore, during mouse embryo-fetal development of skeletal and intestinal systems the detected hybridization signals are believed to reflect PTPPBS γ - mRNA (8). Northern blot analyses, on the other hand, have thus far only been performed with probes that hybridize to all *Ptprr* transcript variants (9-11). Using such a pan-PTPRR cDNA probe on Northern blots of cerebral and cerebellar RNA samples, the large (4.1 kb) PTPBR7 transcript is detected in cerebellum and to a lesser extent in other brain areas, whereas the shorter PTP-SL (3.2 kb) or perhaps PTPPBS γ (predicted to be ~3kb) RNAs appear to be exclusively expressed in cerebellum (Figure 2A, upper panel).

To ascertain the identity of the obtained signals we analyzed RNA samples isolated from various mouse brain regions by Northern blot analysis, using PCR-generated probes that are specific for the unique 5' mRNA parts in the PTPBR7, PTP-SL and PTPPBS γ type transcripts. Indeed, weak hybridization signals that corresponded to the 4.1 kb transcript mentioned above were obtained in all samples with the PTPBR7-specific probe (data not shown). Use of the PTP-SL-specific probe revealed this shorter transcript to be exclusively expressed in cerebellum (Fig. 2A, lower panel). Although PTPPBS γ messengers are detectable in brain by *in situ* hybridization (9), no specific signal resulted upon using the PTPPBS γ -specific probe in Northern blot analysis (data not shown), indicating very low expression levels for these transcript variants.

To perform a more sensitive survey of the isoform-specific expression patterns in brain we used the same RNA samples in RT-PCR experiments (Fig. 2B). Primer sets were chosen in such a way that genomic DNA contaminations would not yield amplicons of the appropriate size. β -actin messenger amplification was used as control for RNA integrity and reverse transcriptase activity. Except for olfactory bulb, PTPPBS γ transcripts indeed were now detectable in the various brain regions. PTPBR7 mRNA was present in all brain tissues, including olfactory bulb (Fig. 2B), but was not detected in RNA samples from other mouse tissues (i.e. heart, lung, liver; data not shown). PTP-SL transcripts thus far had only been detected in cerebellum by *in situ* hybridization and Northern blot analysis (9,10). RT-PCR, however, also reveals PTP-SL messengers in midbrain, brainstem and cortex (Fig. 2B). Taken together, these RNA expression data demonstrate that in the mouse cerebrum the PTPBR7 promoter is responsible for the vast majority of *Ptprr* transcripts. In cerebellum about two-third of the transcripts arise from the PTP-SL promoter and the remaining one third is mainly of the PTPBR7 type (Fig. 2A, upper panel). Only trace amounts of PTPPBS γ mRNAs, not detectable on Northern blots, are present throughout the brain.

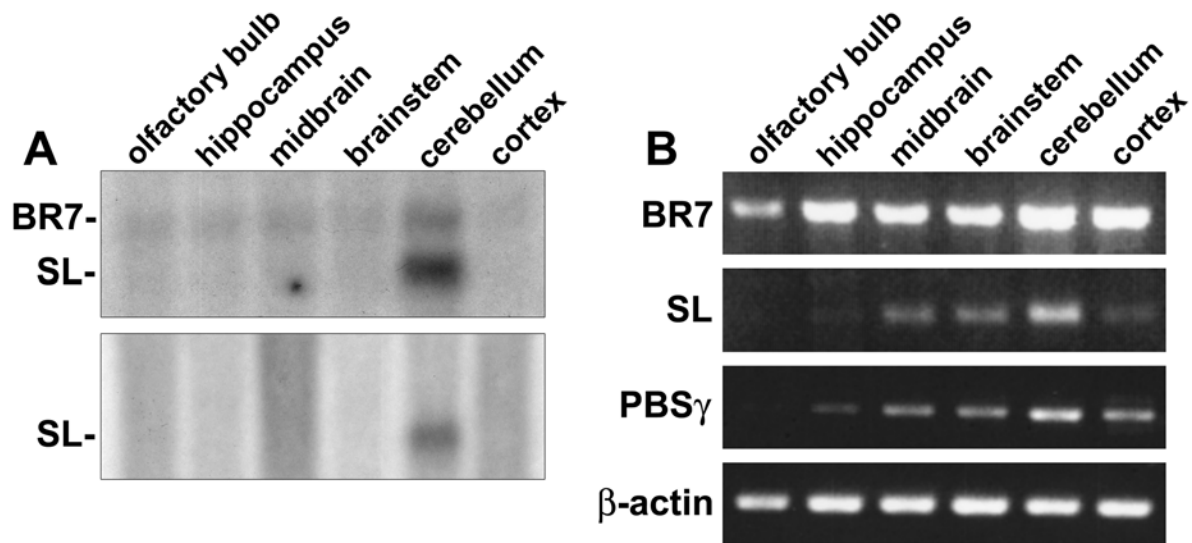


Fig. 2 Expression of *Ptprr* transcript variants in specific brain regions.

A, Northern blot analysis on RNA from different brain regions using full-length PTPBR7 cDNA (upper panel) or the unique PTP-SL 5' untranslated region (lower panel) as a probe. PTPBR7 mRNA is expressed in cerebellum and, to a lesser extent, in the other brain areas. PTP-SL messengers on the other hand are only detectable in cerebellum. PTPPBS γ type transcripts are below detection levels (data not shown). **B**, PTP-SL and PTPPBS γ mRNAs are detectable in total RNA isolated from several cerebral brain parts when using a sensitive transcript-specific RT-PCR assay. PTPBR7 transcripts were detected in all brain regions. Isoform-specific primer sets used were negative on mouse genomic DNA, and β -actin primers were included as positive controls.

Mapping of translation initiation sites in the Ptprr-derived mRNAs

Open reading frames encompassing 656, 549 and 412 codons in the PTPBR7, PTP-SL and PTPPBS γ cDNAs predict the synthesis of 74, 62 and 47 kDa mature proteins, respectively. For PTP-SL it has been suggested that not the first AUG of the major predicted open reading frame (ORF), but the following in-frame AUG codon is used for initiation of translation (10) leaving the exact size of the protein as yet unclear. Likewise, the translation start site used in both PTPPBS γ messenger isoforms (9) is enigmatic. To aid in the determination of the start codons, a pSG5-based full-length PTPPBS γ cDNA expression construct was generated and used, together with similar, existing constructs encoding PTPBR7 and PTP-SL (12), in transfection experiments. All three constructs resulted in multiple immunoreactive products in protein lysates from transiently transfected Neuro-2a cells upon Western blot analysis

using α -SL antiserum (Fig. 3, left three lanes), whereas no signal was obtained for lysates of mock transfected cells (data not shown). For PTPBR7, two immunoreactive bands, around 72 and 65 kDa, respectively, are observed. Expression of PTP-SL cDNA revealed a doublet band around 60 kDa and two additional signals at 42 and 37 kDa. Surprisingly, the latter two immunoreactive bands also appear as the main products using the PTPPBS γ expression construct. These data imply posttranslational modifications, including processing through protease cleavage, and / or the use of alternative AUG start codons.

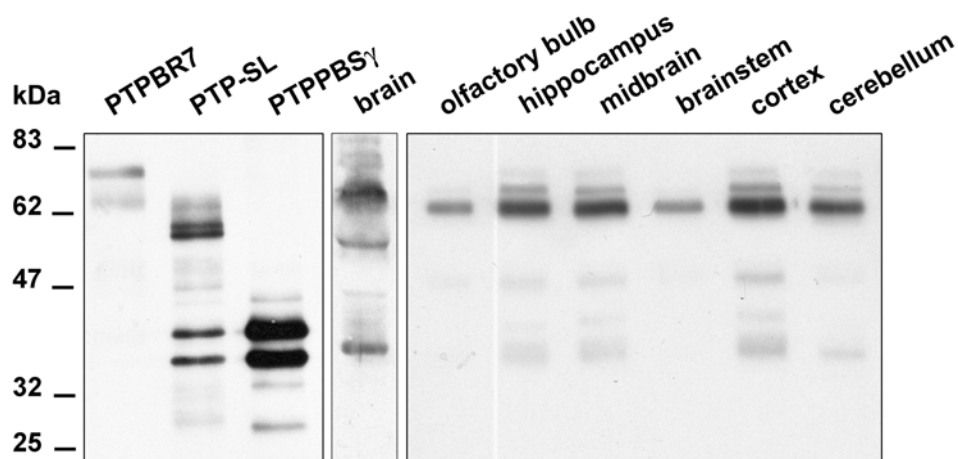


Fig. 3 The three different *Ptprr* transcripts give rise to multiple PTPRR isoforms.

Left panel: Neuro-2a cells were transiently transfected with pSG5/PTPBR7-FL, pSG5/PTP-SL-FL or pSG5/PTPPBS γ -FL expression plasmids. Lysates were used for Western blot analysis exploiting the rabbit α -SL antiserum that is immunoreactive against the catalytic portion in PTPBR7, PTP-SL and PTPPBS γ . Middle panel: Western blot analysis of α -SL immunoreactive proteins detected in mouse total brain lysates. The rightmost panel shows monoclonal antibody 6A6 immunoprecipitates from different brain regions, visualized on blot using STEP-absorbed α -SL that is immunoreactive towards all PTPRR proteins. Please note that the polyvalent antiserum may cross-react with the nearest homologue, STEP, on immunoblots but not in immunoprecipitation experiments. Molecular mass markers (in kDa) are indicated on the left.

To allow unequivocal mapping of the AUG start codons used in the various transcripts, we performed site directed mutagenesis on the PTPBR7, PTP-SL and PTPPBS γ expression constructs. Mutation of the ATG triplet in PTPBR7 cDNA, at nucleotide position 356-358 (BR7-356), into an isoleucine-encoding one led to a complete absence of PTPBR7 expression in transiently transfected Neuro-2a cells (Fig. 4A). A similar mutation at the next in-frame ATG triplet (BR7-719) had no effect at all, indicating that in the PTPBR7 messenger only the start codon at position 356-358 is used and leaving that the 65 kDa species must be derived from a 72 kDa precursor through posttranslational processing. In the PTP-SL expression construct mutations were incorporated such that either one of the suggested two candidate translation start codons (position 103-105 and 145-147 in PTP-SL cDNA; mutants SL-103 and SL-145, respectively) is changed into an isoleucine codon. Upon transfection, these mutants show that not the first but indeed the second AUG codon in the PTP-SL encoding ORF is used for translation initiation (Fig. 4B). The resulting protein product subsequently undergoes an as yet uncharacterized posttranslational modification resulting in a doublet immunoreactive band at 60 kDa. Remarkably, the production of the immunoreactive 42 and 37 kDa proteins are not influenced by these mutations.

Site directed mutagenesis of ATG triplets within the PTPPBS γ expression construct clearly showed that in the PTP reading frame not the first (position 401-403; γ -401) but rather the second (pos. 530-532; γ -530) as well as the third (pos. 647-649; γ -647) AUG codon is used efficiently for translation initiation (Fig. 4C), thus resulting in two PTPPBS γ variants that differ in their N-terminus. Elimination of both of these AUG codons (mutant γ -530/647) totally blocked the synthesis of the PTPPBS γ isoforms. In view of the similarity in electrophoretic mobility of the two 42 and 37 kDa PTPPBS γ species and the two low-molecular weight entities in PTP-SL expressing lysates, we wondered whether the downstream AUG codons that correspond with the PTPPBS γ translation start sites are also being used in PTP-SL messengers for initiation of protein synthesis. Mutation of these ATG codons (at positions 643-645 and 760-762) in PTP-SL cDNA indeed resulted in the elimination of the 42 and 37 kDa protein bands without affecting the production of the 60 kDa doublet (Fig. 4B). These data demonstrate that two downstream AUG codons in PTP-SL mRNA serve as alternative translation initiation sites and result in protein isoforms indistinguishable from the 42 and 37 kDa PTPPBS γ isoforms.

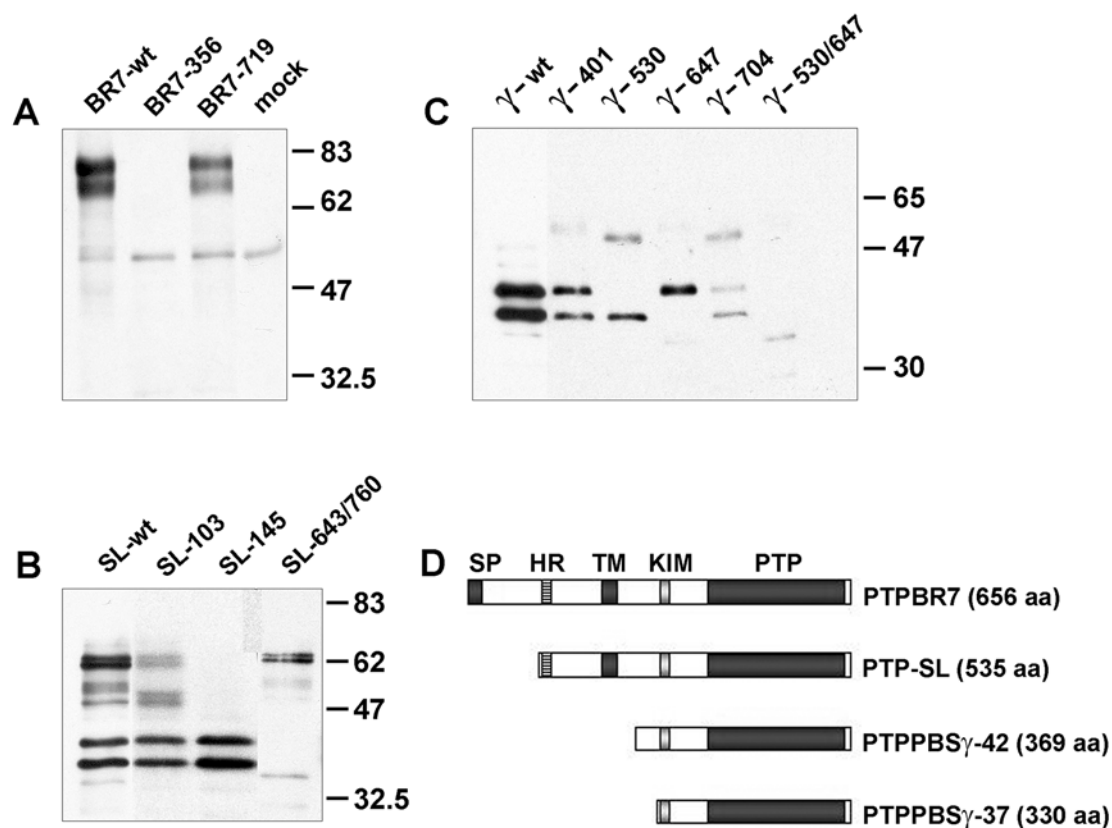


Fig. 4 Determination of the sites of translation initiation in the *Ptprr*-derived transcripts.

Neuro-2a cells were transiently transfected with plasmids containing wild type or mutated full-length PTPBR7 (BR7), PTP-SL (SL) and PTPPBS γ (γ) cDNAs. Nomenclature of mutants (indicated above the lane) corresponds to the position of the first nucleotide in the ATG codon that was altered by site-directed mutagenesis within the respective isoform cDNA (Table 1). Proteins produced were immunoprecipitated using α -PTPRR monoclonal antibody 6A6 and analyzed on Western blots using the α -SL antiserum. **A**, Mutating the ATG triplet at 356 in PTPBR7 cDNA results in complete loss of protein expression (BR7-356), whereas the BR7-719 mutant displays unaltered synthesis. Mock transfected cells revealed a 50 kDa background signal. Note the doublet band for PTPBR7, indicative for posttranslational modifications. Molecular mass markers are indicated (in kDa) on the right. **B**, Similar experiments on PTP-SL cDNA show that mutations at positions 145, 643 and 760 interfere with synthesis of the 60, 42 and 37 kDa immunoreactive bands, respectively. Note the doublet band for PTP-SL around 60 kDa that is reminiscent of posttranslational modification. **C**, Production of the 42 and 37 kDa PTPPBS γ isoforms is abrogated when ATG triplets at positions γ -530 and γ -647 are mutated, respectively. When these AUG mutations are combined (γ -530/647 mutant) both prominent PTPPBS γ bands disappear. The γ -401 and γ -704 mutants have no effects. **D**, Schematic diagrams of the *Ptprr* protein isoforms that result from translation of the corresponding full length messengers in mouse Neuro-2a cells as determined in this study. Signal peptide (SP), hydrophobic region (HR), transmembrane segment (TM), kinase interacting motif (33) and catalytic phosphotyrosine phosphatase domain (PTP) are indicated in the appropriate isoforms.

The resulting four different PTPRR isoforms that are encoded by the gene *Ptprr* are schematically depicted in figure 4D. To investigate whether this catalogue of PTPRR isoforms can actually be detected in brain tissue lysates, we performed Western blot analysis of mouse total brain lysate. Three major immunoreactive proteins, with sizes of approximately 70, 60 and 40 kDa, are apparent using the rabbit α -SL serum (Fig. 3, middle panel). The two upper major bands correspond with the ones seen for PTPBR7 and PTP-SL in the *in vitro* studies, especially when taking into account possible *in vivo* posttranslational modifications as witnessed by the occurrence of double bands for these isoforms in figure 4 (e.g. BR7-719 and SL-643/760). The smaller, 40 kDa band in brain may correspond to a PTPPBS γ isoform.

PTPRR protein localization in mouse brain

To aid in the study of the *in situ* localization of PTPRR proteins in mouse brain tissue, monoclonal antibodies against the common part in all four isoforms were raised. To this end, the GST-SL fusion protein encompassing the PTP domain-containing carboxyl terminal 294 residues (10) was used to immunize mice. Absence of unique amino acid sequences in PTP-SL and PTPPBS γ precluded the generation of PTPRR antibodies that would have been specific for either one of these isoforms. Obtained hybridomas were screened by ELISA using a His-tagged PTP-SL fragment as antigen to eliminate GST-reactive hybridomas. Eight different clones were obtained that secreted antibodies reacting with Neuro-2a cells ectopically expressing PTP-SL in Western analysis (Fig. 5A) and immunofluorescence assays, and remaining negative on mock-transfected cells. Various deletion mutants of the GST-SL fusion protein were exploited to map the epitope-containing region for these monoclonal antibodies. All were found to be immunoreactive towards amino acids 227-292 in PTP-SL (aa numbering according to TPA accession number BN00037), spanning the region just downstream of the KIM domain present in all four PTPRR isoforms.

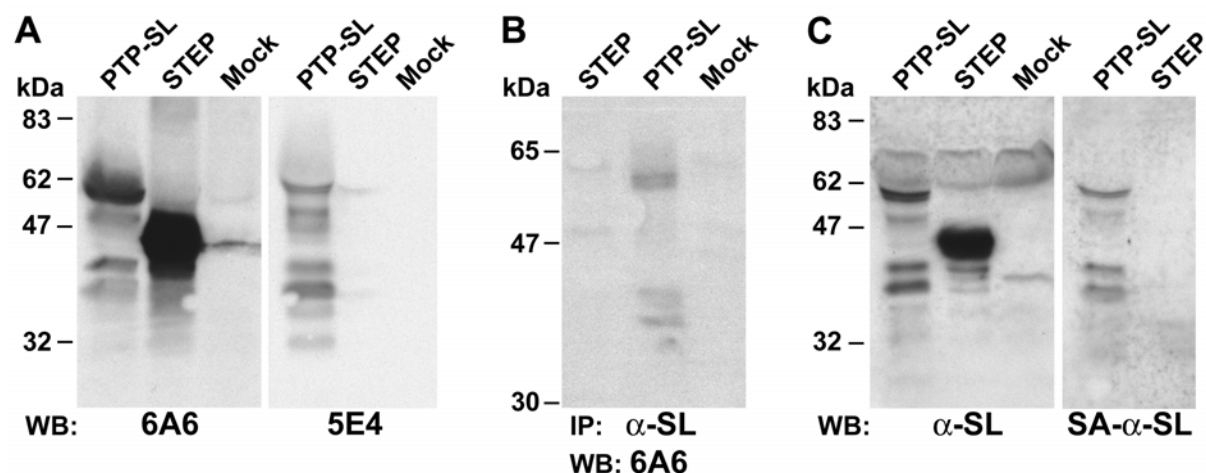


Fig. 5 Immunoreactivity of monoclonal antibodies and polyvalent antiserum directed against the common part in PTPRR protein isoforms.

Neuro-2a cells were transiently transfected with PTP-SL or STEP expression plasmids, as indicated above the lanes. Mock transfected cells were included as negative controls. Lysates were directly subjected to Western blot analysis using (A) monoclonal antibodies (6A6, 5E4) or (C) polyvalent antiserum (α -SL, STEP-absorbed SA- α -SL) directed against the PTPRR PTP moiety. The other six PTPRR monoclonal antibodies that were obtained displayed reactivities similar to 6A6. Proteins were also immunoprecipitated from transfected cell lysates using the different antibodies, and analyzed on Western blots. All eight monoclonal antibodies demonstrated specificities in immunoprecipitation applications that are identical to that of the polyvalent α -SL antiserum shown in panel B. Molecular mass markers (kDa) are indicated on the left.

On the basis of signal intensities on mouse tissue sections three monoclonal antibodies (designated 6A6, 1E3 and 3E11) were selected for use in immunohistochemical assays. Mouse brain horizontal and coronal sections were incubated with a mixture of these anti-PTPRR monoclonal antibodies and specific brain regions revealed immunoreactivity. Clear staining was observed in the Purkinje cells of the cerebellum (Fig. 6A), in both the neuropil and the neurons of the striatum (Fig. 6B). Close to the striatum the major Islands of Calleja and the ventral pallidum also stain positive, and furthermore the hippocampal CA2/CA3 region, subthalamic nucleus, substantia nigra area, and large neurons between the medial and dorsal lateral septum stain very bright (data not shown). Of the five remaining

monoclonal antibodies all except one (5E4) gave similar but much weaker staining patterns (data not shown). To our surprise monoclonal antibody 5E4 firmly stained Purkinje cells of the cerebellum (Fig. 6C), but remained negative in all other brain regions, most notably the striatum (Fig. 6D). This suggested to us a possible cross-reactivity of all other antibodies with striatum-enriched phosphatase (STEP), which is 45% identical in the PTP domain. Indeed, exploiting bacterial and mammalian cells ectopically expressing PTP-SL or STEP proteins, we found that all monoclonal antibodies, except 5E4, as well as the previously used polyvalent α -SL antiserum recognized STEP, both on immunoblots (Fig. 5A) and in immunofluorescence assays (data not shown), while remaining negative on mock-transfected cells. In immunoprecipitation experiments, however, all antibodies were specific for PTP-SL (Fig. 5B). We could successfully remove the STEP cross-reactivity from the polyvalent α -SL serum by passing it over glutathion-sepharose-bound GST-STEP fusion proteins (Fig. 5C), and the resulting PTPRR-specific rabbit serum performed comparable to 5E4 on brain sections (Fig. 6 E-F). Taken together these data show that PTPRR protein isoforms are only present at detectable levels in the cerebellar Purkinje cells, and that previously observed staining patterns in other brain regions (12,18,19) may reflect cross-reactivity with STEP proteins.

The possible cross-reactivity of the α -SL serum with the STEP family of phosphatases made us re-evaluate the immunoblot analysis of PTPRR protein expression in different brain areas. To maximise sensitivity and to eliminate STEP cross-reactivity, we performed immunoprecipitations followed by Western blot analysis on protein lysates of mouse olfactory bulb, hippocampus, midbrain, brainstem, cerebellum and cortex brain areas using monoclonal antibodies and STEP-absorbed α -SL serum. One major immunoreactive band of approximately 65 kDa was seen in all lysates tested (Fig. 3, right panel), which corresponds well with the lower protein band seen for PTPBR7 in the in vitro studies. The minor bands at 70 and 75 kDa detected in most brain parts probably represent a processing intermediate and the full-length PTPBR7 protein, respectively. No other potential in-frame AUG start sites could account for these alternative sizes. Reflecting the lower and more restricted expression of PTP-SL and PTPPBS γ mRNAs, specific signals for these protein isoforms are not apparent in the immunoprecipitation experiment, although the lower band may correspond with PTPPBS γ -37.

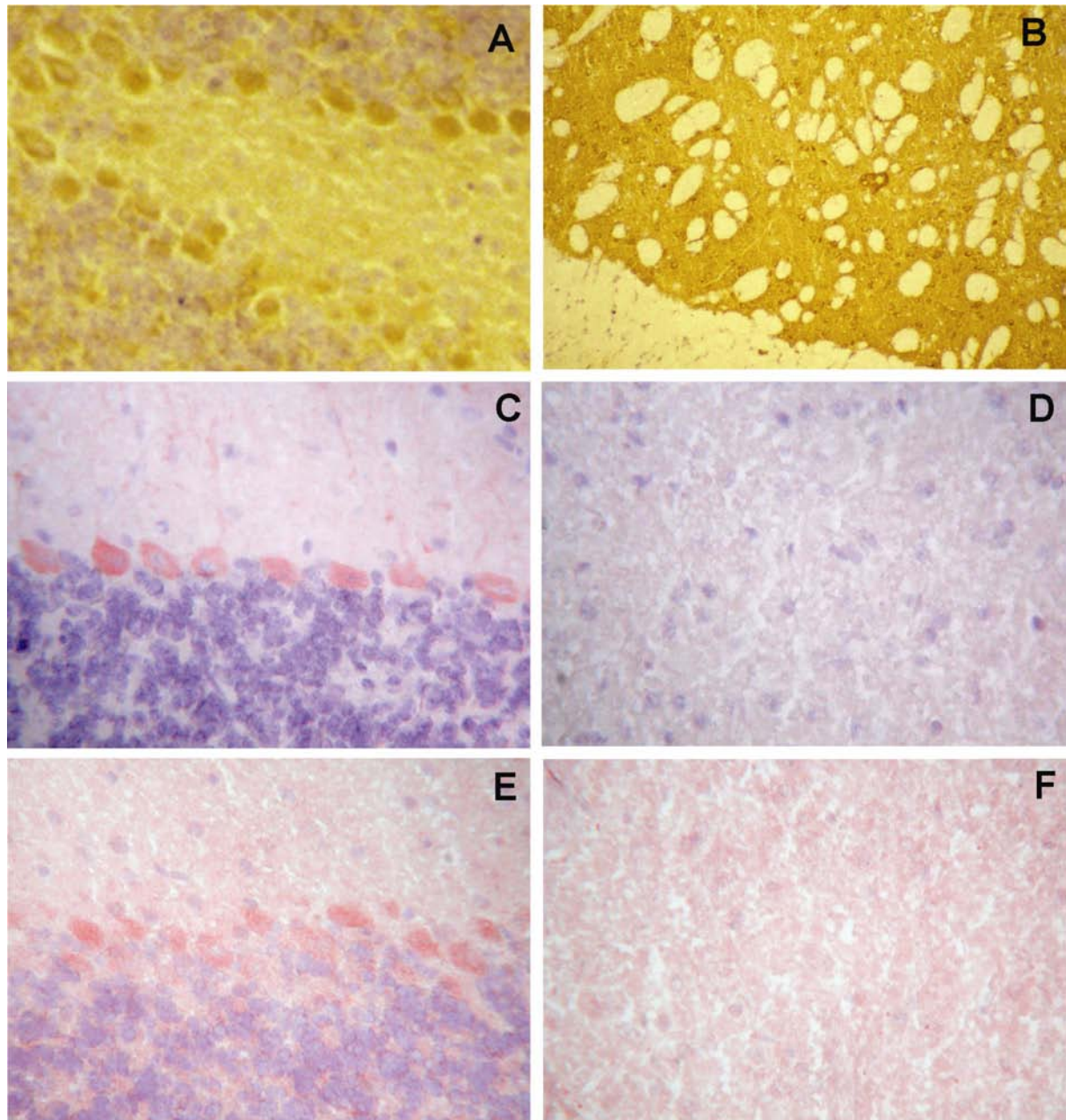


Fig. 6 Immunolocalization of PTPRR protein in mouse brain.

Brain cryosections were stained using a mixture of three different monoclonal antibodies (1E3, 3E11 and 6A6) immunoreactive towards the common part in PTPRR isoforms and that cross-react with STEP. Positive staining is observed in the Purkinje cells of the cerebellum (A), both the neurons and neuropil of the striatum (B). Similar sections were incubated with monoclonal antibody 5E4, which does not cross-react with STEP. Exclusively Purkinje cell staining was observed (C), and no signal could be detected in the striatum (D). The STEP-absorbed α -SL serum also shows a clear Purkinje cell staining (E) and does not react with striatum (F), suggesting that staining of the striatum (B) reflects STEP immunoreactivity.

PTPRR isoforms comprise cell surface, vesicle-associated and cytosolic variants

The presence of hydrophobic protein domains in the PTPBR7 and PTP-SL isoforms has led to the prediction that they may represent receptor-type PTPs (Fig. 4D). Indeed, for PTPBR7 a functional signal peptide and a transmembrane segment have been mapped (11,12). The N-terminal hydrophobic segment in PTP-SL, however, is unable to exert a signal peptide ‘start transfer’ effect (12) and, consequently, the membrane topology of PTP-SL remains elusive. The construction of the PTPPBS γ expression plasmid now enabled us for the first time to make a comparison of the subcellular localizations for the PTPBR7, PTP-SL and PTPPBS γ PTPRR protein isoforms. Transiently transfected Neuro-2a cells were immunostained using the rabbit α -SL antiserum and analyzed by confocal laser scanning microscopy (Fig. 7). The three different PTPRR expression constructs resulted in markedly different subcellular localization patterns. As described before, PTPBR7 and PTP-SL are localized at the Golgi apparatus and at late endosomal vesicles, additionally PTPBR7 is also found at the cell membrane (12,18,19). In contrast, the 42 and 37 kDa PTPPBS γ variants are genuine cytosolic proteins that are excluded from the nucleus. Similar results were obtained when other cell types, e.g. COS-1 cells, were used (data not shown).

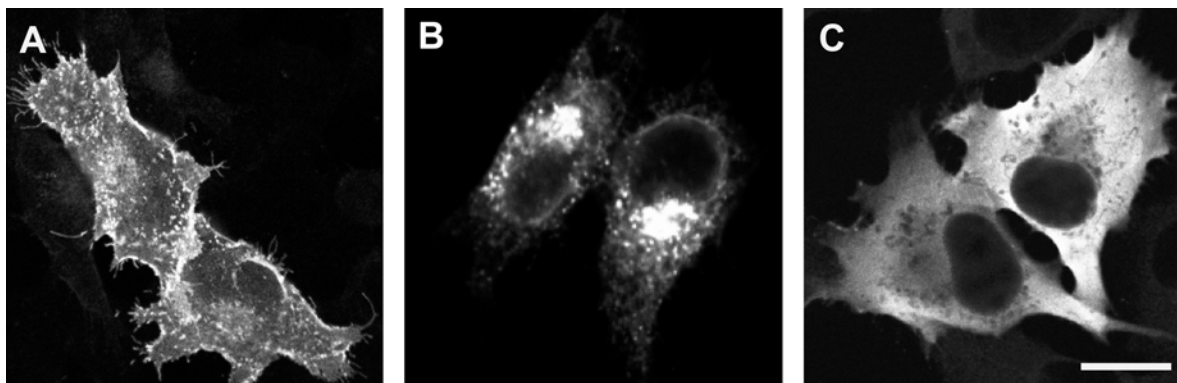


Fig. 7 PTPRR isoforms differ in their subcellular localization.

Neuro-2a cells, transiently transfected with expression plasmids encoding PTPBR7 (A), PTP-SL (B) or PTPPBS γ (C), were stained using α -SL antiserum and analyzed by confocal laser scanning microscopy. Distinct localization patterns for each isoform type can be discerned. PTPBR7 displays a predominant cell surface staining, but also at the Golgi and vesicles throughout the cytoplasm (A). PTP-SL resides at the Golgi apparatus and on vesicles (B). The PTPPBS γ 42 and 37 kDa proteins diffusely stain the cytosol (C). Bar indicates 10 μ m.

Discussion

Here we have characterized the full collection of transcript and protein isoforms that are derived from the mouse gene *Ptprr*. Three different alternative promoters (Fig. 1) were found to give rise to messengers encoding PTPBR7, PTP-SL and two PTPPBS γ protein variants (Figs. 3,4) that differ in their brain expression (Fig. 2) and subcellular localization (Fig. 7) patterns. Results from the human genome project have demonstrated that the phenotypic complexity of higher organisms is achieved only in part by higher gene numbers and that mechanisms that result in the production of multiple protein isoforms from a single gene locus contribute substantially to this (20). A well-studied mechanism to create diversity at the RNA level is alternative splicing, now thought to occur in some two-third of the mammalian primary transcripts (21). Indeed, two *Ptprr* transcript variants arise through an alternative splicing event: PTPPBS γ ⁺ and PTPPBS γ ⁻ (8). However, they contain identical open reading frames and thus do not contribute differentially to the collection of PTPRR protein isoforms. The PTPPBS γ splice variants only differ in their 5' non-translated region due to alternative removal of a 117 nucleotide intronic sequence that according to our genomic analysis spans positions 176-292, rather than 174-290 as reported earlier (9), in the PTPPBS γ ⁺ cDNA.

An alternative, well-studied means to produce multiple protein isoforms from a single gene is through the use of alternative translation initiation sites (22). Also this strategy is used in mouse to create isoform diversity within the *Ptprr* protein products. From the large open reading frame present in PTPPBS γ mRNA variants it is not the first AUG codon that is used as translation start, but instead the second and the third methionine codon (Fig. 4C). Likewise, the first AUG codon in the PTP-SL reading frame is ignored by the ribosome, and rather the one at position 145-147 and to a lesser extend those at 643-645 and 760-762 are used to generate 60, 42 and 37 kDa isoforms, respectively. This translation initiation site choice appears to be depending on the expression system used. COS1 cells transiently transfected with the PTP-SL expression construct show predominance of the start at position 145-147, whereas PC12 cells mainly produce the isoforms known as PTPPBS γ by using the alternative start codons at positions 643-645 and 760-762 (unpublished data).

The pioneering work of Marilyn Kozak has provided detailed knowledge on the translation initiation behavior of mammalian ribosomes. Although surrounding RNA

secondary structure elements are certainly of influence as well, the optimal context for start codon recognition has been determined as GCCRGaugG, with the most important nucleotide types in bold (23). Less optimal start codons may cause ‘leaky scanning’ resulting in translation initiation on further downstream AUGs. Alternatively, direct entry of ribosomes at internal AUG sites in the mRNA might occur (24). Finally, ‘reinitiation’ by ribosomes after translation of small upstream ORFs could explain alternative start site choices (23). Since certain initiation factors dissociate only gradually from the ribosome during the elongation phase, they enable the 40S subunit to resume scanning for AUG start sites after terminating from such very small ORFs. In the case of PTP-SL and PTPPB γ mRNAs indeed very small upstream ORFs near or overlapping the predicted start sites are present. We exclude cryptic promoters or splice sites in the pSG5-based expression constructs as the cause for the synthesis of 60, 42 and 37 kDa PTPRR proteins since identical staining patterns were obtained using pRK5 as vector (data not shown) or when performing *in vitro* translation experiments (9,10).

Yet another key mechanism for generating organismal complexity is alternative use of promoters (25). Alternative promoters may display differences in expression level, tissue specificity or developmental activity. Furthermore, the resulting alternative 5’ mRNA ends may impose differences in mRNA stability and translatability or, most importantly, in the encoded proteins. The three alternative promoters present in the *Ptprr* gene create differences both in expression pattern as well as in coding potential of the distinct mRNA types. PTPBR7 is a receptor-type PTP that is expressed throughout the brain (11). PTP-SL is located at perinuclear vesicular structures (18) and during postnatal Purkinje cell maturation PTP-SL specific transcripts replace the PTPBR7 messenger (12), a developmental expression pattern that is conserved in rat (26). The third, cytosolic protein isoform PTPPB γ is, in contrast to the other two, not only expressed in brain but also during cartilaginous skeleton development and in the gastrointestinal tract (8).

The orthologous human gene, *PTPRR*, has a very similar exon-intron build-up (27) and also encodes multiple isoforms (9). Human PTPPB α and PTPPB γ correspond to mouse PTPBR7 and PTPPB γ , respectively, and expressed sequence tag BQ957212 may represent human PTP-SL. Interestingly, in human tissues yet another isoform has been identified. This PTPPB δ cDNA has a unique 5’ stretch of 23 nucleotides, containing an ATG sequence, which replaces the first 799 basepairs of PTPPB α and will result in a

protein with 3 unique amino acids (9). We could map the human PTPPBS δ -specific stretch in *PTPRR* just 2 nucleotides upstream of the PTPPBS γ -specific exon, meaning that the PTPPBS δ and PTPPBS γ promoters are arranged in tandem. In mouse, no PTPPBS δ -like isoform has been described so far. We could locate a putative PTPPBS δ -like 5' leader sequence (sharing 83% sequence homology) just in front of, and partly overlapping with, the first mouse PTPPBS γ exon, nicely coinciding with the position of the human PTPPBS δ promoter. However, cDNAs containing the implicated mouse genomic segment could not be identified in the databases and even if a mouse PTPPBS δ -type transcript is generated this will not give rise to a mouse PTPPBS δ protein since the human PTPPBS δ ATG start codon reads GTG in mouse.

To monitor PTPRR protein expression *in situ*, we raised monoclonal antibodies against the PTP part that is present in all isoforms. Delineation of protein expression patterns for individual PTPRR isoforms is hampered by the absence of unique sequence stretches in the PTP-SL and 42 and 37 kDa PTPPBS γ proteins. Furthermore, we stumbled upon the finding that a polyvalent antiserum and seven out of eight monoclonal antibodies directed against the common part in the PTPRR isoforms cross-reacted with STEP, that is only 45% identical in its catalytic domain (Fig. 5). Therefore, our previous immunohistochemical data, showing expression in Purkinje cells of the cerebellum, striatal neurons, hippocampal CA2/CA3 region and brain cortex (12,18) should be reconciled. Our present survey by immunoprecipitation and Western blot analysis (Fig. 3) now reveals that PTPRR isoforms, most notably of the PTPBR7 type, are present at low levels in various brain regions but by immunohistochemistry are only detectable in cerebellar Purkinje cells (Fig. 6). The apparent discrepancy between immunoprecipitation and Western blot experiments may be explained in several ways but most likely is due to low sensitivity and limited antigen accessibility. Furthermore, mRNA and protein stabilities are crucial parameters for the ultimate detection levels.

On the basis of the initial mapping of *Ptprr* on chromosome 8 (28) and the conspicuous PTPBR7 to PTP-SL isoform switch during postnatal Purkinje cell development we have considered *Ptprr* a candidate gene for the recessive neurological mouse mutation *nr* (nervous) (12). During the fourth postnatal week 90% of the cerebellar Purkinje cells in *nr* mutant mice start to degenerate and, as a consequence, adult *nr* mice display ataxia and poor motherhood (29). We have PCR amplified and sequenced all *Ptprr* exonic regions in *nr* mice

but no differences were found when compared to wild type controls (data not shown). Furthermore, normal levels and sizes of PTPRR transcripts and proteins were detectable in *nr* mice. Meanwhile, the Mouse Genome Project has revealed that *Ptprr* is located on chromosome 10 rather than 8 (30). Indeed, using a *Ptprr* containing genomic clone from the consortium, we could confirm the chromosome 10 location by fluorescence *in situ* hybridization (data not shown). Obviously, a chimeric genomic clone compromised our original mapping result, and the above eliminates *Ptprr* as *nr* candidate.

Taken together, through the use of three alternative promoters, a single alternative splicing event and alternative use of AUG start codons, the mouse gene *Ptprr* produces four different PTPRR mRNA and protein isoforms. Although the PTPRR isoforms occupy different niches in the cell (Fig. 7), they all have a C-terminal part in common that contains in addition to the catalytic PTP domain a so-called KIM (Kinase Interaction Motif) sequence that allows them to interact with MAP kinases (13,31). Intriguingly, the spatio-temporal regulation of MAP kinase activation is a crucial determinant in cell signaling as demonstrated in the paradigm example of PC12 cell response to growth factor stimulation (32). It is tempting to speculate that the various PTPRR isoforms perform distinct tasks in determining signaling specificity, having PTPBR7 counteracting MAP kinases at the cell surface, with PTP-SL being active during growth factor receptor endocytosis, and PTPPBS γ variants in keeping cytosolic MAP kinases unphosphorylated. Clearly, elucidation of the cell biological impact of the multiple *Ptprr* gene products awaits further experiments.

Acknowledgements

We thank Ad Geurts van Kessel and Gerard Merkx for performing FISH experiments, C.E.E.M. van der Zee for help with mouse brain histological analyses, and Rafael Pulido (Valencia, Spain) for providing STEP expression constructs. R.G.S.C. and W.H. are members of the European TMR Network on Neuronal Protein Tyrosine Phosphatases. This work is financed by grants from the Nijmegen University Medical Center (grant number V.089942 to J.F. and W.H.) and the European Community Research Fund (Research Training Network grant number CT2000-00085).

References

1. Gurd, J. W. (1997) *Neurochem. Int.* **31**, 635-649
2. Hunter, T. (1998) *Harvey Lect.* **94**, 81-119
3. Purcell, A. L., and Carew, T. J. (2003) *Trends Neurosci.* **26**, 625-630
4. Andersen, J. N., Mortensen, O. H., Peters, G. H., Drake, P. G., Iversen, L. F., Olsen, O. H., Jansen, P. G., Andersen, H. S., Tonks, N. K., and Moller, N. P. (2001) *Mol. Cell Biol.* **21**, 7117-7136
5. Bult, A., Zhao, F., Dirkx Jr, R., Sharma, E., Lukacsi, E., Solimena, M., Naegele, J. R., and Lombroso, P. J. (1996) *J. Neurosci.* **16**, 7821-7831
6. Bult, A., Zhao, F., Dirkx, R., Jr., Raghunathan, A., Solimena, M., and Lombroso, P. J. (1997) *Eur. J. Cell Biol.* **72**, 337-344
7. Gil-Henn, H., Volohonsky, G., Toledano-Katchalski, H., Gandre, S., and Elson, A. (2000) *Oncogene* **19**, 4375-4384
8. Augustine, K. A., Rossi, R. M., Silbiger, S. M., Bucay, N., Duryea, D., Marshall, W. S., and Medlock, E. S. (2000) *Int. J. Dev. Biol.* **44**, 361-371
9. Augustine, K. A., Silbiger, S. M., Bucay, N., Ulias, L., Boynton, A., Trebasky, L. D., and Medlock, E. S. (2000) *Anat. Rec.* **258**, 221-234
10. Hendriks, W., Schepens, J., Brugman, C., Zeeuwen, P., and Wieringa, B. (1995) *Biochem. J.* **305**, 499-504
11. Ogata, M., Sawada, M., Fujino, Y., and Hamaoka, T. (1995) *J. Biol. Chem.* **270**, 2337-2343
12. van den Maagdenberg, A. M. J. M., Bachner, D., Schepens, J. T. G., Peters, W., Fransen, J. A. M., Wieringa, B., and Hendriks, W. J. A. J. (1999) *Eur. J. Neurosci.* **11**, 3832-3844
13. Pulido, R., Zuñiga, A., and Ullrich, A. (1998) *EMBO J.* **17**, 7337-7350
14. Walma, T., Spronk, C. A., Tessari, M., Aelen, J., Schepens, J., Hendriks, W., and Vuister, G. W. (2002) *J. Mol. Biol.* **316**, 1101-1110
15. Peterson, G. L. (1977) *Anal. Biochem.* **83**, 346-356
16. Sambrook, J., Fritsch, E. F., and Maniatis, T. (1989) *Cold Spring Harbor Laboratory, Cold Spring Harbor, NY*
17. Church, G. M., and Gilbert, W. (1984) *Proc. Natl. Acad. Sci. USA* **81**, 1991-1995
18. Dilaver, G., Schepens, J., van den Maagdenberg, A., Wijers, M., Pepers, B., Fransen, J., and Hendriks, W. (2003) *Histochem. Cell Biol.* **119**, 1-13
19. Ogata, M., Oh-hora, M., Kosugi, A., and Hamaoka, T. (1999) *Biochem. Biophys. Res. Commun.* **256**, 52-56
20. International Human Genome Consortium. (2001) *Nature* **409**, 860-921
21. Boue, S., Letunic, I., and Bork, P. (2003) *Bioessays* **25**, 1031-1034
22. Kozak, M. (1999) *Gene* **234**, 187-208
23. Kozak, M. (2002) *Gene* **299**, 1-34
24. Kozak, M. (2003) *Gene* **318**, 1-23

Chapter 3

25. Landry, J.-R., Mager, D., and Wilhelm, B. (2003) *Trends Genet.* **19**, 640-648
26. Watanabe, Y., Shiozuka, K., Ikeda, T., Hoshi, N., Suzuki, T., Hashimoto, S., and Kawashima, H. (1998) *Mol. Brain Res.* **58**, 83-94
27. Bektas, A., Hughes, J. N., Warram, J. H., Krolewski, A. S., and Doria, A. (2001) *Diabetes* **50**, 204-208
28. van den Maagdenberg, A. M. J. M., Schepens, J. T. G., Schepens, M. T. M., Merkx, G. F., Darroudi, F., Wieringa, B., Geurts van Kessel, A., and Hendriks, W. J. A. J. (1999) *Cytogenet. Cell. Genet.* **84**, 243-244
29. Sidman, R. L., and Green, M. C. (1970) in *Les Mutants Pathologiques Chez l'Animal. Leur Intérêt pour la Recherche Biomedicale* (Sabourdy, M., ed), pp. 69-79, Editions du Centre National de la Recherche Scientifique, Paris
30. Mouse Genome Sequencing Consortium. (2002) *Nature* **420**, 520-562
31. Zuñiga, A., Torres, J., Ubeda, J., and Pulido, R. (1999) *J. Biol. Chem.* **274**, 21900-21907
32. Marshall, C. J. (1995) *Cell* **80**, 179-185
33. Kim, W. T., Chang, S., Daniell, L., Cremona, O., Di Paolo, G., and De Camilli, P. (2002) *Proc. Natl. Acad. Sci. USA* **99**, 17143-17184

Chapter 4

Proteolytic shedding of the brain-specific receptor-type protein tyrosine phosphatase PTPBR7

Gönül Dilaver, Rinske van de Vorstenbosch, Céline Tárrega[¶], Pablo Ríos[¶],
Rafael Pulido[¶], Karlijn van Aerde[§], Jack Fransen, and Wiljan Hendriks

From the [¶]Instituto de Investigaciones Citológicas, Amadeo de Saboya 4, Valencia 46010,
Spain, and the [§]Department of Experimental Neurophysiology, Centre for Neurogenomics
and Cognitive Research, Vrije Universiteit Amsterdam, De Boelelaan 1087, 1081 HV
Amsterdam, The Netherlands.

Submitted

Summary

The single-copy mouse gene *Ptprr* gives rise to different protein tyrosine phosphate isoforms in neuronal cells through the use of distinct promoters, alternative splicing and multiple translation initiation sites. In the current study, we examined the array of posttranslational modifications that are imposed upon PTPRR protein products PTPBR7, PTP-SL, PTPPBS γ -42 and PTPPBS γ -37, which have distinct N-terminal segments and localize to different parts of the cell. All PTPRR isoforms were found to be short-lived proteins, with half-lives of around 3-5 hours, and are constitutively phosphorylated on one or two of the previously identified protein kinase A and MAP kinase target sites. No evidence was obtained for the predicted N-linked glycosylation of the extracellular segment in the receptor-type PTPRR isoform PTPBR7. Rather, the 72 kDa PTPBR7 protein is subjected to N-terminal proteolytic processing *in vitro* as well as *in vivo*, resulting in yet another PTP isoforms: PTPBR7-65. Mutational analyses revealed that proteolytic cleavage of PTPBR7 occurs C-terminal in between residues 135 and 136, at a site that fits the consensus for furin-like convertases. Labeling and internalization experiments suggest that this cleavage occurs predominantly at the cell membrane and is enhanced by serum-derived factors. However, unlike for other receptor-type PTPs, the resulting N-terminal ectodomain does not remain associated with PTPBR7-65 but appears to be released into the surrounding medium. This regulated shedding of PTPBR7-derived polypeptides at the cell surface further adds to the molecular complexity of PTPRR biology.

Introduction

Protein tyrosine phosphorylation is one of the key mechanisms in cellular signaling and as a consequence determines many cellular processes. The extent of protein-tyrosine phosphorylation is dictated by the balance of activities of protein-tyrosine kinases and protein tyrosine phosphatases (PTPs)¹ (1-3). The family of PTPs includes both intracellular and transmembrane enzymes (4,5). Receptor-linked transmembrane PTPs contain an extracellular domain, a single transmembrane domain and an intracellular region consisting of one or two catalytic domains.

Interestingly, some PTP genes give rise to multiple (transmembrane and cytoplasmic) isoforms by the use of different promoters, alternative splicing, differential initiation sites and post-translational modification (3,5). For example, the STEP (striatal enriched phosphatase) subfamily of PTPs consists of multiple transmembrane and cytosolic isoforms that are the result of alternative splicing (6,7), or proteolytic cleavage (8). Likewise, transmembrane, cytosolic and membrane-associated PTP ϵ isoforms exist, as a result of the use of alternative promoters, differential initiation of translation and proteolytic processing (9,10). It is commonly believed that the generation of multiple isoforms from a single PTP gene through (a combination of) these mechanisms warrants fine-tuning of cellular signaling programs, both in time and space dimensions, thus adding to the organismal complexity of higher eukaryotes.

Recently, we described that the mouse PTP gene, *Ptprr*, harbors the information for the regulated production of multiple messenger RNAs, and ultimately four different PTPRR protein isoforms (PTPBR7, PTP-SL, PTPPBS γ -42, and PTPPBS γ -37) through the use of three distinct promoters, alternative splicing and multiple translation initiation sites (11). The four isoforms have molecular weights of 72, 60, 42 and 37 kDa, respectively, and differ in the length of their N-terminal part (Fig. 1) which result in distinct subcellular localizations. The PTPBR7 protein is a type I transmembrane protein, that localizes at the cell membrane and additionally at vesicles and the Golgi apparatus. PTP-SL is probably membrane-associated and localizes at late endosomal vesicles and the Golgi area (12,13). The 42 and 37 kDa PTPPBS γ proteins are genuine cytosolic proteins that are excluded from the nucleus (11). During these studies, isoform-specific expression experiments in intact cells pointed to post-

translational modifications as an additional mechanism to exacerbate the PTPRR isoform diversity (11).

In the current study we have analyzed in detail the biochemical events imposed upon the PTPRR isoforms following their initial biosynthesis. We report on the fate determination and importance of constitutive phosphorylation for all isoforms. Moreover, we reveal that one protein, PTPBR7, is subjected to conditional proteolytic processing, thus introducing a fifth member, PTPBR7-65, to the PTPRR isoform collection.

Material & Methods

Expression Plasmid Constructs and Site-directed Mutagenesis

To obtain the tetracycline inducible construct pNRTIS/PTPBR7-GFP, the plasmid pPTPBR7-EGFP (13) was linearized with *Hind*III and subjected to a Klenow DNA polymerase fill-in reaction to make it blunt. Subsequently, the PTPBR7-GFP encoding fragment was released by a *Not*I digestion and cloned into the *Eco*RV-*Not*I digested pNRTIS-21 vector (14). Plasmids pSG5/PTP-SL-FL (12), pSG5/PTPBR7-FL (12), pSG5/PTPPBS γ -FL (11) and pHSI (15) have been described elsewhere. Point mutations were introduced into pSG5/PTPBR7-FL and pSG5/PTP-SL-FL using the QuickChange Mutagenesis protocol according to manufacturers specifications (Stratagene Inc., La Jolla, CA, USA). The PTPPBS γ S51A/T73A mutant was expressed using plasmid pLXSN/PTPPBS γ /S51A/T73A, the generation of which will be described elsewhere. In Table 1 the primers used and the mutant nomenclature are listed. All constructs were verified by sequence analysis.

Table 1. Mutant nomenclature and primers used for site directed mutagenesis

| <i>mutant</i> | <i>5'primer</i> | <i>3'primer</i> |
|---------------------|---|--|
| BR7-35/36 | ttggctattcgtcaag cg gagcgcgagttggaagccggtg | caccgcttccaactc gc gcttgacgaatagccaa |
| BR7-51/52 | cattcacaggatatc cg gctagcctggacatcgcac | gtgcgatgccaggctag cg cgatattcctgtaagt |
| BR7-158/159 | taaccggctcattgaag cg gcaaccagggtgagttg | caactcaacctggtc gc gcttcaatgaccggta |
| BR7-171/172 | gtgtcccggaaac cg gaccaggagaaacgcag | ctgcgttcccttgg gc gcttccgggagacac |
| BR7-R133A | gaacataaccctgct gc gatctccccaaggag | ctccttggcggaagatc gc aagcagggttatgtg |
| BR7-R136A | ctgcagctactcct gg gcaagatccgaagcag | ctgcttcggatctc gc ccaaggagtagctgcag |
| BR7- R133A/R136A | gaacataaccctgct gc gatctccccaaggag | ctccttggcggaagatc gc aagcagggttatgtg |
| BR7- S338A/T360A | ctgcagctactcct gg gcaagatccgaagcag | ctgcttcggatctc gc ccaaggagtagctgcag |
| | caggagcgacgaggt gc caatgtatctcttacg | cgtaagagatacatt gg cacctcgtcgtc |
| | ccttgtggccgtc ag ccccccgggagaaggtagc | gctaccttcccgggg gc tgagacggccacaagg |

Several codons of PTPBR7 (Acc.no.: D31898), PTP-SL (Acc.no.: BN000437) and PTPPBS γ (BN000438) were mutated into alanines using the primers above. Numbers correspond to the amino acid position of the different isoforms. The mutated nucleotides are indicated in bold. The SL-217A/T239A and γ -S51A/T73A mutants were obtained using the same primer-sets as for BR7-S338A/T360A. Two numbers indicate mutations of two amino acids.

Antibodies

To generate a polyclonal antiserum (α -BR7) against the unique, N-terminal part of PTPBR7, the segment of mouse PTPBR7 cDNA (Acc. No. D31898) that encodes amino acids 25-118 was obtained by PCR and cloned into pGEX-4T. The resulting pGEX-4T/PTPBR7/25-118 plasmid was introduced into DH5 α strain and GST fusion proteins were induced and isolated as described (16). Purified fusion protein was used to immunize rabbits following standards protocols. The polyvalent rabbit antiserum α -SL (12) and the monoclonal antibody 6A6 (11), both raised against the C-terminal 295 amino acid residues present in all PTPRR isoforms, and the monoclonal antibody directed against sucrase isomaltase, HBB 2/614/88 (17), have been described previously. Beta-tubulin antibody E7 was obtained from the hybridoma bank (DHSB, university of Iowa, Iowa city).

Cell Lines

Neuro-2a (ATCC number: CCL-131) and LoVo (ATCC number: CCL-229) cells were cultured in DMEM/5% Fetal Calf Serum (FCS) and DMEM/10% FCS, respectively. FCS was heat inactivated for 30 min at 56°C, unless otherwise stated. Transient transfections were performed using Lipofectamine-Plus according to the manufacturer's instructions (Invitrogen Life Technologies, Breda, the Netherlands). To obtain a tet-off inducible PTPBR7 stable cell line, Neuro-2a-BR7, Neuro-2a cells were transfected with pNRTIS/PTPBR7-GFP using Lipofectamine-Plus (Invitrogen Life Technologies, Breda, the Netherlands). Six hours after transfection the cells were cultured in tet-off medium, being DMEM/5% FCS containing 800 μ g/ml G418 (Gibco Europe, Breda, The Netherlands) and 0.1 μ g/ml doxycycline (Clontech). Ten to fourteen days after transfection, individual clones were selected, expanded for another 2 weeks, and then split in half. One half was cultured in Tet-on medium (DMEM/5% Tet-system-approved FCS, lacking doxycycline; Clontech). After 1, 2 and 3 days of induction cells were checked for PTPBR7-GFP protein expression. The uninduced counterhalves of positive clones were expanded and used for further studies.

Metabolic Pulse-chase Labeling Experiments

Neuro-2a cells transiently expressing PTPBR7, PTP-SL and PTPPBS γ , or PTPBR7-GFP

upon induction, were starved in methionine- and cysteine-free medium for 1 hour at 37 °C. Cells were then pulse-labeled for 15-30 minutes with methionine- and cysteine-free medium supplemented with 100 $\mu\text{Ci/ml}$ Tran³⁵S-label (ICN Radiochemicals) and chased with normal culture medium for different periods. Subsequently, the cells were washed three times with PBS (phosphate-buffered saline) and lysed (lysis buffer: 100 mM Na₂HPO₄, 1% Triton-X-100, 0.2% bovine serum albumin (BSA), pH 8.0, 1 mM PMSF, 25 mM NaF, 1 mM Na₃VO₄, 2 mM EDTA, and 1 mM sodium pyrophosphate, containing a complete protease inhibitor cocktail; Roche Diagnostics GmbH, Mannheim, Germany). Immunoprecipitations and SDS-PAGE were performed as described previously (11). Radiolabeled proteins were detected using Kodak X-omat autoradiography films at -70°C.

Deglycosylation Experiments

Neuro-2a cells, transiently transfected with PTPBR7, PTP-SL or sucrase isomaltase expression constructs (as a positive control (15)), were metabolically labeled for 3 hours and cell lysates were prepared as described above. Following immunoprecipitation of PTPBR7 or PTP-SL with monoclonal antibody 6A6, or sucrase isomaltase using HBB 2/614/88, the proteins were subjected to digestion with Endoglycosidase H (Endo H) or Endoglycosidase F (Endo F) according to the manufacturers protocol (Roche Diagnostics). Proteins were resolved by SDS-PAGE and visualized by autoradiography.

In vivo [³²P]Orthophosphate Labeling

Transiently transfected Neuro-2a cells were grown for 20 hours in DMEM/5% FCS, washed with phosphate-free medium and cultured in phosphate-free medium containing 0.2 $\mu\text{Ci/ml}$ [³²P]-orthophosphate (Amersham Pharmacia Biotech, UK) for 30 min. Preparation of cell lysates and subsequent immunoprecipitations were done as described above. Proteins were resolved by SDS-PAGE and detected using autoradiography.

Immunofluorescence Assays

Neuro-2a cells transiently transfected with a PTPBR7 expression construct were put on ice, washed three times with PBS and incubated for 1h with a 1:2000 dilution of α -BR7 antiserum. After three subsequent washes with PBS the cells were incubated for 1 hour on ice with a 1:100 dilution in PBS of goat anti-rabbit Alexa-568 (10mg/ml; Jackson

ImmunoResearch Laboratories, Inc., West Grove, PA, USA). Following successive washes with PBS, cells were fixed for 10 min with 1% paraformaldehyde in PHEM buffer (60 mM Pipes, 25 mM Hepes, 10 mM EGTA, 2 mM MgCl₂, pH 6.9), and permeabilized using 0.1% saponin and 20 mM Glycine in PBS for 30 min at room temperature. Subsequently, these cells were incubated for 1h with a 1:2000 dilution of monoclonal antibody 6A6 in SPBS (0.1% saponine in PBS) at room temperature. Following three washes with SPBS, cells were incubated for 1h at room temperature with a 1:100 dilution in SPBS of Alexa-488-conjugated goat anti-mouse IgG (10mg/ml; Jackson ImmunoResearch Laboratories, Inc., West Grove, PA, USA). After three final washes with SPBS and methanol dehydration, cells were mounted on glass slides using Mowiol (Sigma) containing 2.5% sodium azide as anti-fading reagent. Images were examined and collected using confocal laser scanning microscopy (MRC 1024, Bio-Rad).

Immunoprecipitation of Mouse Brain Lysates

Mouse C57BL/6 cerebellar lysates were made by mechanical disintegration in 1.5 ml lysis buffer. The lysates were incubated for 1h at 4°C and insoluble components were pelleted by centrifugation (14,000 rpm) for 30 min at 4°C. Protein concentration in the resulting supernatant was determined according to Lowry (18). Supernatants were first precleared with Sepharose beads and then subjected to immunoprecipitation with α -SL or α -BR7 antisera as described above. Obtained proteins were size-separated by SDS-PAGE, and subsequently visualized by Western blot analysis using monoclonal antibody 6A6.

Metabolic Labeling of Brain Tissue Slices

Brains were removed from decapitated 3-week old C57BL/6 mice and directly placed in ice-cold artificial CSF (aCSF: 126 mM NaCl, 26 mM NaHCO₃, 10 mM glucose, 3 mM KCl, 1.2 mM NaH₂PO₄, 1 mM CaCl₂, 3 mM MgCl₂). Horizontal slices (450 μ m thick), including striatal, hippocampal and cerebellar tissue, were prepared on a vibratome (Leica, Nussloch, Germany) and incubated for at least 1h at room temperature in aCSF with increased CaCl₂ (2 mM) and decreased MgCl₂ (2 mM) levels, under continuous perfusion with 95% O₂, 5% CO₂. After placing the perfusion chambers, each containing three tissue slices, in a 37°C water bath, the medium was supplemented with 350 μ Ci of ³⁵S-methionine. Following a 1h incubation period the slices were transferred into an eppendorf tube and washed twice with

ice-cold PBS through centrifugation. Subsequently, the tissue slices were treated with 500 μ l lysis buffer for 1 hour on ice. Remaining debris was removed by centrifugation at 4°C. Immunoprecipitations with the antisera α -BR7 or α -SL were performed as described above. Proteins were resolved by SDS-PAGE and radiolabeled proteins were detected using autoradiography at -70°C for 2 weeks.

Cell Surface Biotinylation

Neuro-2a cells transiently expressing PTPBR7 were metabolically labeled with Tran³⁵S-label as described above. Cells were washed twice with ice-cold PBS and once with ice-cold biotinylation buffer (10mM boric acid, 150mM NaCl, pH 8.0) before being incubated for 45 min at 4°C in biotinylation buffer supplemented with 0.5 mg/ml Sulfo-NHS-Biotin (Pierce, Rockford, IL, USA). Subsequently, the cells were incubated for 20 min at 4°C in quenching solution (15 mM glycine in PBS) and rinsed twice with cold PBS. Cells were taken up in 500 μ l lysis buffer and transferred to Eppendorf tubes.

Obtained lysates were precleared with protein A sepharose beads, then 40 μ l monoclonal antibody 6A6 together with 30 μ l of protein A-Sepharose CL-4B was added to 500 μ l cell lysate and incubated by overnight rotation at 4°C. Sepharose beads with immunobound proteins were subsequently washed four times in lysis buffer, once in 0.1 M Na₂HPO₄ (pH 8.1) and twice in 0.01 M Na₂HPO₄. One-third of the beads was removed and transferred to another tube containing 2x sample buffer. From the remaining beads the bound proteins were eluted by adding 500 μ l elution buffer (1% triton X-100, 100mM Glycine-HCl pH 2.8) and rotating for 10 min at RT. The resulting supernatant with eluted proteins was transferred to a tube containing 100 μ l 1M Na₂PO₄ (pH 8.1), 50 μ l 10% BSA and 15 μ l 1M NaOH. 60 μ l of streptavidin beads (Pierce, Rockford, IL, USA) were added to this neutralized eluate and the mixture was rotated for 60 min at RT to pull down biotinylated proteins. Finally, the streptavidin beads were washed multiple times as described above and 2x sample buffer was added. Proteins were separated by SDS-PAGE and subjected to autoradiography.

To assess internalization of surface proteins, PTPBR7-expressing Neuro-2a cells on a 9 cm culture dish were washed as indicated above but this time incubated with 8 mM of the cleavable Sulfo-NHS-SS-Biotin (Pierce, Rockford, IL, USA) in 10 mM triethanolamine (pH

7.6), 250 mM sucrose, and 2 mM CaCl₂ at 4°C for 45 min. Subsequently, cells were washed with DMEM containing 0.25% BSA to remove extensive biotin. To allow for biotin internalization, cells were transferred to 37°C for various times, at the end of which the cells were placed on ice and washed twice with PBS containing 10% FCS. To remove remaining cell surface biotin the cells were treated with reducing solution (containing 50 mM glutathione, 0.3 M NaOH, 75 mM NaCl, and 10% serum added just before use) for 20 min at 4°C. Subsequently, the cells were incubated with quenching solution (15 mM glycine and 1% BSA in PBS) at 4°C and rinsed twice with cold PBS before being taken up in 500 µl lysis buffer. Cell lysates were subjected to immunoprecipitation and pull down experiments as described for cell surface biotinylation. Proteins were separated by SDS-PAGE, and visualized by Western blot analysis using the monoclonal antibody 6A6.

Characterization of proteases involved in PTPBR7 cleavage

Furin-negative LoVo cells (19) were transiently transfected with PTPBR7 and PTPBR7-GFP encoding constructs. The next day, cell lysates were made and used for immunoprecipitation and Western blotting as described above. Neuro-2a cells transiently expressing PTPBR7 or PTPBR7-GFP were used to test the influence of the proprotein convertase inhibitor decanoyl-Arg-Val-Lys-Arg-chloromethylketone (Alexis Biochemicals, Lausen, Switzerland). Immediately following transfection, the cells were treated for 20 hours with 25, 50 and 100 µM (final concentration) inhibitor that was added to the medium. Subsequently, cell lysates were made and used for immunoprecipitation and Western blotting as described.

Quantification of Cleavage Products

To induce synthesis of PTPBR7-GFP fusion protein, the pNRTIS/PTPBR7-GFP-containing Neuro-2a cells were cultured for three days in tet-on medium with or without 5% FCS. Cell lysates were made as described above, and following incubation on ice for 30 min the lysates were cleared by centrifugation at 4°C for 10 min. Protein concentrations in the supernatants were determined according to Bradford (20). Equal protein amounts were loaded onto SDS-PAGE gels and subsequently blotted onto nitrocellulose membranes and subjected to immunodetection as described previously (13). The upper half of the blot, containing the proteins larger than 60 kDa, was incubated with α-SL antiserum (1:2000 dilution in 3% non-

fat dry milk, 10 mM Tris-HCl (pH 8.0), 150 mM NaCl, and 0.05% Tween-20). The lower part, with proteins of an apparent molecular weight smaller than 60 kDa, was incubated with the anti-tubulin monoclonal antibody E7. Following respective washes and incubations with appropriate secondary antibodies, immunoreactive bands were visualized by chemiluminescence (Lumilight, Roche Diagnostics, Mannheim, Germany). For quantification purposes, detection was performed using a BioChemi imaging system and chemiluminescence signals were analyzed using the Labworks 4.0 program (UVP BioImaging systems, Cambridge, UK).

Results

Biosynthesis and Processing of the PTPRR Isoforms

Previous studies on PTPRR isoforms indicated post-translational modifications for these phosphatases (11). We therefore investigated possible precursor-product relationships by metabolic labeling experiments using Neuro-2a cells transfected with PTPBR7, PTP-SL or PTPPBS γ -42/37 encoding constructs. Cells were pulse-labeled with ^{35}S -methionine for 15 minutes and chased with normal medium for several different time periods (Fig. 1). Fig. 1A shows that *de novo* synthesized PTPBR7 precursor protein is readily detectable following the applied pulse-labeling period, and after 15 min of chase an additional band just above the 72 kDa precursor protein is appearing. In addition, after 2 hours chase a third band of approximately 65 kDa becomes discernable (indicated with arrow). This 65 kDa protein was repeatedly detected, and only at later time points, indicating that it is derived from the 72 kDa precursor protein by post-translational modification.

A similar analysis was performed for Neuro-2a cells transfected with PTP-SL cDNA (Fig 1B). After 15 min ^{35}S -methionine pulse labeling, newly synthesized PTP-SL protein of 60 kDa is detected. An additional, slower migrating band was observed after 15 min of chase with normal medium, indicative for post-translational modification. As described previously (11), expressing PTP-SL cDNA also results in the production of the 42 and 37 kDa PTPPBS γ protein isoforms through the use of alternative start codons. Indeed these proteins are not the result of PTP-SL processing; they are already present from the 15 min pulse onward and do not reveal altered mobilities over time in this assay. This is corroborated in a parallel experiment using the PTPPBS γ expression construct in Neuro-2a cells, which resulted in the synthesis of the PTPPBS γ -42 and PTPPBS γ -37 isoforms that display unaltered apparent molecular weights over time (Fig. 1C).

From figure 1 it is also clear that all PTPRR isoforms have a rather moderate life span, since the amount of labeled protein detected after 2 hours of chase has decreased significantly. The relative signal intensities allowed us to estimate the half-lives of PTPBR7, PTP-SL, PTPPBS γ -42 and PTPPBS γ -37 to be around 3 hours, 2 hours, 3 and 5 hours, respectively.

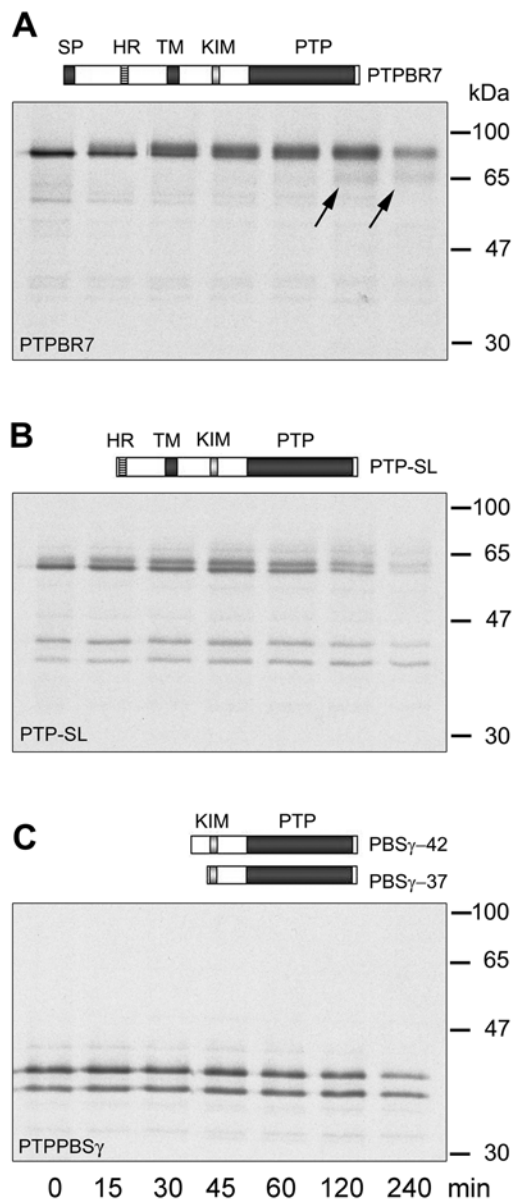


Fig. 1 Biosynthesis and processing of the PTPRR isoforms.

Neuro-2a cells were transiently transfected with pSG5/PTPBR7-FL (**A**), pSG5/PTP-SL-FL (**B**) or pSG5/PTPPBS γ -FL (**C**) expression plasmids. Schematic representations of encoded proteins are shown above the relevant panel. Signal peptide (SP), hydrophobic region (HR), transmembrane segment (TM), kinase interacting motif (KIM) and catalytic phosphotyrosine phosphatase domain (PTP) are indicated. After being metabolically labeled with ^{35}S -methionine for 15 min, cells were chased with normal medium for the indicated time periods (in min). Cell lysates were subjected to immunoprecipitation with monoclonal antibody 6A6. Radiolabeled PTPBR7 (**A**), PTP-SL (**B**) and PTPPBS γ (**C**) protein isoforms were separated by SDS-PAGE and detected by autoradiography. Arrows indicate the appearance at later time points of a 65 kDa PTPBR7 variant. Molecular mass standards are indicated on the right.

No Evidence for N-glycosylation of the PTPRR Isoforms

The upper band that appeared rapidly after the *de novo* synthesis of PTPBR7 and PTP-SL may reflect N-glycosylation or phosphorylation. Glycosylation of PTPBR7 has been suggested before, on the basis of the presence of potential glycosylation sites in the extracellular domain (21). To assess whether glycosylation indeed occurs, Neuro-2a cells were transiently transfected with PTPBR7 and PTP-SL expression constructs and metabolically labeled for 3 hours. This was followed by an immunoprecipitation using the monoclonal antibody 6A6. Part of the obtained PTPRR proteins was also treated with Endo F or Endo H to remove all Asn-linked oligosaccharide chains or only high mannose Asn-linked sugars, respectively. The sucrase isomaltase protein, known to be heavily glycosylated, was taken along as a positive control for the activity of the two deglycosylation enzymes (15). No effect on electrophoretic mobility was observed upon Endo F or Endo H treatment of PTPBR7 and PTP-SL, whereas the sucrase isomaltase protein displayed the expected shifts (Fig. 2A). This indicates that the observed post-translational modification that results in the upward shift of newly synthesized PTPBR7 and PTP-SL is not due to classical N-glycosylation.

PTPRR Isoforms are Phosphorylated

PTP-SL contains two putative phosphorylation sites at serine 217 and threonine 239 (21,22) (NB: position numbers are according to the newly updated database entry BN000437). We therefore investigated whether the upward shift in PTPBR7 and PTP-SL results from phosphorylation, with special emphasis on these sites. Neuro-2a cells expressing either wild-type or mutant PTPBR7, PTP-SL and PTPPBS γ isoforms, were labeled with ^{32}P -orthophosphate for 60 min, and the PTPRR proteins were immunoprecipitated with monoclonal antibody 6A6. Surprisingly, ^{32}P label was detectable in all wild-type isoforms, including the unprocessed as well as the upward shifted PTP-SL and PTPBR7 proteins (the latter is not clearly discernable in the left panel of Fig. 2B). The γ 42-S51A/T73A (and γ 37-S12A/T24A) mutant cannot be phosphorylated at all. Importantly, an almost complete reduction in ^{32}P levels was observed when BR7-S338A/T360A and SL-S217A/T239A mutants were assayed, but these PTPBR7 and PTP-SL mutants still resulted in doublet bands (indicated with arrows) upon immunoblot analysis (Fig. 2B, right panel). These findings rule

out phosphorylation as the post-translational modification causing the upward shift of newly synthesized PTPBR7 and PTP-SL.

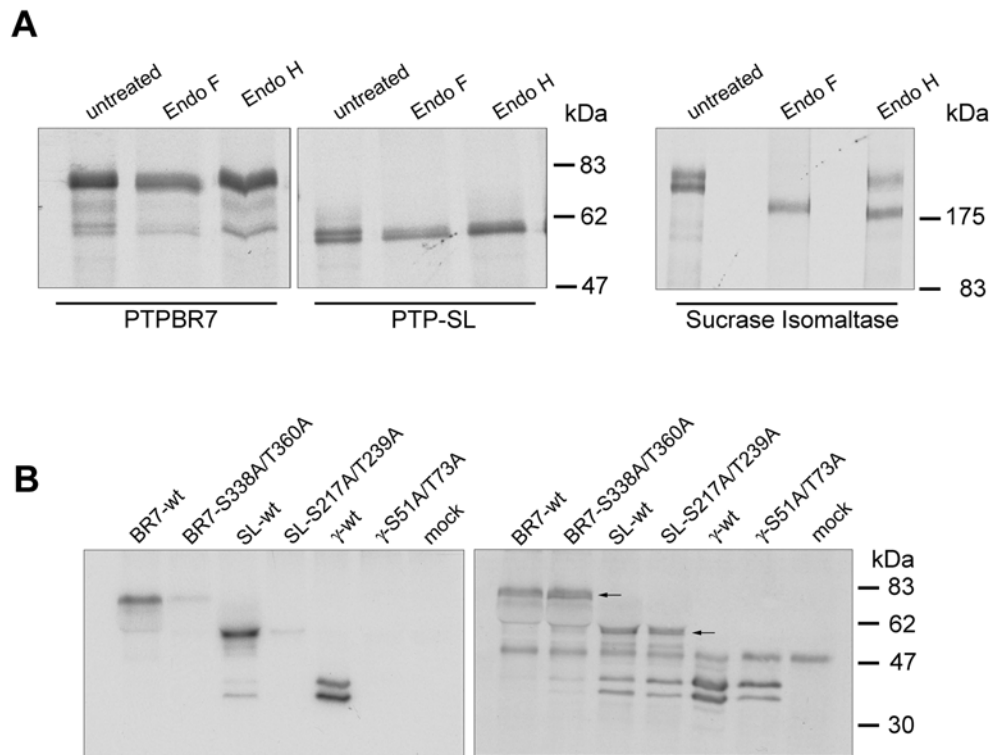


Fig. 2 PTPRR proteins are phosphorylated, but not N-glycosylated.

A, No evidence for N-glycosylation. Neuro-2a cells were transfected with pSG5/PTPBR7-FL (PTPBR7), pSG5/PTP-SL-FL (PTP-SL), or pHSI (Sucrase Isomaltase) expression constructs and metabolically labeled with ^{35}S -methionine for 3 hours. Cell lysates were subjected to immunoprecipitation with 6A6 antibody in the case of PTPBR7 and PTP-SL or with HBB 2/614/88 for sucrase isomaltase. Immuno-purified protein samples were either left untreated or incubated with endoglycosidase F (Endo F) or endoglycosidase H (Endo H). Subsequently, proteins were resolved by SDS-PAGE and visualized by autoradiography. Molecular mass standards are indicated. **B**, Orthophosphate labeling of PTPRR isoforms. Neuro-2a cells were transfected with expression plasmids containing wild-type PTPBR7 (BR7-wt), PTP-SL (SL-wt) or PTPPBS γ (γ -wt) cDNAs, or with corresponding mutant constructs (BR7-S338A/T360A, SL-S217A/T239A, γ -S51A/T73A) in which codons for two candidate phosphorylation sites had been changed into alanine-encoding ones (see Table I for details). Mock transfected cells were taken along as controls. Cells were metabolically labeled with ^{32}P -orthophosphate for 30 min, and lysed. Proteins that were immunoprecipitated with monoclonal antibody 6A6 and separated by SDS PAGE, were subsequently detected by autoradiography (left panel) or by Western blot analysis using α -SL antiserum (right panel). The doublet bands observed for PTPBR7 and PTP-SL are indicated by arrows. The doublet bands observed for PTPBR7 and PTP-SL are indicated by arrows. Molecular mass markers are indicated on the right.

N-terminal Proteolytic Cleavage of PTPBR7

The pulse-chase experiments for PTPBR7 (Fig. 1A), pointed to a 65 kDa protein band that is gradually derived from the 72 kDa PTPBR7 precursor through post-translational modification reminiscent of the proteolytic cleavage as described for several other receptor-type PTPs. If true, the shorter, 65 kDa PTPBR7 variant will lack either C- or N-terminal protein parts. To test this we made use of Neuro-2a cells that had been stably transfected with plasmid pNRTIS/PTPBR7-GFP (Neuro-2a-BR7 cells), which allows conditional expression of a PTPBR7-GFP fusion protein upon removal of doxycycline from the medium. When it is N-terminally cleaved the ~100 kDa GFP-tagged PTPBR7 protein will be turned into a ~90 kDa protein band, whereas C-terminal cleavage would result in a ~65 kDa protein. After two days of PTPBR7-GFP protein induction the Neuro-2a-BR7 cells were metabolically labeled with ³⁵S-methionine for 30 min and chased for up to 24 hours. Fig. 3A shows that detectable amounts of the 100 kDa PTPBR7-GFP precursor protein are present following the applied pulse-labeling period. 30-60 min after biosynthesis, a 90 kDa protein band becomes detectable that gradually replaces the upper precursor. These results strongly suggest N-terminal proteolytic cleavage of the PTPBR7 isoform. Moreover, the gradual increase of the 90 kDa product over time excludes non-specific proteolysis during sample preparations as a cause. Steady-state levels of the PTPBR7-GFP protein in this experiment are presented in the lower panel of Fig. 3A.

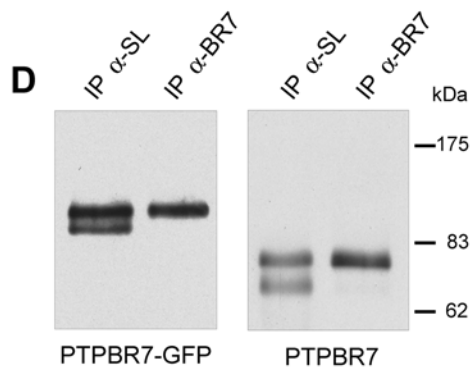
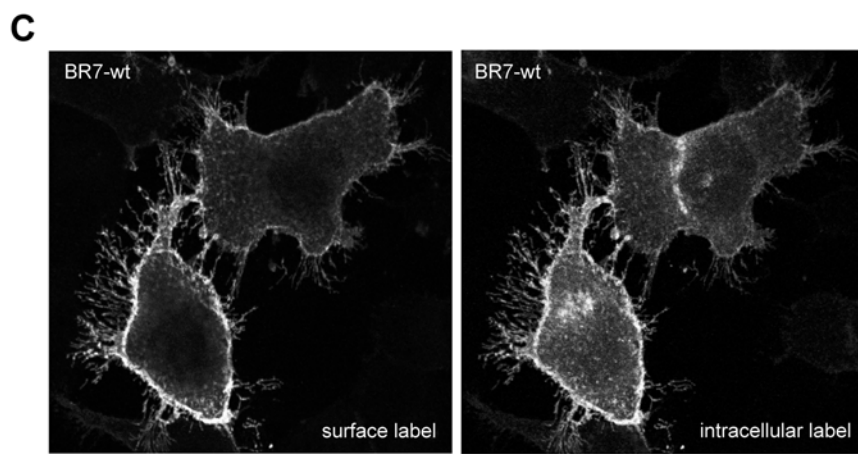
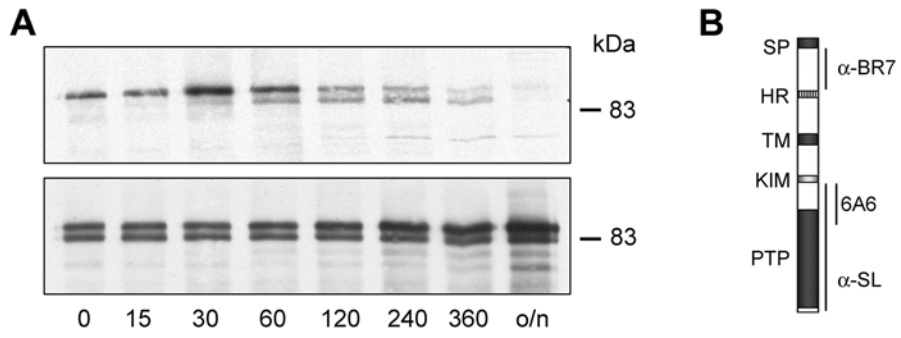
To be able to analyze this proteolytic cleavage in more detail, we generated a rabbit polyclonal antiserum against the N-terminal residues of the PTPBR7 protein (α -BR7) using a bacterially produced GST-BR7 fusion protein as antigen (Fig. 3B). The obtained antiserum recognized exclusively PTPBR7 protein in transfected cells but not in un-transfected control cells using Western blotting and immunofluorescence techniques, demonstrating its specificity. In addition, by performing a surface labeling of Neuro-2a cells expressing PTPBR7 using the α -BR7 antiserum at 4°C before cell fixation (Fig. 3C left panel) the type I transmembrane topology of the PTPBR7 protein could be confirmed. To reveal also the intracellular PTPBR7 molecules the same cells were fixed, permeabilized and stained with monoclonal antibody 6A6 (Fig. 3C right panel). Importantly, no surface staining was observed when PTPBR7 expressing Neuro-2a cells were labeled with the α -SL antiserum or the monoclonal antibody 6A6 without prior fixation and permeabilization (data not shown).

Subsequently, the α -BR7 antiserum was used in immunoprecipitation and Western blotting experiments to test its reactivity towards the PTPBR7 precursor and its cleavage product in PTPBR7 expressing cells. Both Neuro-2a-BR7 as well as transiently transfected Neuro-2a cell-lysates were subjected to immunoprecipitation using the α -BR7 and α -SL antiserum, followed by immunoblot analysis using the monoclonal antibody 6A6. The α -SL antiserum precipitated the two expected protein bands but the α -BR7 antiserum indeed only detected the uncleaved precursor protein (Fig. 3D). These experiments confirm the N-terminal proteolytic cleavage of the PTPBR7 72 kDa precursor into a 65 kDa protein product. The fate of the N-terminal segment that is released following PTPBR7 cleavage was investigated by immunoprecipitation experiments on cell lysates as well as on culture medium using α -BR7 antiserum. In some, but not all experiments, indeed a protein fragment of approximately 12 kDa could be immunoprecipitated from the culture medium (data not shown). No specific PTPBR7-derived low molecular weight protein fragment was obtained from cell lysates in these experiments. Our current belief is therefore that the N-terminal PTPBR7 fragment is shedded from the cell surface and rapidly degraded extracellularly.

Fig. 3 The PTPBR7 protein is N-terminally cleaved. ▶

A, Precursor-protein relationship for GFP-tagged PTPBR7. Neuro-2a-BR7 cells were cultured under doxycycline-free conditions for 2 days to induce expression of the PTPBR7-GFP fusion protein before metabolic labeling with ^{35}S -methionine for 30 min. Cells were then chased with normal culture medium for the indicated time periods (in min), including an overnight incubation (o/n). Following cell lysis, proteins that were immunoprecipitated using monoclonal antibody 6A6 were size-separated by SDS-PAGE and visualized by autoradiography (upper panel) or by immunoblot analysis using α -SL antiserum (lower panel). Molecular mass markers are indicated on the right. **B**, Schematic diagram of full-length PTPBR7 protein. Signal peptide (SP), hydrophobic region (HR), transmembrane segment (TM), kinase interacting motif (50) and catalytic phosphotyrosine phosphatase domain (PTP) are indicated. The regions recognized by α -BR7 and α -SL antisera and by monoclonal antibody 6A6 are indicated. **C**, The α -BR7 antiserum binds to the N-terminal part of PTPBR7 on the cell surface. Intact Neuro-2a cells transiently transfected with pSG5/PTPBR7-FL (BR7-wt) were incubated on ice with the α -BR7 antiserum and subsequently with an appropriate Alexa-568-conjugated second antibody (surface label). Following fixation and permeabilization, cells were also immunostained with monoclonal antibody 6A6 and a suitable Alexa-488-conjugated second antibody (intracellular label). **D**, The α -BR7 antiserum solely detects the 72 kDa PTPBR7 precursor protein. Cell lysates of Neuro-2a cells transiently expressing PTPBR7 (right panel), or of Neuro-2a-BR7 cells conditionally expressing PTPBR7-GFP fusion protein (left panel), were subjected to immunoprecipitation with α -SL (IP α -SL) or α -BR7 (IP α -BR7). Proteins were separated by SDS-PAGE and visualized by immunoblotting using monoclonal antibody 6A6. Molecular mass markers are indicated on the right.

Proteolytic Cleavage of PTPBR7



Endogenous PTPBR7 Processing in the Mouse Brain

Above experiments were conducted with transfected cells. To investigate whether similar processing of PTPBR7 can be observed *in vivo*, we used the α -SL and α -BR7 antisera on mouse cerebellar lysates. Previous immunoprecipitation studies using the monoclonal antibody 6A6 or α -SL antiserum on mouse brain tissue lysates had revealed PTPRR proteins of around 75, 70 and 65 kDa (11). Using the α -BR7 antiserum only the 75 kDa protein is immunoprecipitated (Fig. 4A), supporting the precursor-product relationship as observed in the *in vitro* studies. However, the presence of an additional, possibly intermediate, 70 kDa species in brain points to a more complex processing *in vivo*. Notably, the abundance of the 65 kDa PTPRR protein in brain lysates demonstrates that the majority of PTPBR7 is proteolytically processed.

To substantiate this, brain slices including striatal, hippocampal and cerebellar tissues were metabolically labeled with ^{35}S -methionine for 60 min, homogenized and subjected to immunoprecipitation using the α -SL or α -BR7 antisera. Indeed, the α -BR7 antiserum again results in a single, 75 kDa protein band, whereas the α -SL precipitate contains multiple proteins (Fig. 4B). Irrespective, the fact that the 75 kDa PTPBR7 precursor and the 65 kDa cleavage product were detectable amongst *de novo* synthesized brain proteins strongly supports *in vivo* processing of PTPBR7.

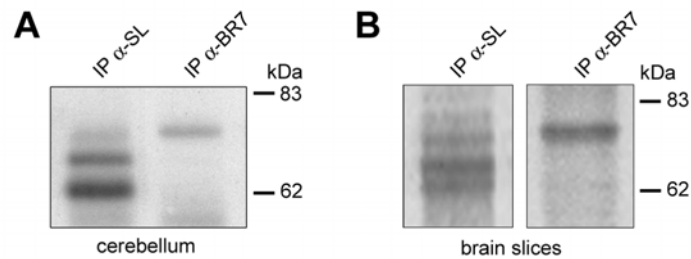


Fig. 4 PTPBR7 steady-state levels and *de novo* synthesis in mouse brain.

A, Endogenous PTPRR expression in mouse cerebellum. Mouse cerebellar protein lysates were subjected to immunoprecipitation using α -SL (IP α -SL) or α -BR7 (IP α -BR7) antiserum. Proteins were separated by SDS-PAGE and visualized on immunoblots using the monoclonal antibody 6A6. Molecular mass markers (kDa) are indicated on the right. **B**, Newly synthesized PTPBR7 proteins in mouse brain slices. Horizontal mouse brain slices were metabolically labeled with ^{35}S -methionine for 60 min before being lysed. Proteins were immunoprecipitated using α -SL (IP α -SL) or α -BR7 (IP α -BR7) antiserum, resolved on SDS-PAGE and visualized by autoradiography. Molecular mass markers are indicated on the right.

Determination of the PTPBR7 Cleavage Site

To establish the position of the cleavage site within PTPBR7 we mutated potential protease recognition sites in the involved N-terminal region. Dibasic cleavage recognition sites are present at multiple positions (Lys35/Lys36, Lys51/Lys52, Lys158/Lys159 and Arg171/Lys172) in PTPBR7, and an Arg-Ile-Phe-Arg-Gln sequence at position 133-137 resembles the RXXRX consensus for furin-like convertases. Appropriate PTPBR7 mutant proteins were expressed in Neuro-2a cells, immunoprecipitated using monoclonal antibody 6A6 and analyzed by SDS-PAGE and western blotting. Mutating the paired lysine/arginine residues into alanines had no effect on PTPBR7 cleavage (data not shown). The changing of Arg136 within the potential convertase site into an alanine, however, significantly reduced PTPBR7 cleavage (Fig. 5A). When both Arg133 and Arg136 were mutated, as in BR7-R133A/R136A, PTPBR7 cleavage was completely abolished. We can exclude that this relates to a protein folding and transportation defect since both mutants are being expressed at the plasma membrane as revealed by cell surface immuno-labeling (Fig. 5B).

Since mutations in the potential proprotein convertase target site within PTPBR7 abrogated cleavage, we tested whether convertases like furin are involved. Transient transfection of furin-negative LoVo colon carcinoma cells (19) with expression constructs encoding PTPBR7 or PTPBR7-GFP revealed normal processing of PTPBR7, as witnessed by the presence of the 65 kDa cleavage product on immunoblots (data not shown). Also, treatment of Neuro-2a cells transiently expressing PTPBR7 with different concentrations of the peptide-based convertase inhibitor decanoyl-Arg-Val-Lys-Arg-chloromethylketone (24) did not result in reduced PTPBR7 cleavage (data not shown), arguing against processing of PTPBR7 by proprotein convertases.

Earlier experiments had already indicated that the N-terminal PTPBR7 segment is detectable at the plasma membrane (Fig. 3B), but did not reveal whether the immunostaining reflected the precursor or the cleavage product. To pinpoint the subcellular location where PTPBR7 is being cleaved, metabolic ³⁵S-methionine pulse-chase labeling of PTPBR7-expressing Neuro-2a cells was followed by cell surface biotinylation at 4°C. To monitor exclusively newly synthesized PTPBR7 that had reached the plasma membrane, an immunoprecipitation with monoclonal antibody 6A6 was performed and, subsequently, eluted immuno-purified proteins were applied to streptavidin beads (Fig. 5C). Newly

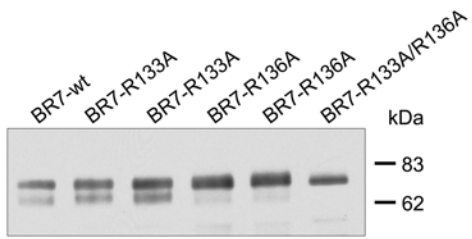
synthesized PTPBR7 precursor proteins were found to reach the cell surface after some 30 min. After two hours, also the cleaved PTPBR7 product is discernable at the cell surface.

Cleavage of cell surface receptors, including receptor tyrosine kinases and phosphatases can take place at the *trans*-Golgi network on the way to the cell surface, at the cell surface itself, and even after subsequent internalization. The latter options are still open for PTPBR7 cleavage, and were examined by exploiting cleavable Sulfo-NHS-SS-Biotin. Cells expressing PTPBR7 were biotinylated at 4°C and chased for 0, 15 and 60 min at 37°C before remaining surface biotin was removed by glutathione treatment. Subsequently, cells were lysed and PTPBR7 proteins were immunoprecipitated using monoclonal antibody 6A6 and, after elution, affinity-purified over streptavidin beads (Fig. 5D). Although PTPBR7 was readily biotinylated at the cell surface, we could not detect internalized PTPBR7 proteins after 15 or 60 minutes. Taken together, the data strongly suggest that cleavage of PTPBR7 occurs predominantly at the cell surface, and that PTPBR7 is not significantly endocytosed under these conditions or is degraded very rapidly following internalization.

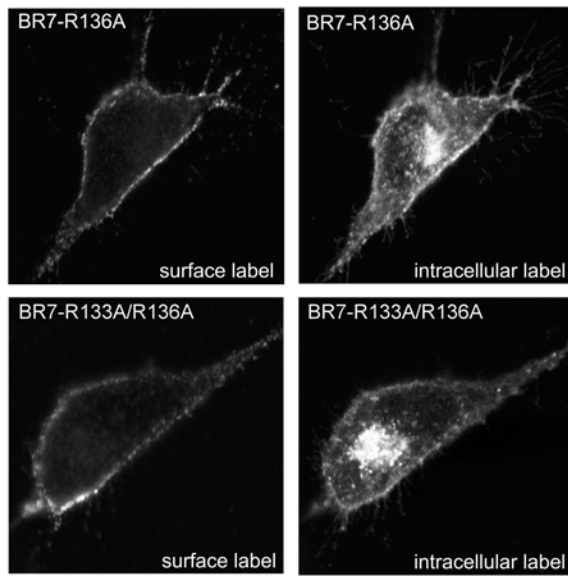
Fig. 5 PTPBR7 is proteolytically cleaved upon reaching the cell surface. ►

A, Cleavage site determination. Neuro-2a cells were transiently transfected with pSG5/PTPBR7-FL (BR7-wt) or mutant versions resulting in alanine substitutions for Arg-133 and/or Arg-136 in PTPBR7 (BR7-R133A, BR7-R136A, BR7-R133A/R136A; for details see Table 1). PTPBR7 proteins were immunoprecipitated using monoclonal antibody 6A6 and analyzed on Western blot using the α -SL antiserum. Molecular mass markers (kDa) are indicated on the right. **B**, Cell surface expression of PTPBR7 mutants. Transiently transfected Neuro-2a cells expressing mutant PTPBR7 forms (BR7-R136A, BR7-R133A/R136A) were stained at 4°C with the α -BR7 antiserum (surface label). After fixation and permeabilization, the same cells were immunostained using monoclonal antibody 6A6 (intracellular label). **C**, PTPBR7 is processed at the cell surface. Neuro-2a cells transiently transfected with pSG5/PTPBR7-FL were metabolically labeled with ³⁵S-methionine for 15 min and subsequently cultured in normal medium for the indicated time period (in min). Cell surface proteins were biotinylated immediately before the cells were lysed, and subsequently PTPBR7 proteins were immunoprecipitated using monoclonal antibody 6A6. Immuno-purified proteins were eluted from the beads and one part was used for SDS-PAGE and subjected to autoradiography to reveal newly synthesized PTPBR7 proteins (top panel). The other part was subjected to a streptavidin pull-down assay. Obtained samples were then resolved by SDS-PAGE and proteins were visualized by autoradiography. The middle panel displays intracellular, non-biotinylated, newly synthesized PTPBR7 proteins. In the bottom panel the newly synthesized PTPBR7 proteins that were on the cell surface during biotinylation are displayed. Arrows indicate the 65 kDa PTPBR7 cleavage product. Molecular mass markers are indicated on the right. **D**, No detectable internalization of surface-exposed PTPBR7 proteins. Neuro-2a-BR7 cells were induced for 2 days to express PTPBR7-GFP before being labeled extracellularly with Sulfo-NHS-SS-Biotin for 45 min at 4°C. Next, the cells were incubated at 37°C for the indicated times (in min) to allow internalization. Subsequently, except for the control sample (ctrl), the surface biotin tag was removed by glutathione treatment at 4°C. Cells were then lysed and PTPBR7-GFP proteins were immunopurified using monoclonal antibody 6A6. One part was used for SDS-PAGE and immunoblotting to visualize steady-state PTPBR7-GFP levels with α -SL serum (top panel). The other part was depleted of biotinylated (and thus internalized) proteins using streptavidin beads, and remaining (untagged) proteins were size-separated on SDS gels and visualized through immunoblotting with α -SL (middle panel). The biotinylated PTPBR7-GFP proteins that had been captured on the streptavidin beads were analyzed in the same way (bottom panel). Molecular Mass standards are indicated on the right.

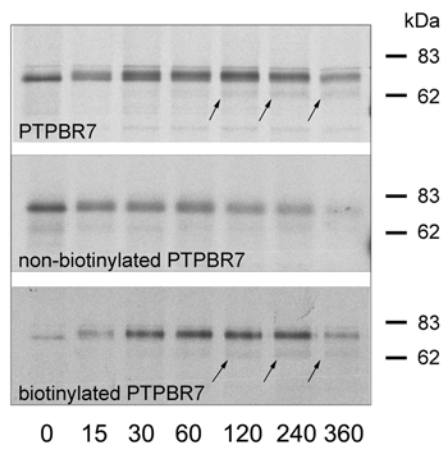
A



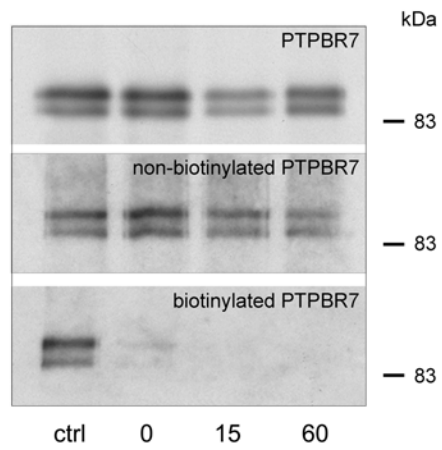
B



C



D



Serum-enhanced Proteolytic Cleavage of PTPBR7

On average, steady-state levels of PTPBR7 and its cleavage product displayed a molar ratio of about 2:1 in the previous experiments (e.g. Fig. 3A). Because environmental triggers may influence the proteolytic cleavage process, we also tested the effect of several culture conditions on PTPBR7 cleavage efficacy using Neuro-2a-BR7 cells. No differences in precursor-product ratios were observed when cells were treated with EGTA, ionomycin, CaCl₂, the PKC inhibitor staurosporin, phorbol ester TPA, NH₄Cl₂, chloroquine, PMSF, E64 or wortmannin, nor when cells were grown at different cell-densities (data not shown). However, a significantly different precursor-product ratio was found when cells were cultured without serum (Fig. 6). Quantification of the observed immunoblot signals for the two protein bands revealed that 90% of PTPBR7 protein remains uncleaved in the absence of serum. Although apparently the total PTPBR7 protein level is increased under serum-free conditions, pulse-labeling studies revealed that this is not due to altered protein stability (data not shown).

The above raises the possibility that PTPBR7 cleavage is performed by serum proteinases with specificity for basic residues. Indeed the former experiments were all performed using serum that had been heat-inactivated through a 30-minute incubation at 56°C, which may allow residual proteinase activity. We therefore investigated PTPBR7 cleavage in Neuro-2a cells that were transiently expressing PTPBR7 or PTPBR7-GFP using serum that had been heat-inactivated at 56°C, at 60°C, or had been left untreated. A partial reduction of PTPBR7 cleavage was noticed for cells cultured in 60°C heat-inactivated FCS when compared to cells incubated with untreated or 56°C-treated FCS (data not shown). Thus, serum components strongly contribute to PTPBR7 cleavage *in vitro*, but in the end do not result in full depletion of the PTPBR7 precursor protein.

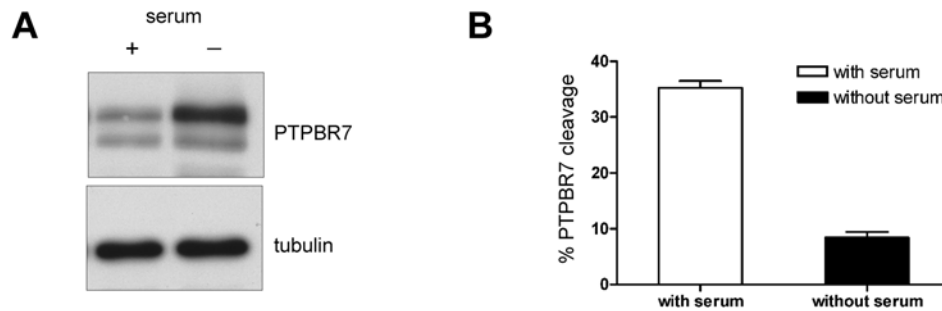


Fig. 6 PTPBR7 cleavage is enhanced by serum.

A, Effect of serum withdrawal on PTPBR7 cleavage. Neuro-2a-BR7 cells were grown in tet-on medium with (+) or without (-) serum for three days. Equal amounts of lysates were separated by SDS-PAGE and blotted onto membranes of which the upper part (proteins >60 kDa) was immunoblotted with α -SL antiserum (PTPBR7, upper panel) and the lower part with α -tubulin antibody E7 (tubulin, lower panel). A representative example out of five experiments is shown. **B**, Quantitative representation of PTPBR7-GFP processing efficacy. Relative intensities of the ~100 and ~90 kDa α -SL immunoreactive bands were determined from the immunoblot results (as in *A*) by direct imaging and quantification of the respective luminescent signals. The percentage contributed by the ~90 kDa cleavage product was determined for cells grown with (white bar) or without (black bar) serum. Results are the means \pm S.D. of five individual experiments; $p < 0.005$ according to Student's *t* test.

Discussion

The current study shows that post-translational modifications considerably add to the complexity of the PTPRR isoform collection. Interestingly, all PTPRR isoforms are being constitutively phosphorylated and display relatively short half-lives of 3-5 hours. Furthermore, both PTPBR7 and PTP-SL undergo an as yet uncharacterized modification that results in a slight reduction of their electrophoretic mobility in SDS-PAGE, leaving open the possibility of sugar modifications that differ from the classical N-glycosylation. Finally, the 72 kDa PTPBR7 protein was found to undergo N-terminal proteolytic processing *in vitro* as well as *in vivo*, pointing to a physiological role for this process.

Cells must be able to respond to rapid changes in both their internal and external environments. Post-translational modifications like proteolytic cleavage of specific proteins, represents such a sensitive and rapid response to environmental cues that enables a programmatic change in cell state. Over the last years several papers have reported proteolytic cleavage of PTPs and progress has been made in understanding the molecular details. Intracellular proteolytic cleavage by the enzyme calpain has been observed for e.g. PTP ϵ (10), PTP-STEP (8), and PTP-MEG (25). For PTP ϵ this results in an altered subcellular localization pattern (10). Proteolytic cleavage of PTP-STEP₆₁, a PTP that is rather similar to PTPBR7, is calcium dependent (8) and is enhanced by ischemia-induced calcium influx in rat brain (26). Cleavage within extracellular domains, probably mediated by the endopeptidase furin, has been reported for LAR (27,28), PTP σ (16,29,30), PTP μ (29) and IA-2 (32). Interestingly, the resulting extracellular and transmembrane parts of these PTPs remain non-covalently associated at the cell surface. Subsequent shedding of the LAR extracellular segment was shown to require an additional, inducible, extracellular proteolytic cleavage step (29). In contrast, the cleaved IA-2 phosphatase-like receptor also undergoes an inducible second processing step, but this concerns an intracellular calpain-mediated cleavage that appears instrumental in the mobilization of secretory granules (33).

The R-I-F-R-Q sequence within the PTPBR7 precursor protein that appeared crucial for its processing fits the consensus cleavage site for proprotein convertases, broadly expressed endopeptidases that generally cleave their targets after the second R in the recognition site (34). They act along the constitutive, unregulated secretory pathway, thus at the *trans*-Golgi network or close to the membrane. Results obtained with a furin-negative cell

line and with a broad proprotein convertase inhibitor, however, argue against convertases as the responsible enzymes for PTPBR7 cleavage. Furthermore, biotinylation experiments suggest that cleavage of the PTPBR7 precursor takes place at the plasma membrane.

The physiological effect of PTPBR7 cleavage remains as yet unresolved. It is conceivable that proteolytic processing of PTPBR7 results in the release of a soluble intercellular regulator into the extracellular space (35,36). For example, proteolytic cleavage of the extracellular domain of an interleukin-1 decoy receptor generates a soluble molecular trap that binds free interleukin-1, thereby down-regulating IL-1 signaling (37,38). The signaling potential of RPTP ectodomains is well documented for phosphacan, that corresponds to the extracellular domain of RPTP β/ζ (39,40) and is an important regulator of neuronal development (41-43). Phosphacan is a high-affinity ligand of several immunoglobulin superfamily neural cell adhesion molecules and binds to the extracellular matrix proteins tenascin-C and R (44-46). It is unclear as yet whether the PTPBR7 ectodomain is released following cleavage and may perform similar functions. Results thus far exclude that it remains non-covalently attached to the transmembrane PTPBR7-65 part. Unfortunately, we could not unequivocally demonstrate the presence of this ~ 12 kDa PTPBR7 ectodomain in the surrounding medium, which may imply rapid degradation.

The half-lives of the PTPRR isoforms are relatively short, around 3-4 hours, which is fairly comparable to that of some other PTPs, such as RPTP μ (31). There are many PTPs, however, that are far more stable, like the heavily glycosylated RPTP α and RPTP ϵ (10). The relative instability of proteins has been related to the presence of proline (P), glutamic acid (E), serine (S), and threonine (T) rich regions (PEST sequences) within them and that would serve as a signal for rapid proteolytic degradation (47). We screened PTPRR isoforms for possible PEST sequences using web-based search tools, but no such motifs could be discerned. For several proteins it has been shown that rapid degradation is important for differentiation and developmental programs, for example in the I κ B signaling pathway (48). Thus the high turnover of the PTPRR isoforms may reflect an additional regulation mechanism in the signal transduction pathways.

Extracellular triggers may influence the proteolytic cleavage process. For example, proteolytic cleavage of RPTP μ is upregulated when cell density is increased (31), and also staurosporin administration or serum starvation has been reported to affect cleavage of

proteins (49). Although many regulators did not to affect PTPBR7 cleavage (data not shown), serum deprivation had a pronounced influence (Fig. 6). Steady-state levels of the ectopically expressed PTPBR7 appear higher under serum-free conditions, but metabolic pulse-chase labeling experiments revealed unaltered protein stability in the absence of serum. Furthermore, a normal location at the plasma membrane under these conditions excluded transport defects as the cause of the altered precursor-product ratio (data not shown). We conclude, therefore, that the proteolytic processing of PTPBR7 is enhanced, either directly or indirectly, by serum-derived factors. This is corroborated by the finding that heat-inactivation of the FCS at 60 instead of (our default) 56°C partly impairs PTPBR7 processing. Since PTPBR7 cleavage also does occur under serum-free conditions (Fig. 6) and can be witnessed in *in vivo* brain material (Fig. 4) the physiological enzymes remain undefined.

All PTPRR isoforms contain a KIM (kinase interacting motif) sequence by which they can interact with the MAP kinases ERK1/2/5 and p38 (22,50,51) and, as a result, block their nuclear translocation (50). PKA-mediated phosphorylation of a crucial serine residue within the KIM sequence abolishes the interaction and allows MAP kinase signaling to proceed (23). Proteolytic cleavage of PTPBR7 as observed in this study may provide an additional way to regulate the impact of PTPRR isoforms on MAP kinase signaling pathways.

Intriguingly, *in vivo* the major PTPRR isoform is apparently the proteolytically processed PTPBR7 65 kDa species (Fig. 4). This processing of the larger PTPBR7 precursor into an N-terminally truncated PTPBR7-65 protein is in a way reminiscent of the *Ptprr* gene promoter switch that occurs during cerebellar development and that results in the replacement of the PTPBR7-encoding transcript by the shorter PTP-SL mRNA in Purkinje cells (12). To unravel the functional consequences of both phenomena provides a further challenge.

Acknowledgments

We thank Hans Lodder and Yvonne Gouwenberg from the Centre for Neurogenomics and Cognitive Research, Vrije Universiteit Amsterdam for their technical assistance, and Frank Böhmer (Jena, Germany) for generously providing the pNRTIS-21 construct. We also thank Yvet Noordman and Rick Wansink for help and advice, and anonymous reviewers for valuable suggestions. This work was supported in part by an EU Research Training Network Grant (HPRN-CT-2000-00085) on Neuronal Protein Tyrosine Phosphatases to R.P. and W.H., and a grant from Ministerio de Ciencia y Tecnologia, Spain (Grant BMC2003-02696) to R.P. P.R. is a recipient of a fellowship from Generalitat Valenciana (Spain).

References

1. Hunter, T. (1998) *Harvey Lect.* **94**, 81-119
2. Hunter, T. (2002) *Keio J. Med.* **51**, 61-71
3. Paul, S., and Lombroso, P. J. (2003) *Cell. Mol. Life Sci.* **60**, 2465-2482
4. Andersen, J. N., Mortensen, O. H., Peters, G. H., Drake, P. G., Iversen, L. F., Olsen, O. H., Jansen, P. G., Andersen, H. S., Tonks, N. K., and Moller, N. P. (2001) *Mol. Cell Biol.* **21**, 7117-7136
5. Alonso, A., Sasin, J., Bottini, N., Friedberg, I., Osterman, A., Godzik, A., Hunter, T., Dixon, J. E., and Mustelin, T. (2004) *Cell* **117**, 699-711
6. Bult, A., Zhao, F., Dirkx Jr, R., Sharma, E., Lukacsi, E., Solimena, M., Naegele, J. R., and Lombroso, P. J. (1996) *J. Neurosci.* **16**, 7821-7831
7. Bult, A., Zhao, F., Dirkx, R., Jr., Raghunathan, A., Solimena, M., and Lombroso, P. J. (1997) *Eur. J. Cell Biol.* **72**, 337-344
8. Nguyen, T., Paul, S., Xu, Y., Gurd, J. W., and Lombroso, P. J. (1999) *J. Neurochem.* **73**, 1995-2001
9. Gil-Henn, H., Volohonsky, G., Toledano-Katchalski, H., Gandre, S., and Elson, A. (2000) *Oncogene* **19**, 4375-4384
10. Gil-Henn, H., Volohonsky, G., and Elson, A. (2001) *J. Biol. Chem.* **276**, 31772-31779
11. Chirivi, R., Dilaver, G., van de Vorstenbosch, R. A., Schepens, J., Croes, H. J. E., Wanschers, J., Fransen, J., and Hendriks, W. (2004) *Genes Cells* **9**, 919-933
12. van den Maagdenberg, A. M. J. M., Bachner, D., Schepens, J. T. G., Peters, W., Fransen, J. A. M., Wieringa, B., and Hendriks, W. J. A. J. (1999) *Eur. J. Neurosci.* **11**, 3832-3844
13. Dilaver, G., Schepens, J., van den Maagdenberg, A., Wijers, M., Pepers, B., Fransen, J., and Hendriks, W. (2003) *Histochem. Cell Biol.* **119**, 1-13
14. Tenev, T., Böhmer, S., Kaufmann, R., Frese, S., Bittorf, T., Beckers, T., and Böhmer, F. (2000) *Eur. J. Cell Biol.* **79**, 261-271
15. Ouwendijk, J., Moolenaar, C. E. C., Peters, W. J. M., Hollenberg, C. P., Ginsel, L. A., and Fransen, J. A. M. (1996) *J. Clin. Invest.* **97**, 633-641
16. Frangioni, J. V., and Neel, B. G. (1993) *Anal. Biochem.* **210**, 179-187
17. Hauri, H. P., Sterchi, E. E., Bienz, D., Fransen, J. A. M., and Marxer, A. (1985) *J. Cell Biol.* **101**, 838-851
18. Peterson, G. L. (1977) *Anal. Biochem.* **83**, 346-356
19. Takahashi, S., Nakagawa, T., Kasai, K., Banno, T., Duguay, S., van de Ven, W., Murakami, K., and Nakayama, K. (1995) *J. Biol. Chem.* **270**, 26565-26569
20. Bradford, M. M. (1976) *Anal. Biochem.* **72**, 248-254
21. Ogata, M., Oh-hora, M., Kosugi, A., and Hamaoka, T. (1999) *Biochem. Biophys. Res. Commun.* **256**, 52-56
22. Pulido, R., Zuñiga, A., and Ullrich, A. (1998) *EMBO J.* **17**, 7337-7350
23. Blanco-Aparicio, C., Torres, J., and Pulido, R. (1999) *J. Cell Biol.* **147**, 1129-1136

24. Jean, F., Stella, K., Thomas, L., Liu, G., Xiang, Y., Reason, A. J., and Thomas, G. (1998) *Proc. Natl. Acad. Sci. USA* **95**, 7293-7298
25. Gu, J., and Majerus, P. W. (1996) *J. Biol. Chem.* **271**, 27751-27759
26. Gurd, J. W., Bissoon, N., Nguyen, T., Lombroso, P. J., Rider, C. C., Beesley, P. W., and Vanucci, S. J. (1999) *J. Neurochem.* **73**, 1990-1994
27. Streuli, M., Krueger, N. X., Arineillo, P. M., Tang, M., Munro, J. M., Blattler, W. A., Adler, D. A., Disteché, C. M., and Saito, H. (1992) *EMBO J.* **11**, 897-907
28. Serra-Pages, C., Saito, H., and Streuli, M. (1994) *J. Biol. Chem.* **269**, 23632-23641
29. Aicher, B., Lerch, M. M., Muller, T., Schilling, J., and Ullrich, A. (1997) *J. Cell Biol.* **138**, 681-696
30. Rock, M. T., Brooks, W. H., and Roszman, T. L. (1997) *J. Biol. Chem.* **272**, 33377-33383
31. Gebbink, M. F. B. G., Zondag, G. C. M., Koningstein, G. M., Feiken, E., Wubbolts, R. W., and Moolenaar, W. H. (1995) *J. Cell Biol.* **131**, 251-260
32. Hermel, J. M., Dirx Jr, R., and Solimena, M. (1999) *Eur. J. Neurosci.* **11**, 2609-2620
33. Ort, T., Voronov, S., Guo, J., Zawalich, W., and Solimena, M. (2001) *EMBO J.* **20**, 4013-4023
34. Steiner, D. F. (1998) *Curr. Opin. Chem. Biol.* **2**, 31-39
35. Hooper, N. M., Karran, E. H., and Turner, A. J. (1997) *Biochem. J.* **321**, 265-279
36. Mantovani, A., Locati, M., Vecchi, A., Sozzani, S., and Allavena, P. (2001) *Trends. Immunol.* **22**, 328-336
37. Fernandez-Botran, R., Chilton, P. M., and Ma, Y. (1996) *Adv. Immunol.* **63**, 269-336
38. Heaney, M. L., and Golde, D. W. (1996) *Blood* **87**, 847-857
39. Maurel, P., Rauch, U., Flad, M., Margolis, R. K., and Margolis, R. U. (1994) *Proc. Natl. Acad. Sci. U S A* **91**, 2512-2516
40. McKeon, R. J., Juryneec, M. J., and Buck, C. R. (1999) *J. Neurosci.* **19**, 10778-10788
41. Bandtlow, C. E., and Zimmermann, D. R. (2000) *Physiol. Rev.* **80**, 1267-1290
42. Butler, C. D., Schnetz, S. A., Yu, E. Y., Davis, J. B., Temple, K., Silver, J., and Malouf, A. T. (2004) *J. Neurosci.* **24**, 462-473
43. Ivanova, A., Agochiya, M., Amoyel, M., and Richardson, W. D. (2004) *Gene Expr. Patterns* **4**, 161-166
44. Margolis, R. K., Rauch, U., Maurel, P., and Margolis, R. U. (1996) *Perspect. Dev. Neurobiol.* **3**, 273-290
45. Margolis, R. U., and Margolis, R. K. (1997) *Cell Tissue Res* **290**, 343-348
46. Milev, P., Monnerie, H., Popp, S., Margolis, R. K., and Margolis, R. U. (1998) *J. Biol. Chem.* **273**, 21439-21442
47. Reichsteiner, M., and Rogers, S. W. (1996) *Trends Biochem. Sci.* **21**, 267-271
48. Schaecher, K., Goust, J. M., and Banik, N. L. (2004) *Neurochem. Res.* **29**, 1443-1451

Chapter 4

49. Columbaro, M., Mattioli, E., Lattanzi, G., Rutigliano, C., Ognibene, A., Maraldi, N. M., and Squarzoni, S. (2001) *FEBS lett.* **509**, 423-429
50. Zuñiga, A., Torres, J., Ubeda, J., and Pulido, R. (1999) *J. Biol. Chem.* **274**, 21900-21907
51. Buschbeck, M., Eickhoff, J., Sommer, M. N., and Ullrich, A. (2002) *J. Biol. Chem.* **277**, 29503-29509
52. Kim, W. T., Chang, S., Daniell, L., Cremona, O., Di Paolo, G., and De Camilli, P. (2002) *Proc. Natl. Acad. Sci. USA* **99**, 17143-17184

Chapter 5

Differential localization of the protein tyrosine phosphatases PTPBR7 and PTP-SL in early endocytic compartments

Gönül Dilaver, Frank de Lange, Mietske Wijers, Huib Croes, Jan Kuiper,
Wiljan Hendriks and Jack Fransen

Submitted

Summary

The precise subcellular localization of protein tyrosine phosphatases (PTPs) is a crucial factor in defining their physiological functions. Neural expression of the mouse gene *Ptprr* results in multiple neuronal PTPs, among which PTPBR7 and PTP-SL. The PTPBR7 isoform is a type I transmembrane protein and localizes to the plasma membrane, the Golgi apparatus and vesicles. PTP-SL is membrane-associated and found at the Golgi apparatus and at vesicles that are in part from endocytic origin. In the current study, we compared in detail the vesicular localization of these two PTPRR isoforms. We show by immunofluorescence and immuno-gold labeling that PTPBR7 and PTP-SL are mainly located and co-localize in late endosomes and in the Golgi area in Neuro-2a cells. PTPBR7, however, shows additional localization on early endosomes as well. Intriguingly, distinct vesicles can be discerned that are positive for PTP-SL alone, for PTPBR7 alone, or that contain both PTPRR isoforms. PTPBR7 and PTP-SL vesicles are highly motile in both anterograde and retrograde directions. The dynamic aspects of the positive vesicles together with their differential presence suggest a specific role for these PTPRR isoforms in the endocytic pathway.

Introduction

Protein tyrosine phosphatases (PTPs) and protein tyrosine kinases (PTKs) are the enzyme classes that are instrumental in determining the spatial and temporal balance between tyrosine-phosphorylated and non-phosphorylated targets. Thus they coordinately regulate cellular responses to intra- and extracellular cues. For many cellular proteins these phosphorylation and dephosphorylation events take place at separate cellular locations (1-3). Subcellular compartmentalization indeed is an important paradigm in signaling pathways as nicely demonstrated for epidermal growth factor receptor (EGFR) and the protein tyrosine phosphatase 1B (4,5).

In previous studies we have shown that the mouse PTPRR protein tyrosine phosphatase family consists of five isoforms, PTPBR7, PTP-SL, PTPPBS γ -42 and PTPPBS γ -37, and an proteolytic product PTPBR7-65, that are derived from the single-copy *Ptprr* gene through the use of different promoters and differential translation initiation events (6,7). These PTPRR isoforms differ in the length of their N-terminal part and in subcellular localization, variables that also differ between all other major PTP subtypes: the receptor-like, membrane associated and cytosolic members of this huge protein family. PTPBR7 is a type I transmembrane protein, which localizes to the plasma membrane, the Golgi apparatus and vesicles. PTP-SL is membrane-associated, although lacking a functional signal peptide, and localizes to the Golgi apparatus and vesicles that are in part from endocytic origin (6,8). The PTPPBS γ isoforms on the other hand are cytosolic proteins (7). All isoforms have an identical C-terminal core containing the catalytic PTP domain and a so-called kinase interaction motif (9) that allows them to associate with the MAP kinases Erk1/2/5 and p38 (10-12). Binding of MAP kinases to KIM-containing PTPs results in inactivation of the MAP kinases, through dephosphorylation of the regulatory tyrosine residue, and prevents their nuclear translocation (11).

Since the precise subcellular localization of the PTPs is of importance for the regulation of phosphorylation cascades we performed a detailed analysis of PTPBR7 and PTP-SL decorated vesicles to increase our knowledge about the extend of overlap between these two major PTPRR gene products. PTPBR7 and PTP-SL were both found to be present on late endocytic compartments, but PTPBR7 shows an additional localization in early endosomes. We also observed that PTPBR7 and PTP-SL decorated vesicles are highly motile

in both anterograde and retrograde directions. Our observations therefore suggest a role for these phosphatases in the endocytic pathway.

Material & Methods

Expression plasmid constructs

The tetracycline-responsive pNRTIS/PTP-SL-EGFP construct was generated as follows. The pPTP-SL-EGFP plasmid (8) was first linearized with *HindIII* and sticky ends were blunted using Klenow DNA polymerase. Subsequently the PTP-SL-EGFP encoding part was released from the plasmid backbone with *NotI*. The obtained DNA fragment was cloned in between the *EcoRV* and *NotI* site of the pNRTIS-21 plasmid (13; kindly provided by dr. Frank Böhmer, Jena, Germany). The mammalian expression constructs pSG5/PTP-SL-FL, pSG5/PTPBR7-FL, pSG8/PTPBR7-FL-VSV and pPTPBR7-EGFP have been described elsewhere (6,8).

Cell lines and Antibodies

Neuro-2a cells (ATCC number: CCL-131) were cultured in DMEM supplemented with 5% Fetal Calf Serum. To obtain the Neuro-2a-SL cell line, which carries an inducible tet-off PTP-SL-EGFP expression construct, Neuro-2a cells were transfected with pNRTIS/PTP-SL-EGFP DNA using Lipofectamine-Plus (Invitrogen Life Technologies, Breda, the Netherlands). Six hours after transfection the cells were cultured in medium containing 800 µg/ml G418 (Gibco Europe, Breda, The Netherlands) and 0.1 µg/ml doxycycline (Clontech) (tet-off medium). Ten to fourteen days after transfection, several individual clones were selected and plated on 96 well dishes. After expanding the individual clones for 2 weeks, cells were split in two halves. One half of the cells was cultured in tet-off medium whereas the other half was cultured in tet-on medium (DMEM supplemented with 5% tet-system approved Fetal Bovine Serum (Clontech) lacking doxycycline). After 1, 2 and 3 days of induction cells were checked for PTP-SL-EGFP expression by fluorescence microscopy. The uninduced counterparts of positive clones were expanded and used for further studies. The tet-off inducible PTPBR7 stable cell-line, Neuro-2a-BR7, was generated similarly and is described elsewhere (14).

The polyvalent antisera α -SL (6), α -BR7 (14), and α -EGFP (15), and the monoclonal antibodies 6A6 (7), and P5D4 (against the VSV-G epitope tag) (16) have been described. The polyclonal α -SL antiserum and the monoclonal antibody 6A6 recognize the C-terminal PTP region of the PTPRR isoforms, whereas α -BR7 recognizes the N-terminal part that is unique

for the PTPBR7 isoform. For some applications the α -SL antiserum was first preabsorbed over a GST-STEP fusion protein column (7) in order to eliminate cross reactivity with the striatum-enriched phosphatase STEP. The beta-tubulin antibody E7 was obtained from the hybridoma bank (DHSB, university of Iowa, Iowa City).

Immunofluorescence assay

Primary hippocampal neurons were prepared and cultured as described previously (17). Neurons were fixed for 30 min with 1% paraformaldehyde in PHEM buffer (60 mM Pipes, 25 mM HEPES, 10 mM EGTA, 2 mM MgCl₂, pH 6.9) and permeabilized using 0.1% saponin in PBS containing 20 mM Glycine (SPBS) for 30 min. Subsequently, cells were incubated for 1h with a 1:200 dilution of STEP-absorbed α -SL antiserum or a 1:2000 dilution of α -BR7 antiserum in SPBS at room temperature. Following three washes with SPBS, cells were incubated with Alexa488-conjugated goat-anti-rabbit IgG (1:100 dilution in SPBS of 10mg/ml; Jackson ImmunoResearch Laboratories, Inc., West Grove, PA, USA) at room temperature for 1h. Finally, after three washes with SPBS and methanol dehydration, cells were mounted on glass slides using Mowiol (Sigma). Images were collected using confocal laser scanning microscopy (MRC 1024, Bio-Rad).

To perform double labeling experiments with PTPBR7-EGFP or PTP-SL-EGFP and tubulin, the Neuro-2a-BR7 and Neuro-2a-SL cell lines were plated on glass coverslips and protein expression was induced for two days. Then the cells were fixed, permeabilized and stained as described above. To visualize tubulin, the E7 antibody (1:2000 dilution) was used followed by Alexa568-conjugated goat-anti-mouse. Fluorescence of the EGFP-fusion proteins was recorded directly. PTPBR7-EGFP or PTP-SL-EGFP expressing cells grown on coverslips were treated with 10 μ g/ml Nocodazole for 3 hours prior to washing, fixation and mounting to disrupt the Golgi apparatus.

Dextran uptake experiment

Neuro-2a cells cultured on glass cover slips were transiently transfected with pPTPBR7-EGFP or pPTP-SL-EGFP using Lipofectamine-Plus (Invitrogen Life Technologies). To visualize endocytic vesicles and late endosomes, cells were first washed and incubated for 1 hour with serum-free medium. Then the medium was replaced by serum-free medium containing 5 mg/ml Dextran-AlexaFluor-546 (Molecular Probes). Cells were incubated at

37°C for 5, 10, 20 or 60 minutes to allow for endocytosis, at the end of which the cells were placed on ice and washed twice with cold PBS to stop membrane and Dextran trafficking in the cell. Subsequently, the cells were fixed for 30 min with 1% paraformaldehyde in PHEM buffer. This was followed by washing and mounting as described above.

For triple labeling purposes Neuro-2a cells were first co-transfected with pPTP-SL-EGFP and pPTPBR7-VSV as described above. To visualize whether PTPBR7 and PTP-SL co-localize in endosomal compartments, cells were allowed for 2 mg/ml Dextran-AlexaFluor-633 uptake as described for the double labeling experiments. Subsequently, the cells were washed, fixed, permeabilized and stained as described above. To visualize PTPBR7-VSV the P5D4 antibody (1:200) was used followed by Alexa568-conjugated goat-anti-mouse IgG (10mg/ml; Jackson ImmunoResearch Laboratories, Inc., West Grove, PA, USA). Images were collected using confocal laser scanning microscopy (MRC 1024, Bio-Rad).

BSA-gold uptake experiment

Ultrastructural localization studies were performed on Neuro-2a cells transfected with pPTPBR7-EGFP or pPTP-SL-EGFP. After 24 hours the transfected cells were incubated with serum-free medium for 1 hour at 37°C. Then the cells were incubated with BSA complexed to 5nm gold particles in serum-free medium for 5, 15, 30, and 60 minutes at 37°C. Subsequently, cells were fixed for 30 min with 1% paraformaldehyde in PHEM buffer. Fixed cells were stored until use in 1% PFA. Before sectioning, cells were pelleted in 10% gelatin and post-fixed in 1% PFA for 24 hours. Ultrathin cryosectioning was performed as described before (18,19). Sections were incubated with α -EGFP (1:2000 dilution) followed by Protein A complexed to 10 nm or 15nm gold. Electron microscopy was performed using a Jeol 1010 electron microscope operating at 80 kV.

Live cell studies

Stable cell lines conditionally expressing PTPBR7-GFP (Neuro-2a-BR7) or PTP-SL-GFP (Neuro-2a-SL) were used for live-cell imaging. Cells were plated on 35-mm-diameter glass-bottom dishes (Willco wells BV, Amsterdam, The Netherlands) and protein expression was induced for two days. Live cell confocal microscopy was performed on a Zeiss LSM510Meta confocal microscope (Carl Zeiss GmbH, Jena, Germany) equipped with a temperature-controlled stage and CO₂ incubator (type S).

Measurements on vesicle dynamics were made from movies that were taken at ~ 1 frame/s. Analyses were performed with the public domain image analysis package ImageJ (Version 1.32j; Wayne Rasband, NIH, USA; <http://rsb.info.nih.gov/ij/>) using the Kymograph plugin (<http://www.embl.de/eamnet/html/kymograph.html>). In short, maximum projections were made highlighting the trajectories over which vesicle movement had occurred. From these projections tracks were selected to generate kymographs - or time-space-plots - from which velocities were obtained by extracting slope values (dx/dt).

Results

Localization of endogenous PTPRR isoforms in primary neurons

For the functional understanding of the PTPBR7 and PTP-SL PTPRR isoforms, knowledge on their precise subcellular localization is of relevance. We first studied the endogenous subcellular localization of the PTPRR isoforms in primary hippocampal neurons, using the α -SL and the α -BR7 antisera. The α -SL antiserum recognizes the C-terminal region of all PTPRR isoforms. To eliminate its cross-reactivity with the STEP phosphatases this α -SL antiserum was first passed over a column carrying GST-STEP fusion protein before being used (7). The α -BR7 antiserum specifically recognizes the unprocessed ~72 kDa PTPBR7 (14).

Both antisera resulted in a punctate staining pattern throughout the neurons (Fig. 1A and C). Higher magnification (Fig. 1B and D) shows a clear dotted fluorescence pattern in dendrites, indicating that endogenous PTPRR isoforms also localize to vesicles. In view of the reported RNA and protein expression profiles in mouse brain (6,7), it is most likely that the observed vesicular pattern in hippocampal neurons solely represents the PTPBR7 isoform. This endogenous localization is remarkably similar to the vesicular staining observed in transfected cell lines earlier (8). As the level of endogenous PTPRR proteins in the hippocampal primary neurons is very low, and these cells are not easy to manipulate we continued our studies using ectopic expression in Neuro-2a cells.

Co-localization of PTPBR7 and PTP-SL vesicles with endosomal markers

In previous investigations both PTPBR7 and PTP-SL were found at vesicles that are, at least in part, from endocytic origin (6,8). To relate the PTPRR-positive vesicles more precisely to different stages of the endocytic pathway and reveal the extent of overlap in PTP-SL and PTPBR7 localization, we performed experiments using fluorescent Dextran uptake in Neuro-2a cells transiently expressing EGFP-tagged PTPRR isoforms (Figs. 2 and 3). After 5 min of Dextran uptake, revealing the early endosomes (20), no co-localization with Dextran was obtained for either one of the PTPs (Fig. 2A-C and 3A-C). After 10 minutes of endocytotic labeling, numerous Dextran-containing vesicles were also found positive for PTPBR7, predominantly at the periphery of the cells (Fig. 2D-F). Co-localization of PTP-SL and Dextran at this time point could also be detected, albeit to a much lesser extent (Fig. 3D-F).

After 20 min of Dextran uptake the localization of both phosphatases showed a high degree of overlap with that of endocytosed Dextran, mainly in vesicles close to the Golgi area (late endosomes) (Fig. 2G-I and 3G-I). These experiments corroborate our finding that PTPBR7 and PTP-SL are present on endosomes (8). Furthermore, they demonstrate that whereas PTP-SL locates predominantly to the late endosomes, PTPBR7 is also present at endosomes from earlier stages.

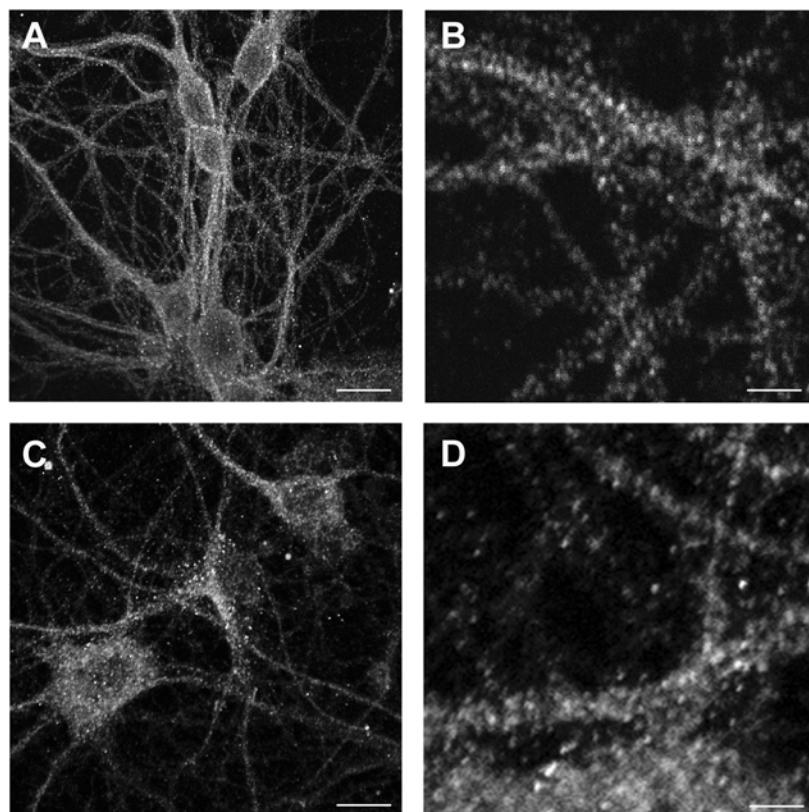


Fig. 1 Endogenous localization of PTPRR isoforms in neuronal cells.

Primary hippocampal neurons were isolated and cultured for two weeks. PTPRR proteins were immunohistochemically detected using the antisera α -BR7 (A and B) or STEP-absorbed α -SL (C and D). Bars in A and C indicate 10 μ m and in B and D 1 μ m.

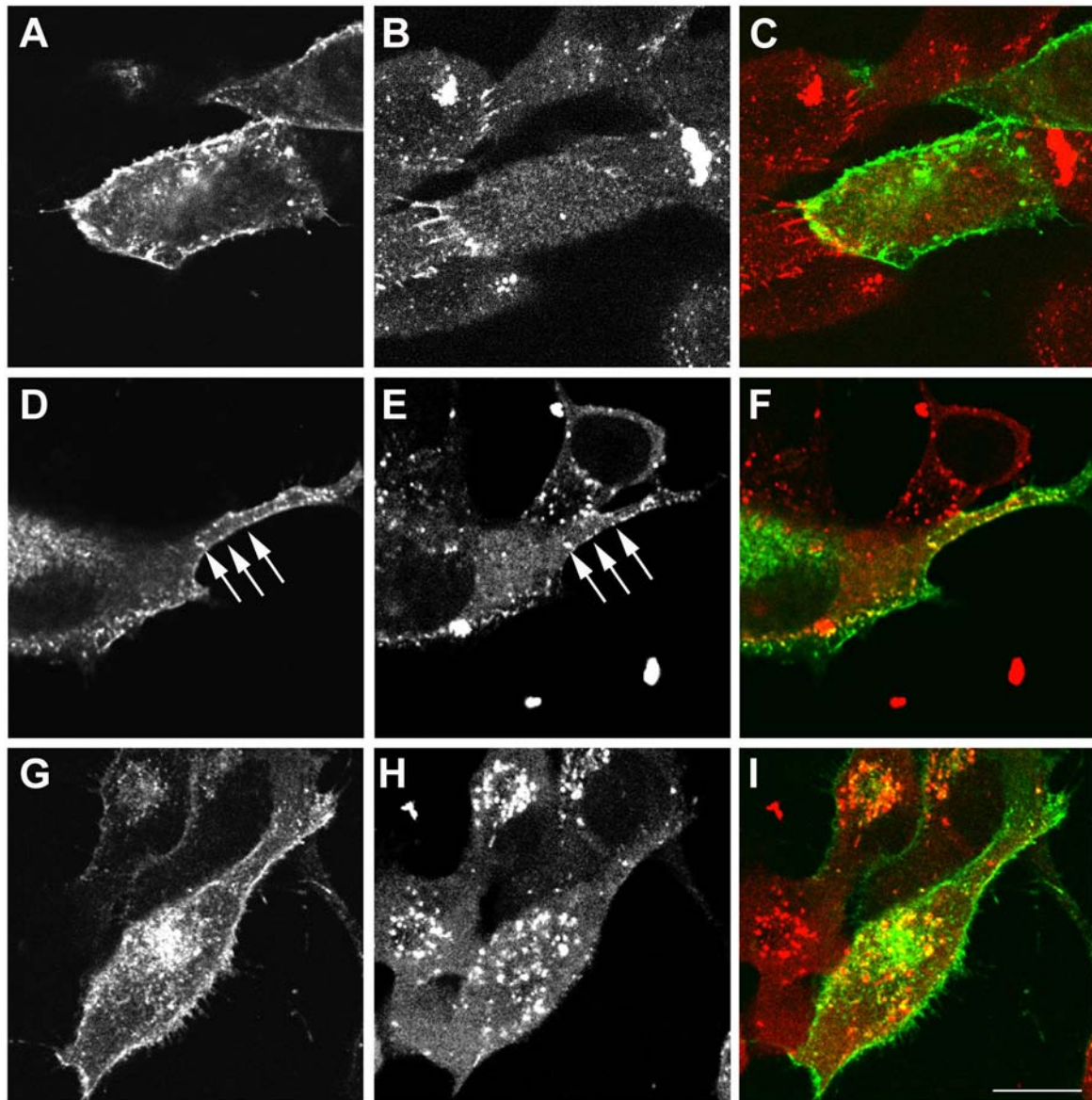


Fig. 2 PTPBR7 localizes to early and late endosomes.

Neuro-2a cells were transiently transfected with construct pPTPBR7-EGFP. PTPBR7-EGFP fluorescence (A, D, and G) and Alexa549-labeled Dextran uptake (B, E, and H) after 5 min (A-C), 10 min (D-F) and 20 min (G-I) were recorded directly using confocal microscopy. Yellow color in panels C, F and I indicates overlap of PTPBR7-EGFP (green) and Alexa549 Dextran (red) signals. Arrows point to dextran-containing vesicles, which are also positive for PTPBR7 (D and E). Bar indicates 10 μ m.

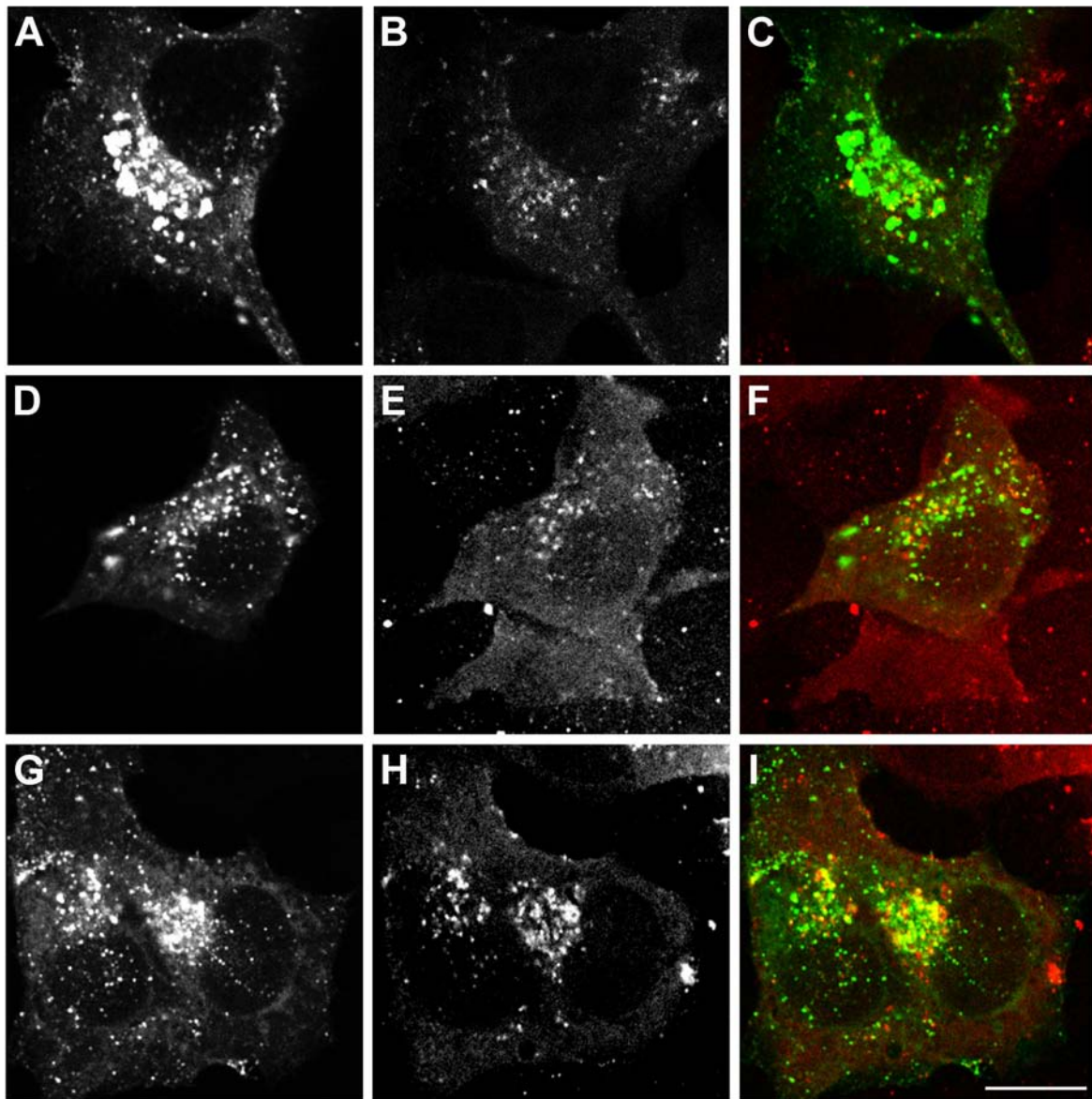


Fig. 3 PTP-SL localizes to late endosomes.

Neuro-2a cells were transiently transfected with construct pPTP-SL-EGFP. PTP-SL-EGFP fluorescence (A, D, and G) and Alexa549-labeled Dextran uptake (B, E, and H) after 5 min (A-C), 10 min (D-F) and 20 min (G-I) were recorded directly using confocal microscopy. The yellow color in panels C, F and I shows the overlap of PTP-SL-EGFP (green) and Dextran (red) signals. Bar indicates 10 μ m.

To substantiate this finding we next studied localizations in the earlier stages of the endocytic pathway in more detail, at the ultrastructural level. To this end, we performed an endocytosis assay using uptake of 5nm BSA-gold in Neuro-2a cells transiently transfected with PTPBR7-EGFP or PTP-SL-EGFP (Fig. 4). The tagged PTPBR7 and PTP-SL proteins were detected using a GFP-directed antiserum with proven suitability for immunoelectron microscopy (8,21). After 5 min BSA-gold uptake, gold particles were found at invaginations of the plasmamembrane (coated pits) and small vesicles (Fig. 4A and B). Co-localization with these early endosomal organelles was only found for PTPBR7-EGFP (Fig. 4B) and not for PTP-SL-EGFP (Fig. 4A). In contrast, after 15 min of continuous uptake the BSA-gold-containing vesicles, representing endocytic organelles at later stages, were positive for both PTPBR7-EGFP and PTP-SL-EGFP (Fig. 4C and D). Both PTP-SL-EGFP (Fig. 4E and 4F) and PTPBR7-EGFP (data not shown) displayed extensive colocalization after 30-60 min of BSA-gold internalization, in larger, late endosomes (Fig. 4E) and in structures near the Golgi apparatus (Fig. 4F). These results firmly establish the differential localization of these two PTPRR isoforms over the early stages of endocytosis.

Partial co-localization of PTPBR7 and PTP-SL

The apparent overlap in localization observed between PTPBR7 and PTP-SL at the late endosomal compartments, prompted us to answer the question whether PTPBR7 and PTP-SL themselves co-localize at single vesicles. Neuro-2a cells were co-transfected with expression plasmids encoding GFP-tagged PTP-SL and VSV-tagged PTPBR7, and the resulting immunofluorescence patterns revealed that there is indeed a substantial overlap between PTPBR7 and PTP-SL at the Golgi apparatus and in vesicles surrounding it (Fig. 5 A-C). In addition, we also observed single positive vesicles, with fluorescence derived from only PTPBR7 or PTP-SL. Interestingly, single-positive PTPBR7 vesicles are particularly found in the vicinity of the plasma membrane, reminiscent of the early endocytic compartment in which PTP-SL is sparse (Fig. 5A-C). We also used the double transfected Neuro-2a cells in a 20 min fluorescent Dextran uptake experiment, to label the late endosomal compartment. The triple labeling experiments demonstrated that indeed PTPBR7 and PTP-SL co-localize at late endosomal vesicles in these cells (Fig. 5D-F).

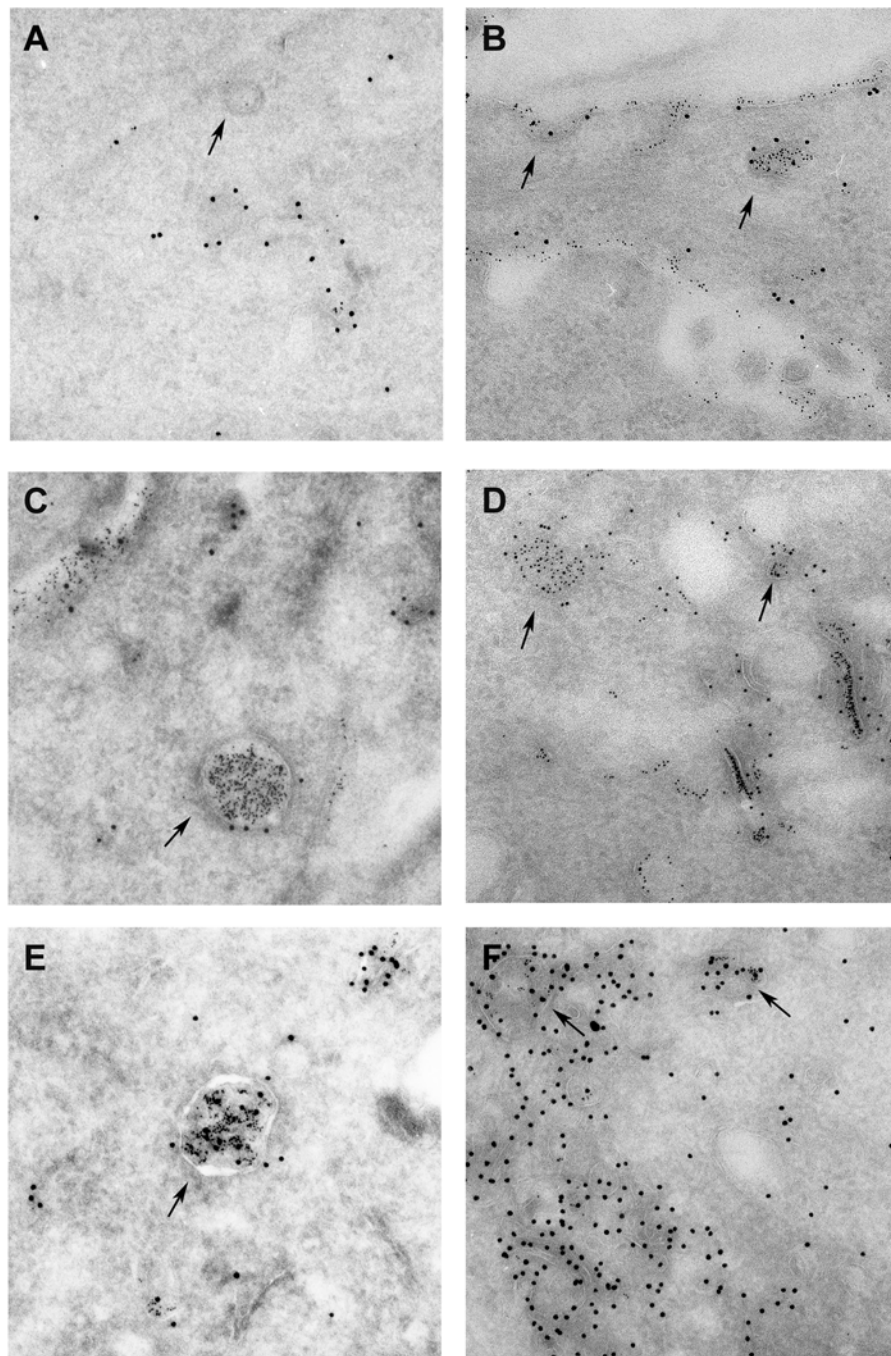


Fig. 4 Differential localization of PTPBR7 and PTP-SL to endosomal organelles. Immunoelectron microscopy analysis of transiently transfected Neuro-2a cells expressing PTP-SL-EGFP (A, C, E and F) or PTPBR7-EGFP (B and D) after BSA-gold uptake (5nm gold) for 5 min (A and B), 15 min (C and D) and 30-60 min (E and F). The EGFP fusion proteins were visualized using α -EGFP antiserum and Protein A complexed to 15 nm (A, B, C, E, and F) gold or to 10 nm gold (D). The arrows point to early endosomes in A and B, to late endosomes in C and E, or to structures near the Golgi in F.

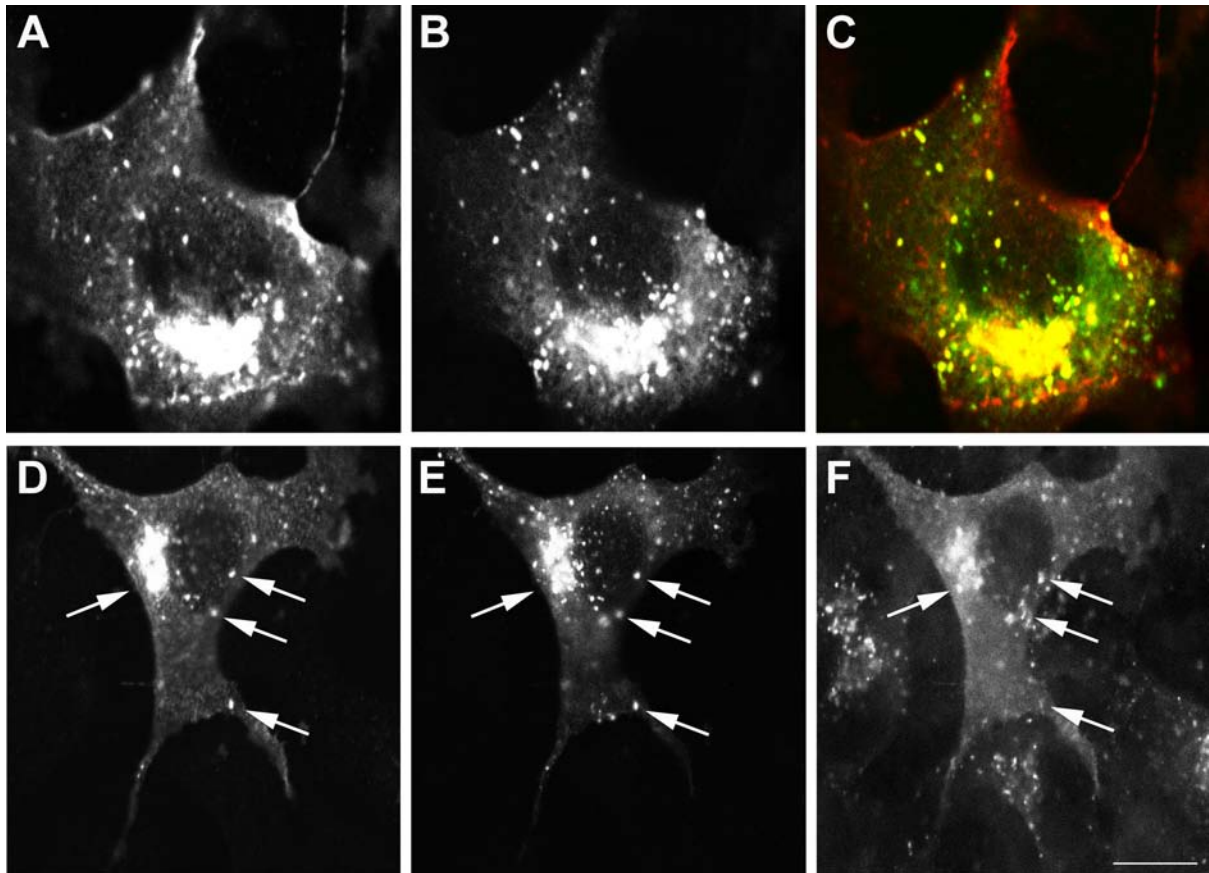


Fig. 5. Some endocytic vesicles contain PTPBR7 as well as PTP-SL.

Neuro-2a cells were co-transfected with pPTP-SL-EGFP and pSG8/PTPBR7-FL-VSV. EGFP fluorescence of PTP-SL-EGFP was recorded directly (B and E) and PTPBR7 proteins were visualized immunohistochemically using the P5D4 antibody against the VSV tag (A and D). Yellow color in panel C indicates overlap of PTP-SL-EGFP (green) and PTPBR7 (red) signals. After 20 min of Alexa-633-labeled Dextran uptake triple-labeled vesicles that are positive for PTPBR7 (D), PTP-SL (E) and Dextran (F) can be detected (arrows). Bar indicates 10 μ m.

PTPBR7 and PTP-SL dynamics in live cells

Vesicular trafficking pathways, essential for delivering membrane components, ligands and solute molecules to various intracellular compartments, commonly involve so-called recycling/shuttling mechanisms to ensure membrane homeostasis throughout the cell. Hence the dynamics and directionality of vesicle movement are relevant characteristics. To investigate whether PTPBR7 and PTP-SL are present on anterograde and/or retrograde vesicles traveling between the plasma membrane and the Golgi apparatus we analyzed the dynamics of these vesicles exploiting the intrinsic fluorescence of EGFP-tagged PTPRR isoforms. To exclude over-expression artifacts we generated stable cell lines, Neuro-2a-BR7 and Neuro-2a-SL, in which expression of PTPBR7-EGFP or PTP-SL-EGFP fusion proteins can be induced up to moderate levels upon removal of doxycycline from the medium. The subcellular localization of the tagged PTPBR7 and PTP-SL proteins as displayed in these stable cell lines (Fig. 6 A and C) is in concordance with that observed in transiently transfected Neuro-2a cells (Figs. 2-3). The Golgi association of PTPBR7 and PTP-SL in these stable cell-lines was confirmed by the observation that the fluorescence pattern was dispersed upon Nocodazole treatment (not shown), a drug known to disrupt the Golgi apparatus.

Monitoring of the dynamics of the PTPBR7-EGFP and PTP-SL-EGFP proteins in living cells revealed a stable Golgi region and highly motile vesicles (Fig. 6 B and D) that move both to and from the Golgi apparatus (Fig. 6E). Also in other areas of the cell anterograde and retrograde movement of both PTPBR7 and PTP-SL positive vesicles were observed. Vesicles moved with quite different velocities (speeds up to 1.6 $\mu\text{m/s}$ could be measured), but when we calculated the average vesicle speed no significant differences were found between PTPBR7 ($0.14 \pm 0,036 \mu\text{m/s}$) and PTP-SL ($0.17 \pm 0,027 \mu\text{m/s}$) positive vesicles.

The observed trafficking pattern of the PTPBR7 and PTP-SL vesicles is reminiscent of movement along microtubule tracks in the cell (Fig. 6B and D). To test this, we performed an immunofluorescence assay using an anti-tubulin antibody (E7) on the Neuro-2a cells stably expressing PTPBR7-EGFP and PTP-SL-EGFP fusion proteins (Fig. 7). This revealed that indeed PTPBR7-EGFP and PTP-SL-EGFP positive vesicles localize mainly along microtubuli.

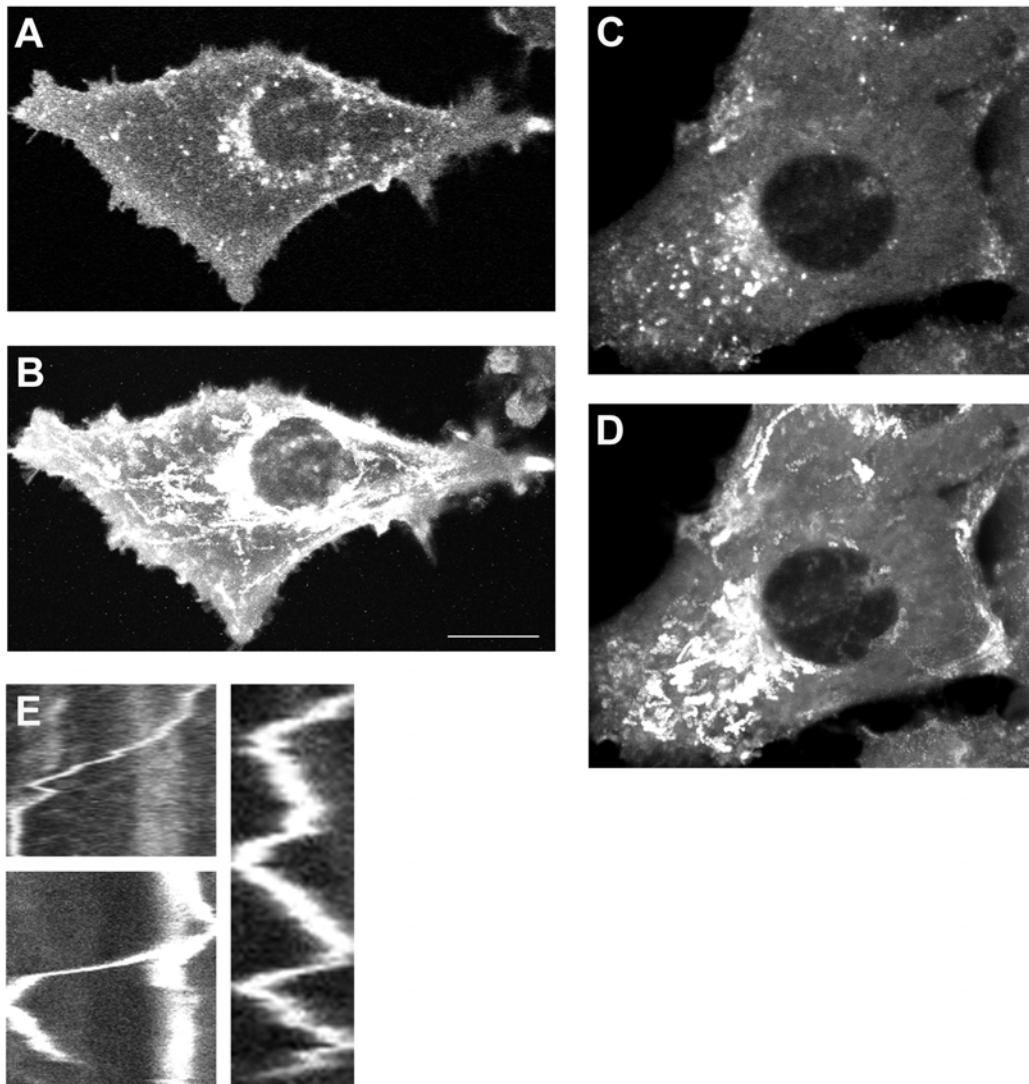


Fig. 6 Dynamic aspects of PTPBR7 and PTP-SL positive vesicles.

Neuro-2a-BR7 (A and B) and Neuro-2a-SL (C and D) cells were cultured under doxycycline-free conditions for 2 days to induce expression of the EGFP fusion proteins. Images of the fluorescence of PTPBR7-EGFP (A) and PTP-SL-EGFP (C) were acquired from live cells. 600 images for PTPBR7-EGFP and 300 images for PTP-SL-EGFP were collected with 1 s time interval. The projections of the images of PTPBR7-EGFP (B) and PTP-SL-EGFP (D) reveal the motility of the vesicles. Representative kymograms for PTP-SL-positive vesicles (E) demonstrate bi-directional movement. PTPBR7 positive vesicles yielded the same results (data not shown). Bar indicates 10 μm in A-D.

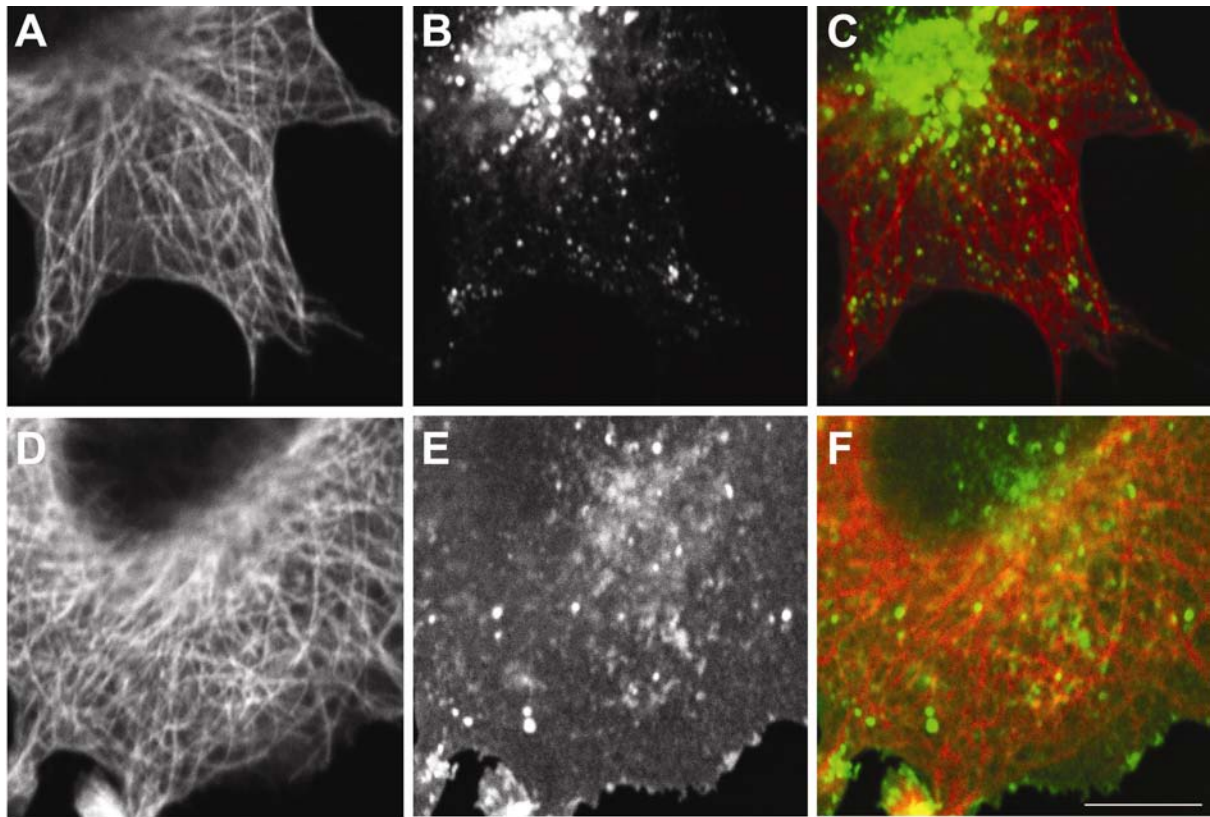


Fig. 7 PTPBR7 and PTP-SL positive vesicles localize along microtubule tracks.

Neuro-2a-SL (A-C) and Neuro-2a-BR7 (D-F) cells were cultured under doxycycline-free conditions for 2 days to induce expression of the EGFP fusion proteins. Fluorescence of PTP-SL-EGFP (B) and PTPBR7-EGFP (E) was recorded directly. Microtubuli (A, D) were stained immunohistochemically using an antibody directed against β -tubulin. Panels C and F display merged images of EGFP-tagged PTPRR autofluorescence (green) and the microtubuli immunostaining (red). Bar indicates 10 μ m.

Discussion

The PTPRR isoforms PTPBR7 and PTP-SL both localize at the trans-Golgi network and on endocytic vesicles in neuronal cells (8). In the current study we show by immunofluorescence and immuno-gold labeling studies that PTPBR7 and PTP-SL display clear but subtle differences in their endosomal localization. Proteins that are internalized first end up in the early endosomes and can be recycled to the cell surface via a rapid or a slow route through recycling endosomes, but a direct route can also connect these endosomes to the late endosomes, multivesicular bodies and ultimately the *trans*-Golgi network or lysosomes (22). To facilitate these transport processes in the endocytic compartment, a dynamic network of endocytic vesicles can be discerned (e.g. (23)). Indeed, labeling of these PTPRR isoforms revealed highly motile vesicles trafficking to and from the Golgi apparatus, which appeared rather stable by itself. In addition, vesicles trafficking in both anterograde and retrograde fashion were observed outside the *trans*-Golgi area, in other parts of the cell (Fig. 7). Especially for PTPBR7 vesicles in the periphery of the cells were noted, most likely representing early endosomes. Together, our data reveal that PTPBR7 is present on vesicles throughout the endocytic pathway from the plasma membrane to the Golgi apparatus. In contrast, PTP-SL is only present on vesicles participating in the later stages of endocytosis, close to the *trans*-Golgi network.

The differential localization of PTPBR7 and PTP-SL on vesicles of the endocytic machinery leaves us with three options with respect to their functioning. To start with, it could be that the PTPRR isoforms are merely cargo proteins that for example need to be delivered to lysosomes for degradation. In line with this, all PTPRR isoforms are short-lived proteins with half-lives varying from 3 to 5 hours (14). However, we did not observe any colocalization of PTPRR proteins with lysosomal marker proteins (8). Furthermore, as cargo proteins these phosphatases would rather be expected to travel in one direction and to accumulate at a certain location within the cell. We did, however, observe both anterograde and retrograde movements for PTPRR-positive vesicles. We therefore favor the two remaining options, namely that these phosphatases are either involved in localized signaling or make part of the endocytic transport machinery itself.

Besides its main function of delivering membrane components, ligands and solute molecules to various intracellular compartments, endocytosis is also intricately coupled to

regulated signal transduction (3). For many growth factor signaling pathways indeed the impact of receptor internalization and timely signal shutdown through dephosphorylation has been documented. The prototypic example is the EGF tyrosine kinase, which can be internalized upon ligand binding (5). Phosphorylation dynamics of the EGF receptor were successfully imaged and revealed that EGFR at the plasma membrane is phosphorylated and hence internalized upon ligand binding and subsequently dephosphorylated by PTP1B, which resides at the ER membrane, resulting in receptor silencing (signal termination) and RTK break down in lysosomes (24). In addition, tyrosine phosphorylation of Eps15, an endocytic protein, by EGFR itself is also required for ligand-induced EGFR endocytosis (25). Recently, localized signaling has been demonstrated for human sef (acronym of similar expression to *fgf* genes), a new MAPK scaffold (26). Sef resides on the Golgi apparatus, and acts there as a spatial regulator for ERK signaling by specifically blocking ERK nuclear translocation without inhibiting its activity in the cytoplasm (26). A comparable role for PTPRR isoforms is easy to imagine since these phosphatases interact with the MAP kinases ERK1/2/5 and p38 through their KIM domain. The interaction not only results in the dephosphorylation of the MAP kinase but it also blocks its translocation to the nucleus, thus eliminating downstream responses at the transcriptional level (12,27). Up to now, these effects have been reported following overexpression of PTPRR isoforms; whether they are capable of performing these tasks under more physiological circumstances remains to be investigated.

The third option, involvement of PTPRR proteins in endocytic vesicle transport itself, is also still open. Accurate packaging of cargo and (coated) vesicle formation and membrane fusion *in vivo* requires tight regulation, for which phosphorylation is indeed one of the mechanisms (28). Four different heterotetrameric adaptor protein complexes, AP-1 to AP-4, are involved in the sorting of cargo proteins into transport vesicles that traffic between the different organelles of the cell (29,30). It has been shown that phosphorylation of serine and threonine residues within the clathrin coat proteins plays an important role during clathrin-mediated endocytosis (31,32). Also growth factor or hormone induced tyrosine phosphorylation of coat proteins, like clathrin heavy chain and dynamin, has been reported to influence clathrin redistribution and MAP kinase signaling (33,34). Likewise, EGF-induced tyrosine phosphorylation of the β 2 subunit of AP-2 turned out to be important in regulating EGFR protein turnover of (35). And very recently, the direct impact of PTP activity on intracellular trafficking was established for PTP-MEG2, which is localized to secretory

vesicle membranes. PTP-MEG2 can bind and dephosphorylate NSF, a key regulator of vesicle fusion, thereby local releasing NSF activity and promoting secretory vesicle fusion (36).

We have previously shown that the phosphatase domains of PTPBR7 and PTP-SL interact with the β 4-subunit of the AP-4 complex in a yeast two-hybrid system and also co-localize in neuronal cells (8). Using immuno-gold labeling, AP-4 complexes have been found at the Golgi complex as well as on early and late endosomes (37), pointing to a role for AP-4 in sorting processes at these sites. Interestingly, co-expression of PTP-SL and β 4-adaptin in Neuro-2a cells leads to an altered subcellular localization for PTP-SL. Under these conditions PTP-SL is displaced from the Golgi apparatus and vesicles and redistributes throughout the cytoplasm (8). Combined with the conspicuous overlap in subcellular localization of the AP-4 complex and PTPRR isoforms, this finding is in line with a role for these PTPs in regulating the AP-4 complex itself. One may even envisage differential roles for PTPBR7 and PTP-SL in the regulation of AP-4 mediated processes.

In conclusion, we have shown that two PTPRR isoforms, which differ in their N-terminal sequence, show a differential localization in the early endocytic compartments. PTP-SL is localized to the Golgi apparatus and late endosomes, whereas PTPBR7 was additionally found at the plasma membrane, at membrane curvatures and invaginations and in the very early stages of endocytosis. These data suggest a specialized function for each of these phosphatases in the endocytic pathway. Whether the PTPRR isoforms are involved in localized tyrosine dephosphorylation of MAP kinases and/or function in cellular processes directly connected to the regulation of endocytosis remains to be established.

Acknowledgements

We thank Bas Wanschers and Rinske van de Vorstenbosch for technical assistance, and Frank Böhmer (Jena, Germany) for generously providing the pNRTIS-21 construct. This work was supported in part by a grant from the Dutch Organization for Scientific Research N.W.O. to support J.K.

References

1. Kholodenko, B. N. (2002) *Trends Cell Biol.* **12**, 173-177
2. Sorkin, A., and von Zastrow, M. (2002) *Nat. Rev. Mol. Cell. Biol.* **3**, 600-614
3. Gonzalez-Gaitan. (2003) *Nat. Rev. Mol. Cell. Biol.* **4**, 213-224
4. Burke, P., Schooler, K., and Wiley, H. S. (2001) *Mol. Biol. Cell* **12**, 1897-1910
5. Haj, F. G., Verveer, P. J., Squire, A., Neel, B. G., and Bastiaens, P. I. H. (2002) *Science* **295**, 1708-1711
6. van den Maagdenberg, A. M. J. M., Bachner, D., Schepens, J. T. G., Peters, W., Fransen, J. A. M., Wieringa, B., and Hendriks, W. J. A. J. (1999) *Eur. J. Neurosci.* **11**, 3832-3844
7. Chirivi, R., Dilaver, G., van de Vorstenbosch, R. A., Schepens, J., Croes, H. J. E., Wanschers, J., Fransen, J., and Hendriks, W. (2004) *Genes Cells* **9**, 919-933
8. Dilaver, G., Schepens, J., van den Maagdenberg, A., Wijers, M., Pepers, B., Fransen, J., and Hendriks, W. (2003) *Histochem. Cell Biol.* **119**, 1-13
9. Kim, W. T., Chang, S., Daniell, L., Cremona, O., Di Paolo, G., and De Camilli, P. (2002) *Proc. Natl. Acad. Sci. USA* **99**, 17143-17184
10. Pulido, R., Zuñiga, A., and Ullrich, A. (1998) *EMBO J.* **17**, 7337-7350
11. Zuniga, A., Torres, J., Ubeda, J., and Pulido, R. (1999) *J. Biol. Chem.* **274**, 21900-21907
12. Buschbeck, M., Eickhoff, J., Sommer, M. N., and Ullrich, A. (2002) *J. Biol. Chem.* **277**, 29503-29509
13. Tenev, T., Böhmer, S., Kaufmann, R., Frese, S., Bittorf, T., Beckers, T., and Böhmer, F. (2000) *Eur. J. Cell Biol.* **79**, 261-271
14. Dilaver, G., van de Vorstenbosch, R. A., Tarrega, C., Rios, P., Pulido, R., van Aerde, K., Fransen, J., and Hendriks, W. (2004) *submitted*
15. Cuppen, E., Gerrits, H., Pepers, B., Wieringa, B., and Hendriks, W. (1998) *Mol. Biol. Cell* **9**, 671-683
16. Kreis, T. E. (1986) *EMBO J.* **5**, 931-941
17. Janssen, E., Kuiper, J., Hodgson, D., Zingman, L. V., Alekseev, A. E., Terzic, A., and Wieringa, B. (2004) *Mol. Cell. Biochem.* **256**, 59-72
18. Fransen, J. A., Ginsel, L. A., Hauri, H. P., Sterchi, E., and Blok, J. (1985) *Eur. J. Cell Biol.* **38**, 6-15
19. Schweizer, A., Fransen, J. A., Bachi, T., Ginsel, L., and Hauri, H. P. (1988) *J. Cell Biol.* **107**, 1643-1653
20. Möbius, W., van Donselaar, E., Ohno-Iwashita, Y., Shimada, Y., Heijnen, H. F. G., Slot, J. W., and Geuze, H. J. (2003) *Traffic* **4**, 222-231
21. Cuppen, E., Wijers, M., Schepens, J., Fransen, J., Wieringa, B., and Hendriks, W. (1999) *J. Cell Sci.* **112**, 3299-3308
22. Gruenberg, J. (2001) *Mol. Cell Biol.* **2**, 721-730
23. Lebrand, C., Corti, M., Goodson, H., Cosson, P., Cavalli, V., Mayran, N., Faure, J., and Gruenberg, J. (2002) *EMBO J.* **21**, 1289-1300

Chapter 5

24. Offterdinger, M., Georget, V., Girod, A., and Bastiaens, P. I. H. (2004) *J. Biol. Chem.* **279**, 36972-36981
25. Confalonieri, S., Salcini, A. E., Puri, C., Tacchetti, C., and Di Fiore, P. P. (2000) *J. Cell Biol.* **150**, 905-912
26. Torii, S., Kusakabe, M., Yamamoto, T., Maekawa, M., and Nishida, E. (2004) *Dev. Cell* **7**, 33-44
27. Zuñiga, A., Torres, J., Ubeda, J., and Pulido, R. (1999) *J. Biol. Chem.* **274**, 21900-21907
28. Korolchuk, V., and Banting, G. (2003) *Biochem. Soc.* **31**, 857-860
29. Boehms, M., and Bonifacino, J. S. (2002) *Gene* **286**, 175-186
30. Boehms, M., and Bonifacino, J. S. (2001) *Mol. Biol. Cell* **12**, 2907-2920
31. Wilde, A., and Brodsky, F. M. (1996) *J. Cell Biol.* **135**, 635-645
32. Slepnev, V. I., Ochoa, G., Butler, M. H., Grabs, D., and De Camilli, P. (1998) *Science* **281**, 821-824
33. Wilde, A., Beattie, E. C., Lem, L., Riethof, D. A., Liu, S. H., Mobley, W. C., Soriano, P., and Brodsky, M. (1999) *Cell* **96**, 677-687
34. Ahn, S., Maudsley, S., Luttrell, L. M., Lefkowitz, R. J., and Daaka, Y. (1999) *J. Biol. Chem.* **274**, 1185-1188
35. Huang, F., Jiang, X., and Sorkin, A. (2003) *J. Biol. Chem.* **278**, 43411-43417
36. Huynh, H., Bottini, N., Williams, N., Cherepanov, V., Musimeci, L., Saito, K., Bruckner, S., Vachon, E., Wang, X., Kruger, J., Chow, C., Pellicchiaia, M., Monosov, E., Greer, P. A., Trimble, W., Downy, G. P., and Mustelin, T. (2004) *Nat. Cell Biol.* **6**, 831-839
37. Barois, N., and Bakke, O. (2005) *Biochem. J.* **385**, 503-510

Chapter 6

General Discussion

Over the past decades it has become clear that the biological processes of signal transduction and membrane trafficking are intertwined. At the onset of our studies, the protein tyrosine phosphatase PTP-SL, a signaling molecule, was found to be present on transport vesicles mainly belonging to the endocytic compartment (1). PTP-SL is involved in the ERK-MAPK signaling pathway (2-4), but interestingly, it was also found to interact with the β 4-adaptin subunit of the AP-4 adaptor complex, an important component of the vesicular transport machinery. In the previous chapters of this thesis, we describe studies that further point to a possible role for PTP-SL, and other PTPRR family members, in vesicle trafficking between the Golgi-apparatus and endocytic compartments and localized signaling.

The PTPRR protein family

Previous work has revealed the existence of two PTPs in mouse, PTPBR7 and PTP-SL, that were in part identical, suggesting that they originated from the same gene, termed *Ptprr* (1,5,6). In this thesis, I report on the characterization of the various PTPRR isoforms in neuronal cells and demonstrate that the single copy mouse gene *Ptprr* gives rise to four mRNAs that encode PTPBR7, PTP-SL and two PTPPBS γ protein variants through the use of distinct promoters, alternative splicing and differential translation initiation starts (Chapter 3). In addition, the receptor-type PTPBR7 protein isoform was found to undergo N-terminal proteolytic cleavage at a furin-like convertase consensus site, adding an additional, fifth, member for which the name PTPBR7-65 was coined (Chapter 4). A schematic representation of the domain composition and intracellular distribution of all PTPRR isoforms is depicted in Figure 1.

Localization studies that focused on the different PTPRR isoforms, described in Chapters 2 and 5, revealed that PTPBR7 and PTP-SL are both present and co-localize in late endocytic compartments and in the Golgi area. PTPBR7 shows an additional localization at the plasma membrane (1,7), and interestingly on early endosomes as well (Chapter 5). The 42 and 37 kDa PTPPBS γ proteins are genuine cytosolic proteins (Chapter 3). The differential subcellular localization of all PTPRR isoforms within the dynamic vesicular network of the cell is portrayed in Figure 2.

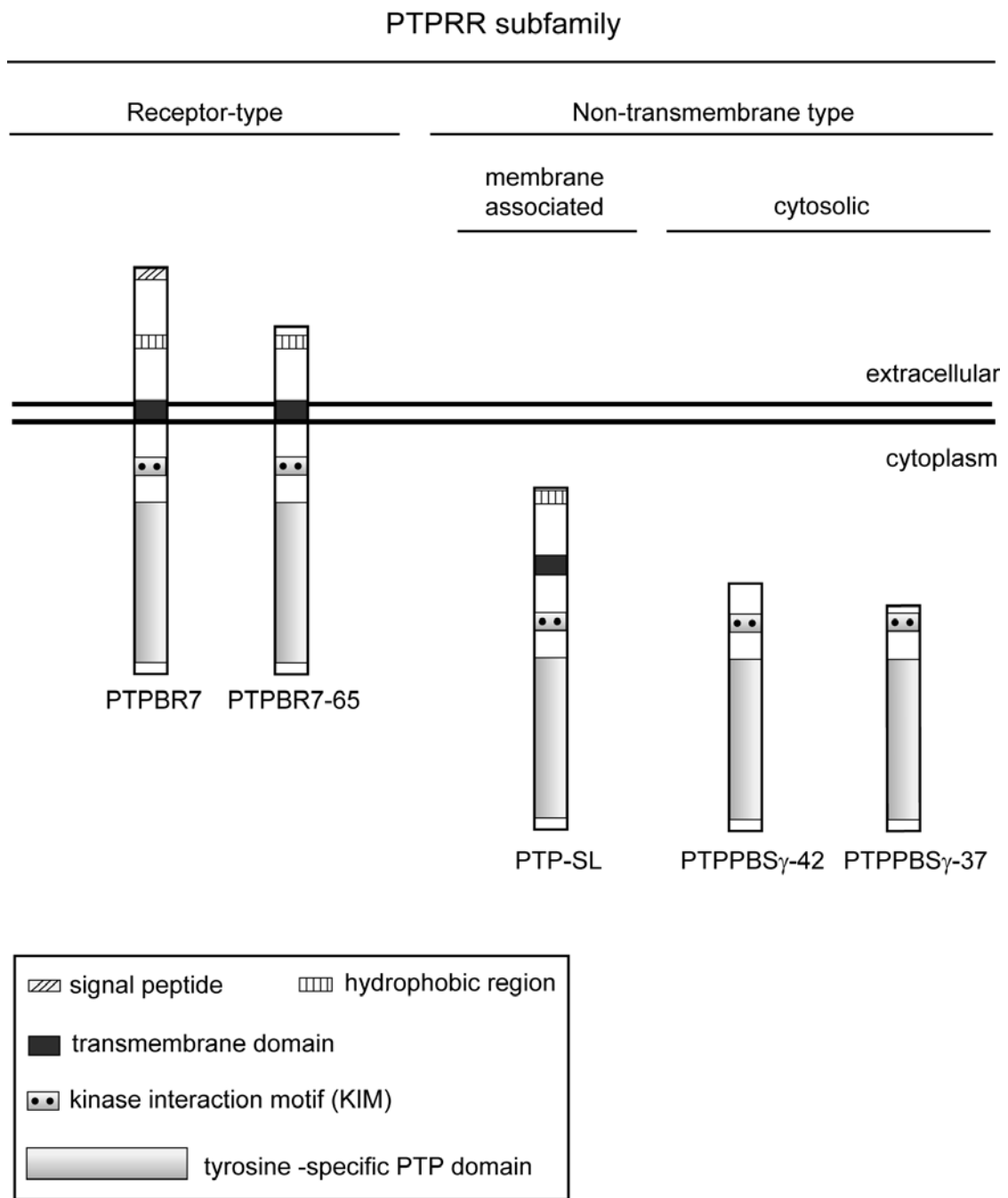


Figure 1. Schematic representation of the set of protein products encoded by the gene *Ptprr*. Structural characteristics of the depicted domains are shown in the boxed inset. PTPBR7-65 is generated through proteolytic cleavage.

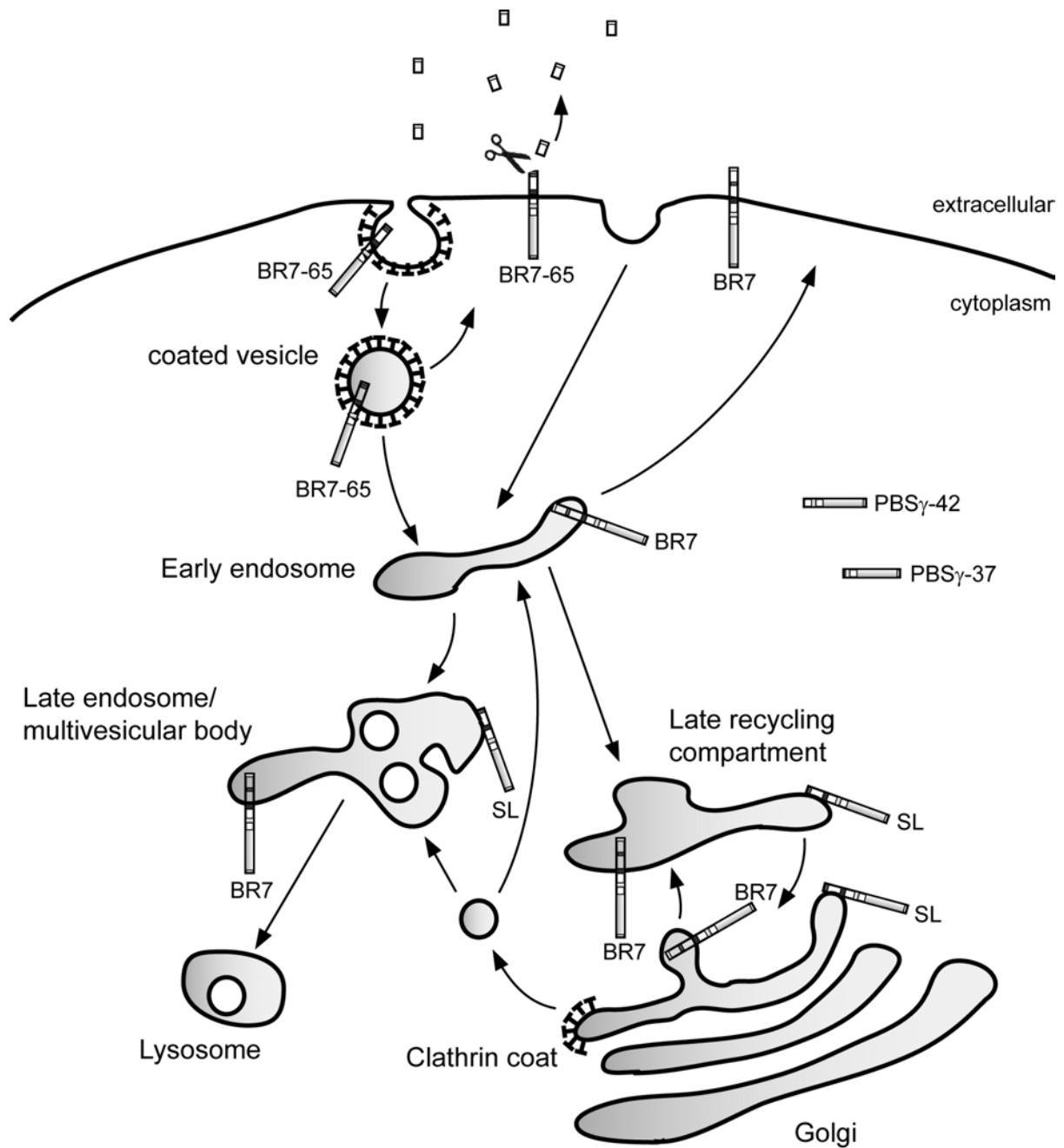


Figure 2. Schematic representation of the distribution of the individual PTPRR isoforms within the different endocytic compartments. The AP-4 complex is localized to the Golgi-apparatus and late endocytic vesicles. See also Figure 1 in chapter 1.

Sine this generation of multiple isoforms is conserved in other mammals (5,6,8), the question arises why so many different PTPRR isoforms exist. Generally speaking, the generation of multiple isoforms from a single gene is believed to warrant fine-tuning of cellular programs, both in time and space, thus adding to the phenotypic complexity of higher organisms (9). Because the catalytic activity of PTPs is generally exceeding that of the counteracting tyrosine kinases by several orders of magnitude, the need for tight regulation of PTP activity *in vivo* is evident. This can be accomplished by a number of mechanisms, including subcellular localization, post-translational modification, steady state protein levels, and dimerization (10,11). Clearly, by generating PTPRR isoforms that behave differently regarding these characteristics, the organism can achieve a high level of control.

The PTPRR isoforms are identical in their C-terminal region that includes the single catalytic phosphatase (PTP) domain, the kinase interaction motif (KIM) and the kinase specificity region (KIS), but they differ in the length and sequence of their N-terminal part (Figure 1). As a consequence, the PTPRR subfamily turns out to comprise receptor-type transmembrane molecules, membrane-associated proteins and cytosolic variants that localize to different subcellular compartments (Figure 2). All subfamily members are subjected to post-translational modifications (Chapter 4). They all can be phosphorylated on the MAPK and PKA target sites as identified in PTP-SL and this may function as a checkpoint in the ERK-MAP kinase signaling pathway (2,3,12). Whether these serine/threonine phosphorylation events have any direct effect on the PTPRR enzymatic activity still remains to be investigated. It should be noticed that the PTPRR isoforms are actually short-lived proteins, with half-lives of just several hours (Chapter 4) and this lability likely reflects the importance of their regulatory role. This may explain why we have not been able to generate stably transfected cell lines that constitutively overexpress PTPRR isoforms, and instead, were forced to use either transient assays or turn to inducible expression systems (Chapters 4-5).

Regulation of PTPRR isoform activity

Interestingly, we found that the PTPRR-isoform PTPBR7 is subjected to N-terminal proteolytic cleavage (Chapter 4). This cleavage occurs predominantly at the cell membrane and is enhanced by serum-derived factors. Unlike for other receptor-type PTPs, like PTP-LAR (13,14) or PTP μ (15), the resulting N-terminal ectodomain does not remain associated with the shortened PTPBR7 version, termed PTPBR7-65, but appears to be released into the surrounding medium. Occurrence of these truncated and shed products of PTPBR7 not only adds to the structural diversity of the PTPRR family, but also to the complexity of its biological role. One of the intriguing questions now is whether or not the extracellular part functions as a ligand. Equally interesting is to find out whether there is some kind of ligand for PTPBR7 itself. If so, such a ligand may well regulate or fine-tune PTPBR7's activity, reminiscent of the situation for growth factors for the receptor-type kinases.

In the regulation of PTPBR7 activity at the cell membrane, dimerization of the protein could play a role in analogy to models now proposed for other PTPases (16-20). These studies were triggered by the observation that upon crystallization the active RPTP- α PTP domain adopts a homo-dimer conformation that results in the inhibition of its activity (18,21). Although the crystal structure of the PTPRR catalytic domain does not reveal signs of dimerization (22), it is still possible that PTPBR7 transmembrane chains are dimerized through ligand binding to the N-terminal region. In support of this, recent findings in our lab point to the existence of PTPBR7 / PTP-SL homo and heterodimers in transfected cells (Y. Noordman; personal communication). It will be a challenge to unravel the eventual regulatory effects of dimerization and proteolytic processing on the intrinsic catalytic activity of PTPBR7 at the plasma membrane.

Taken together, the gene *Ptprr* generates multiplicity (by the use of alternative splicing, alternative promoter and alternative translation initiation sites), diversity (by post-translational modifications) and specificity (by targeting the different isoforms to distinct subcellular compartments), and thus creates ample possibilities for spatial and temporal signaling, which will be discussed below.

PTPRR isoforms and endosomal transport

Two isoforms encoded by the gene *Ptprr* (PTPBR7 and PTP-SL) reside on subcellular compartments belonging to the endocytotic transport system (Chapters 2 and 5). Since the endocytic process is coupled to many cellular processes including signal transduction (reviewed in (23-25)), their presence on endosomes could reflect basically two functions: participation in the regulation of the endocytotic transport route itself, and/or involvement in localized signaling events, i.e. the local dephosphorylation of MAP kinases.

PTP-SL is present on the *trans*-Golgi and on vesicles participating in the later stages of endocytosis. Interestingly, the phosphatase domain of PTP-SL was found to interact with the β 4-subunit of the AP-4 complex in a yeast two-hybrid system (Chapter 2). Four different heterotetrameric adaptor complexes, AP-1 to AP-4, have been described that are involved in the sorting of cargo proteins into transport vesicles that traffic between the different organelles of the cell (26,27). The precise role of the AP-4 complex in transport routes is not yet known but current data suggest that it mediates sorting processes at the *trans*-Golgi and endosomal membranes (28-30). Our microscopy studies revealed that PTP-SL and β 4-adaptin localize to the Golgi-apparatus and vesicles throughout the cytoplasm in neuronal cells (Chapter 2). Co-transfection studies, however, failed to demonstrate a direct interaction between PTP-SL and β 4-adaptin by immunoprecipitation. This may be explained by the intriguing finding that co-expression of PTP-SL and β 4-adaptin in Neuro-2a cells resulted in an altered subcellular localization for PTP-SL: the phosphatase no longer resided at the Golgi-apparatus and vesicles but appeared dispersed throughout the cytoplasm. These findings point to a functional link between PTP-SL and β 4-adaptin, but may also be taken as evidence that both proteins compete for the same subcellular localization. It would be interesting to test whether PTP-SL mutants, i.e. catalytic inactive ones, are also displaying this dispersion effect upon co-expression with β 4-adaptin.

It is intriguing why PTP-SL, but not β 4-adaptin, is redistributed throughout the cytoplasm in such co-expression experiments. PTP-SL contains two hydrophobic regions and originally was predicted to be a transmembrane protein (31). However, a functional start-transfer signal could not be identified (1), leaving the topology of PTP-SL as yet enigmatic. The observed redistribution into the cytosol further argues against PTP-SL being a transmembrane protein and, taken together, all data suggest a membrane-associated status

with displaceable binding characteristics. Future subcellular fractionation studies should add to this matter.

PTPBR7 proteins were found at membrane curvatures and early endosomes in an endocytosis assay at the ultrastructural level, in which C-terminally-tagged PTPBR7-EGFP proteins were detected using an α -EGFP antiserum (Chapter 5). Surprisingly, we could not detect internalized PTPBR7 through biotinylation-internalization protocols (Chapter 4). Since PTPBR7 is subjected to N-terminal proteolytic cleavage at the cell surface (Chapter 4) it is conceivable that only cleaved PTPBR7 protein, i.e. PTPBR7-65, gets internalized. This shorter PTPBR7 variant lacks two-thirds of the residues that can be biotinylated in the small extracellular part, thus introducing a severe limitation for the detection of biotinylated and internalized PTPBR7 molecules.

Assuming that the localization of PTPBR7 at coated membrane curvatures and early endosomes at the ultrastructural level is indicative for a regulatory role in internalization processes, its influence could be either positive or negative. In support of a negative regulatory role, preliminary experiments indicated a reduced uptake of dextran or transferrin by neuronal cells stably expressing PTPBR7-GFP when compared to non-expressing control cells (own unpublished data). However, these experiments should be pursued further in order to establish the significance of this finding. If indeed PTPBR7 turns out to inhibit endocytosis, it will be extremely interesting to study whether catalytic activity or structural properties (i.e. proteolytic cleavage) of PTPBR7 is required for this. Likewise, knock-down of PTPBR7 proteins in cultured PC12 cells (the only neuroendocrine cell line known to express endogenous PTPBR7) by siRNA-mediated RNA interference might shed light on this possible role in endocytosis.

In live imaging studies we demonstrated that PTPBR7 and PTP-SL vesicles are highly motile and that the motion is bi-directional, since PTPRR vesicles traveling both to and from the Golgi-apparatus were observed (Chapter 5). Also in other areas of the cell anterograde and retrograde transport of PTPRR vesicles was detected. The presence of PTPBR7 and PTP-SL on highly motile vesicles of the endocytic pathway is in line with a dynamic role for these phosphatases in the regulation of endocytic transport routes in neurons. Intriguingly, serum deprivation of Neuro-2a cells stably expressing PTPBR7-GFP was found to result in behavioral changes of the PTPBR7 organelles (our unpublished data). In these preliminary live-imaging studies, we observed increased dynamic trafficking of PTPBR7 vesicles as well

as the formation of tubular structures upon serum deprivation. No such differences, in particular no tubule formation, were noted for PTP-SL vesicles.

Dynamic tubular networks have been described for some biological membranes, such as those of the endoplasmic reticulum, the Golgi-apparatus, and endosomes (32,33). Microscopy of living cells has demonstrated that membrane tubules also participate in transport events between cellular compartments (34-36). Many intracellular membrane tubules are generated by microtubule motors that pull developing membrane tubules along a preformed microtubule track (37,38). We have demonstrated that PTPBR7 and PTP-SL vesicles are localized along microtubules (Chapter 5). It is very likely, therefore, that microtubules are involved in the formation of PTPBR7 tubular structures. Upon serum deprivation Neuro-2a cells start to differentiate; they leave the cell cycle, become flatter and form neurite-like extensions. The presence of PTPBR7 but not PTP-SL in the tubular structures during differentiation of Neuro-2a cells may therefore point to distinct roles of these PTPRR isoforms in neuronal differentiation.

PTPRR isoforms and endosomal signaling

Following up on the above, it is interesting to note that the expression of PTPBR7 messenger RNA in PC12 cells is transiently increased nine-fold following treatment with nerve growth factor (NGF), a well-known inducer of PC12 differentiation (39). NGF binds to and activates trkA receptors at the presynaptic terminal and, subsequently, the activated trkA-NGF complex is internalized into endocytic vesicles that fuse with a 'signaling endosome', eventually causing sustained activation of ERK-MAP kinases and induction of neuronal differentiation. In contrast, EGF stimulation of PC12 cells results in a transient activation of the ERK-MAPK pathway which leads to a mitotic response (40,41). Thus, the magnitude and duration of MAPK signals are critical determinants of the ultimate biological response.

As stated, all PTPRR isoforms have an identical C-terminus containing a kinase interacting motif (42) allowing interaction with MAP kinases ERK1/2/5 and p38 (2,4,43). It remains to be determined whether PTPRR isoforms are required for regulating transient or sustained activation of MAPKs. However, up-regulation of PTPBR7 is apparently necessary for neuronal differentiation in PC12 cells and it is tempting to relate this to trkA signaling on

endosomes, with PTPBR7 enabling a negative feedback loop in NGF signaling. Finally, our data support the model in which the different PTPRR isoforms perform distinct tasks in localized signaling, with PTPBR7 counteracting receptors and MAP kinases at the cell surface and during early endocytosis, while PTP-SL acts in the later stages of endocytic transport, and PTPPBS γ isoforms preserve the unphosphorylated state of cytosolic MAP kinases.

Physiological relevance

Most of our understanding of the PTPRR subfamily of protein tyrosine phosphatases is based on studies with cells in culture. Although more work is needed to further extend our biochemical understanding of the regulation of - and regulation by PTPRR isoforms, there is also a need to translate this knowledge to the tissue and organism level. Two PTPRR isoforms are expressed in the Purkinje cells of the cerebellum ((1,44) and Chapter 3). Although PTPBR7 is initially expressed during Purkinje cell development, PTP-SL expression takes over post-natally and remains high in adult Purkinje cells (1). This specific, complementing, neuronal expression pattern of the two isoforms would be in line with an important regulatory role in the cerebellar nervous system. Such a role for PTPs in cerebellar development would not be unprecedented. For instance, tyrosine phosphatase activity of PTP β/ζ was found to be required for proper Purkinje dendrite development (45) and PTP σ knock-out mice show behavioral deficits including abnormal limb flexion, fine intention tremor, ataxic gait and defects in proprioception (46). Very recently, a PTPRR knock-out mouse strain was generated in our lab and the first tests indeed point to motor coordination defects (R. Chirivi and C.E.E.M. van der Zee, personal communication), in support of a critical role for PTPRR in the development or physiological integrity of the cerebellum. It is conceivable that PTPRR isoforms are involved in neuronal plasticity, which is required for cerebellum-coordinated behavior, and therefore it will be interesting to study long-term potentiation (LTP) in hippocampal and cerebellar slice cultures from wild-type and PTPRR knock-out specimen. The impact of phosphorylation in the regulation of LTP is nicely demonstrated by, for example, the PKA-mediated phosphorylation of the active zone protein RIM1 α , which induces presynaptic plasticity at cerebellar parallel fiber synapses (47).

Furthermore, the receptor-type RPTP- α appeared to be required for LTP in hippocampal slice cultures (48), and the STEP family of PTPs were shown to regulate hippocampal LTP either through direct dephosphorylation of the NMDA receptor or through an indirect mechanism that leads to inactivation of Src-family tyrosine kinases (49,50). Clearly, the identification of bona-fide substrates for PTPRR isoforms in neuronal tissue, eventually through the exploitation of materials derived from wild type and PTPRR knock-out animals and cells, will further shed light on the regulatory potential of this PTP subfamily on signaling processes within the neuronal circuitry.

Future prospects

It is clear that much more work needs to be done to fully understand how the many PTPRR isoforms are regulating complex cellular processes. This will require a combination of biochemical, structural, morphological, and advanced imaging approaches. Analysis of the composition of transport vesicles in brain by protein mass spectrometry may identify new PTPRR interacting proteins and help to elucidate the molecular mechanisms by which these PTPs might influence signaling and trafficking. Fluorescent imaging techniques will provide new perspectives on the movement of these proteins and their interactions with cellular components in living cells. It will be a challenge to visualize signal transduction-based protein dephosphorylation by PTPRR isoforms in living cells or tissues in order to learn more about their spatial and temporal characteristics in localized signaling. Fluorescent probes that allow the imaging of protein phosphorylation in living cells are now becoming available (51) and fluorescence resonance energy transfer (FRET) techniques enable the study of PTPRR - MAPK interactions *in vivo*. And last but not least, the ongoing analysis of PTPRR knockout mice will reveal further clues towards the significance of PTPRR protein isoforms for development, health and disease.

References

1. van den Maagdenberg, A. M. J. M., Bachner, D., Schepens, J. T. G., Peters, W., Fransen, J. A. M., Wieringa, B., and Hendriks, W. J. A. J. (1999) *Eur. J. Neurosci.* **11**, 3832-3844
2. Pulido, R., Zuñiga, A., and Ullrich, A. (1998) *EMBO J.* **17**, 7337-7350
3. Zuñiga, A., Torres, J., Ubeda, J., and Pulido, R. (1999) *J. Biol. Chem.* **274**, 21900-21907
4. Buschbeck, M., Eickhoff, J., Sommer, M. N., and Ullrich, A. (2002) *J. Biol. Chem.* **277**, 29503-29509
5. Augustine, K. A., Rossi, R. M., Silbiger, S. M., Bucay, N., Duryea, D., Marshall, W. S., and Medlock, E. S. (2000) *Int. J. Dev. Biol.* **44**, 361-371
6. Augustine, K. A., Silbiger, S. M., Bucay, N., Ulias, L., Boynton, A., Trebasky, L. D., and Medlock, E. S. (2000) *Anat. Rec.* **258**, 221-234
7. Ogata, M., Sawada, M., Fujino, Y., and Hamaoka, T. (1995) *J. Biol. Chem.* **270**, 2337-2343
8. Watanabe, Y., Shiozuka, K., Ikeda, T., Hoshi, N., Suzuki, T., Hashimoto, S., and Kawashima, H. (1998) *Mol. Brain Res.* **58**, 83-94
9. International Human Genome Consortium. (2001) *Nature* **409**, 860-921
10. Paul, S., and Lombroso, P. J. (2003) *Cell. Mol. Life Sci.* **60**, 2465-2482
11. Alonso, A., Sasin, J., Bottini, N., Friedberg, I., Osterman, A., Godzik, A., Hunter, T., Dixon, J. E., and Mustelin, T. (2004) *Cell* **117**, 699-711
12. Blanco-Aparicio, C., Torres, J., and Pulido, R. (1999) *J. Cell Biol.* **147**, 1129-1136
13. Streuli, M., Krueger, N. X., Arineillo, P. M., Tang, M., Munro, J. M., Blattler, W. A., Adler, D. A., Disteché, C. M., and Saito, H. (1992) *EMBO J.* **11**, 897-907
14. Serra-Pages, C., Saito, H., and Streuli, M. (1994) *J. Biol. Chem.* **269**, 23632-23641
15. Gebbink, M. F. B. G., Zondag, G. C. M., Koningstein, G. M., Feiken, E., Wubbolts, R. W., and Moolenaar, W. H. (1995) *J. Cell Biol.* **131**, 251-260
16. Desai, D. M., Sap, J., Schlessinger, J., and Weiss, A. (1993) *Cell* **73**, 541-554
17. Wallace, M. J., Fladd, C., Batt, J., and Rotin, D. (1998) *Mol. Cell. Biol.* **18**, 2608-2616
18. Bilwes, A. M., den Hertog, J., Hunter, T., and Noel, J. (1996) *Nature* **382**, 555-559
19. Meng, K., Rodriguez-Peña, A., Dimitrov, T., Chen, W., Yamin, M., Noda, M., and Deuel, F. (2000) *Proc. Natl. Acad. Sci. USA* **97**, 2603-2608
20. Nam, H. J., Poy, F., Krueger, N. X., Saito, H., and Frederick, C. A. (1999) *Cell* **97**, 449-457
21. Jiang, G., den Hertog, J., Su, J., Noel, J., Sap, J., and Hunter, T. (1999) *Nature* **401**
22. Szedlacsek, S. E., Aricescu, A. R., Fulga, T., Renault, L., and Scheidig, A. J. (2001) *J. Mol. Biol.* **311**, 557-568
23. Kholodenko, B. N. (2002) *Trends Cell Biol.* **12**, 173-177
24. Gonzalez-Gaitan. (2003) *Nat. Rev. Mol. Cell. Biol.* **4**, 213-224
25. Korolchuk, V., and Banting, G. (2003) *Biochem. Soc.* **31**, 857-860
26. Boehms, M., and Bonifacino, J. S. (2001) *Mol. Biol. Cell* **12**, 2907-2920
27. Boehms, M., and Bonifacino, J. S. (2002) *Gene* **286**, 175-186

28. Dell'Angelica, E. C., Mullins, C., and Bonifacino, J. S. (1999) *J. Biol. Chem.* **274**, 7278-7285
29. Hirst, J., Bright, N. A., Rous, B., and Robinson, M. S. (1999) *Mol. Biol. Cell* **10**, 2787-2802
30. Barois, N., and Bakke, O. (2005) *Biochem. J.* **385**, 503-510
31. Hendriks, W., Schepens, J., Brugman, C., Zeeuwen, P., and Wieringa, B. (1995) *Biochem. J.* **305**, 499-504
32. Lee, C., and Chen, L. B. (1988) *Cell* **54**, 37-46
33. Mollenhauer, H. H., and Morre, D. J. (1998) *Histochem. Cell Biol.* **109**, 533-543
34. Hirschberg, K., Miller, C. M., Ellenberg, J., Presley, J. F., Siggia, E. D., Phair, R. D., and Lippincott-Schwartz, J. (1998) *J. Cell Biol.* **143**, 1485-1503
35. Martinez-Menarguez, J. A., Geuze, H. J., Slot, J. W., and Klumperman, J. (1999) *Cell* **98**, 81-90
36. Polishchuk, R. S., Polishchuk, E. V., Marra, P., Alberti, S., Buccione, R., Luini, A., and Mironov, A. A. (2000) *J. Cell Biol.* **148**, 45-58
37. Robertson, A. M., and Allan, V. J. (2000) *Mol. Biol. Cell* **11**, 941-955
38. Roux, A., Capello, G., Cartaud, J., Prost, J., Goud, B., and Bassereau, P. (2002) *Proc. Natl. Acad. Sci. USA* **99**, 5394-5399
39. Sharma, E., and Lombroso, P. J. (1995) *J. Biol. Chem.* **270**, 49-53
40. Marshall, C. J. (1995) *Cell* **80**, 179-185
41. Grewal, S. S., York, R. D., and Stork, P. J. S. (1999) *Curr. Opin. Neurobiol.* **9**, 544-553
42. Kim, W. T., Chang, S., Daniell, L., Cremona, O., Di Paolo, G., and De Camilli, P. (2002) *Proc. Natl. Acad. Sci. USA* **99**, 17143-17184
43. Zuñiga, A., Torres, J., Ubeda, J., and Pulido, R. (1999) *J. Biol. Chem.* **274**, 21900-21907
44. Chirivi, R., Dilaver, G., van de Vorstenbosch, R. A., Schepens, J., Croes, H. J. E., Wanschers, J., Franssen, J., and Hendriks, W. (2004) *Genes Cells* **9**, 919-933
45. Tanaka, M., Maeda, N., Noda, M., and Marunouchi, T. (2003) *J. Neurosci.* **23**, 2804-2814
46. Wallace, M. J., Batt, J., Fladd, C. A., Henderson, J. T., Skarnes, W., and Rotin, D. (1999) *Nat. Genet.* **21**, 334-338
47. Lonart, G., Schoch, S., Kaeser, P. S., Larkin, S., Südhof, T. C., and Linden, D. J. (2003) *Cell* **115**, 49-60
48. Petrone, A., Battaglia, F., Wang, C., Dusa, A., Su, J., Zagzag, D., Bianchi, R., Casaccia-Bonnet, P., Arancio, O., and Sap, J. (2003) *EMBO J.* **22**, 4121-4131
49. Nguyen, T. H., Liu, J. P., and Lombroso, P. J. (2002) *J. Biol. Chem.* **277**, 24274-24279
50. Pelkey, K. A., Askalan, R., S., P., Kalia, L. V., Nguyen, T. H., and Pitcher, G. M. (2002) *Neuron* **34**, 127-138
51. Sato, M., Ozawa, T., Inukai, K., Asano, T., and Umezawa, Y. (2002) *Nat. Biotech.* **20**, 287-294

Abbreviations

Abbreviations

| | |
|---------|--|
| aCSF | arteficial cerebro-spinal fluid |
| AP | adaptor complex |
| BSA | bovine serum albumin |
| c-AMP | cyclic-adenosine monophosphate |
| CLSM | confocal laser scanning microscopy |
| COPI/II | coat protein complexes |
| EDTA | ethylenediaminetetraacetate |
| EGF | epidermal growth factor |
| EGFP | enhanced green fluorescent protein |
| EGFR | epidermal growth factor receptor |
| ELISA | enzyme-linked immunosorbent assay |
| Endo F | endoglycosidase F |
| Endo H | endoglycosidase H |
| ER | endoplasmic reticulum |
| ERK | extracellular regulated kinase |
| FACS | fluorescence activated cell sorting |
| FCS | fetal calf serum |
| FRET | fluorescence resonance energy transfer |
| GFP | green fluorescent protein |
| GGA | Golgi-localized, γ -ear containing, ARF-binding protein |
| JNK | c-Jun N-terminal kinase |
| KIM | kinase interacting domain |
| KIS | kinase specificity domain |
| LTP | long-term potentiation |
| MAPK | mitogen-activated protein kinase |
| MEK | map kinase kinase |
| MKK | map kinase kinase |
| mRNA | messenger ribonucleic acid |
| MVB | multi veiscular bodies |
| NAGT | N-acetylglucosaminytransferase |

| | |
|-----------------|--|
| NGF | nerve growth factor |
| NMDA | N-methyl-D-aspartate |
| NSF | N-ethylmaleimide-sensitive factor |
| ORF | open reading frame |
| PAGE | poly acryl amide gel electroforese |
| PBS | phosphate buffered saline |
| PFA | paraformaldehyde |
| PKA | protein kinase A |
| PTP | protein tyrosine phosphatase |
| PTPBR7 | protein tyrosine phosphatase brain clone number 7 |
| PTPPBS | protein tyrosine phosphatase PC12/Br7/SL |
| PTPPBS γ | protein tyrosine phosphatase |
| PTP-SL | protein tyrosine phosphatase STEP-like |
| RNA | ribonucleic acid |
| RTK | receptor tyrosine kinase |
| RT-PCR | reverse transcriptase-polymerase chain reaction |
| SDS | sodium dodecyl sulfate |
| Sef | acronym for similar expression to <i>fgf</i> genes |
| STEP | striatal enriched phosphatases |
| TGN | trans Golgi complex |

Abbreviations

Samenvatting (Summary in Dutch)

Samenvatting

Voor het optimaal functioneren van levende organismen moeten door de lichaamscellen eiwitten aangemaakt, getransporteerd, gemodificeerd en uiteindelijk weer afgebroken worden. Deze celbiologische processen worden zeer nauwkeurig gereguleerd o.a. door reversibele fosforylering van eiwitten. Eiwitfosforylering (binden van een fosfaatgroep aan een eiwit) gebeurt door enzymen die kinases genoemd worden, terwijl andere enzymen, fosfatases genaamd, de eiwitten kunnen defosforyleren. In de afgelopen decennia is gebleken dat reversibele fosforylering een essentiële rol speelt bij de overdracht van signalen in de cel. Kinases en fosfatases zijn dan ook betrokken bij een veelvoud van levensprocessen, waaronder embryonale ontwikkeling, celbeweging en neuronale celdifferentiatie. Een aantal van de kinases en fosfatases is gelokaliseerd op specifieke organellen in de cel, waaronder transportblaasjes. Dit suggereert dat deze enzymen, naast een rol bij lokale communicatieprocessen binnen de cel, ook een rol spelen bij de regulatie van het intracellulaire transport.

Voordat ik mijn promotieonderzoek begon, was er vastgesteld dat de fosfotyrosine fosfatase PTP-SL voorkomt op transportblaasjes in de cel. Het PTP-SL eiwit behoort tot de PTPRR proteïne tyrosine fosfatase subfamilie en wordt in verband gebracht met signaaloverdrachtscades via zogenaamde MAPKs (mitogen-activated protein kinases). In dit proefschrift worden studies beschreven waarin de moleculaire diversiteit van verschillende PTPRR familieleden onderzocht is, in het bijzonder voor wat betreft de isovorm-specifieke lokalisatie en de mogelijke betrokkenheid bij intracellulair transport.

In hoofdstuk 2 wordt de verkenning van de (moleculaire) omgeving van een tweetal PTPRR-isovormen, te weten PTPBR7 en PTP-SL, beschreven. Bestudering van de subcellulaire localisatie van deze fosfatases in zenuwcellen liet zien dat PTPBR7 en PTP-SL in het Golgi-apparaat en in late endosomale structuren gevonden worden. Daarnaast bevindt het PTPBR7-eiwit zich ook op het celmembraan. De intracellulaire lokalisaties van PTPBR7 en PTP-SL vertonen grote gelijkenis met die van het β 4-adaptin eiwit, een subunit van het AP-4 adaptor complex. De heterotetramere adaptor complexen, AP-1 t/m AP-4, zijn betrokken bij het sorteren van eiwitten die door transportblaasjes vervoerd worden. Het tegelijkertijd tot expressie brengen van PTP-SL en β 4-adaptin in zenuwcellen bleek een dramatische verandering in de lokalisatie van PTP-SL tot gevolg te hebben: in plaats van

rond het Golgi-apparaat en transportblaasjes wordt PTP-SL dan vrij gevonden in het cytoplasma. De lokalisatie van β 4-adaptine bleek overigens niet veranderd. Hoewel in het ‘yeast 2-hybrid systeem’ zelfs aanwijzingen voor een directe interactie tussen PTP-SL en β 4-adaptine werden verkregen, kon een complex van deze twee eiwitten in neuronale cellen niet worden aangetoond. De genoemde resultaten wijzen echter wel op een mogelijk regulerende rol van PTPRR fosfatases in het blaasjestransport in cellen.

Uit de literatuur en sequentie-databanken valt af te leiden dat er mogelijk meerdere eiwitten (isovormen) gecodeerd werden door het muizengen *Ptprr*. In hoofdstuk 3 hebben we een gedetailleerde analyse uitgevoerd waarbij zo volledig mogelijk de transcripten en eiwitproducten horende bij het gen *Ptprr* zijn bepaald. Uit deze experimenten is gebleken dat het gen *Ptprr* aanleiding geeft tot vier verschillende eiwit-isovormen (PTPBR7, PTP-SL, PTPPBS γ -42 en PTPPBS γ -37) door het gebruik van verschillende promoters, alternatieve splicing en meerdere translatie-initiatie sites. De vier isovormen verschillen in hun N-terminale gedeelte, wat resulteert in PTPRR subtypes die ook op (sub)cellulair niveau verschillen: PTPBR7 is een receptorachtig transmembraan eiwit, PTP-SL blijkt membraangeassocieerd, en de twee PTPPBS γ isovormen zijn cytosolische eiwitten.

Hoofdstuk 4 handelt over de posttranslationale modificaties die de PTPRR eiwit-isovormen kunnen ondergaan. Alle isovormen blijken op een tweetal plekken gefosforyleerd te kunnen worden. Daarnaast is gebleken dat alle PTPRR isovormen een relatief korte levensduur, van enkele uren, hebben. Ook werd aangetoond dat PTPBR7 proteolytisch gekliefd kan worden op een furine-achtige convertase consensus site in het N-terminale gedeelte. De klieving gebeurt vooral extracellulair en neemt toe in aanwezigheid van serum in het medium. Hiermee wordt dus een vijfde PTPRR isovorm gecreëerd: PTPBR7-65.

Een gedetailleerde analyse van de subcellulaire localisatie van PTPBR7 en PTP-SL, door middel van lichtmicroscopische (immunofluorescentie) en electronenmicroscopische studies (ultrastructureel), staat beschreven in hoofdstuk 5. Aangetoond wordt dat PTPBR7 en PTP-SL tegelijkertijd aanwezig kunnen zijn in dezelfde ‘late’ endosomen. Belangwekkend is ook dat de aanwezigheid van PTPBR7 op ‘vroeg’ endosomen kon worden aangetoond met behulp van electronenmicroscopie. Deze resultaten zouden stroken met een model waarbij PTPBR7 en PTP-SL bij verschillende stadia van de endocytotische route betrokken zijn. Met behulp van microscopische studies aan levende cellen (live imaging) hebben we verder de bewegelijkheid van PTP-SL- en PTPBR7-positieve transportblaasjes onderzocht. Zowel

PTPBR7 als PTP-SL blaasjes vertonen een grote mate van mobiliteit, en transport van blaasjes van en naar het Golgi-apparaat kon worden waargenomen. Ook in andere delen van de cel is tweerichtingsverkeer van blaasjes waargenomen. De aanwezigheid van PTPBR7 en PTP-SL in zeer bewegelijke blaasjes in specifieke delen van de endocytotische route impliceert een dynamische rol voor deze fosfatases in intracellulair transport.

Hoofdstuk 6 tenslotte, bevat een afrondende bespreking van de resultaten uit het in de voorafgaande hoofdstukken beschreven onderzoek en er worden enkele suggesties gedaan voor vervolgstudies. Vooral wordt hierbij gewezen op de nieuwe mogelijkheden voor het bestuderen van de fosforylering van signaaloverdrachteiwitten in levende cellen met geavanceerde microscopische beeldvormingstechnieken.

Samengevat kan gesteld worden dat één enkel gen, *Ptprr*, in staat is om via verschillende mechanismen een groot repertoire aan functioneel verwante eiwitten te genereren. Doordat deze eiwitten naar specifieke plaatsen in de cel gedirigeerd worden, ontstaat een veelvoud aan mogelijkheden voor locale en ‘tijdelijke’ communicatie op het raakvlak van signaaltransductie en eiwittransport.

Dankwoord

Bana yardım eden ve destek veren herkese teşekkür ederim.

Ik wil graag iedereen bedanken die heeft bijgedragen aan het tot stand komen van dit proefschrift.

I would like to thank everyone who has contributed to accomplish this thesis.

Curriculum Vitae

Gönül Dilaver werd geboren op 7 april 1973 te Doetinchem. In 1991 behaalde zij haar HAVO-diploma aan het Graafschap College in Doetinchem alwaar zij in 1993 ook haar VWO-diploma behaalde. Van september 1993 tot februari 1999 studeerde zij Medische Biologie aan de Radboud Universiteit Nijmegen. Zij deed haar hoofdvakstages op de afdeling Cellulaire Dierfysiologie van de Radboud Universiteit Nijmegen en op de afdeling Celbiologie van het Universitair Medisch Centrum (UMC) St. Radboud. Voor een extra stage verbleef ze 6 maanden in Londen waar ze onderzoek deed op de Research- en Developmentafdeling van het farmaceutische bedrijf Glaxo-Wellcome (GSK). In de periode 1999 – 2004 was zij als onderzoeker (AIO) verbonden aan de afdeling Celbiologie van het Nijmegen Center for Molecular Life Sciences (NCMLS), UMC St. Radboud. In het kader van haar promotie verrichtte zij hier onderzoek naar de functie van een nieuw gevonden eiwit in de hersenen. De resultaten van haar onderzoek staan beschreven in dit proefschrift.

Vanaf 2005 is ze werkzaam als beleidsmedewerker op het onderwijsbureau van de studie Biomedische Wetenschappen, UMC St. Radboud.

Curriculum Vitae

Publications

Kaptein, A., Jansen, M., **Dilaver, G.**, Kitson, J., Dash, L., Wang, E., Owen, M. J., Bodmer, J., Tschopp, J. And Farrow, S. N. Studies on the interaction between TWEAK and the death receptors WSL-1/TRAMP (DR3). (2000) *FEBS Lett.* 24321, 1-7

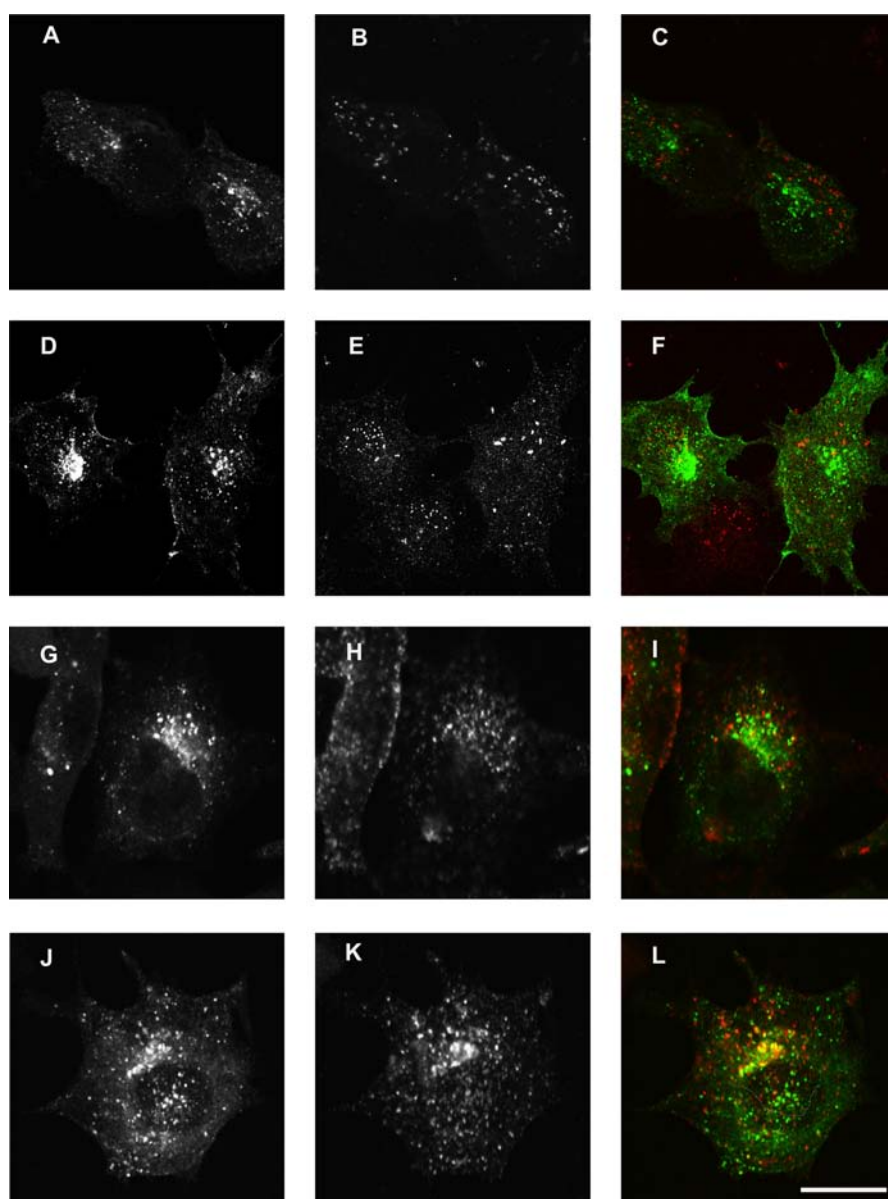
Dilaver, G., Schepens, J., van den Maagdenberg, A., Wijers, M., Pepers, B., Fransen, J., and Hendriks, W., Colocalisation of the protein tyrosine phosphatases PTP-SL and PTPBR7 with β 4 adaptin in neuronal cells. (2003) *Histochem. Cell Biol.* 119, 1-13

Chirivi, R. G. S^{*}, **Dilaver, G^{*}**, van de Vorstenbosch, R., Wanschers, B., Schepens, J., Croes, C., Fransen, J., Hendriks, W. Characterization of multiple transcripts and isoforms derived from the mouse protein tyrosine phosphatase gene *Ptprr*. (2004) *Genes cells* 9, 919-933

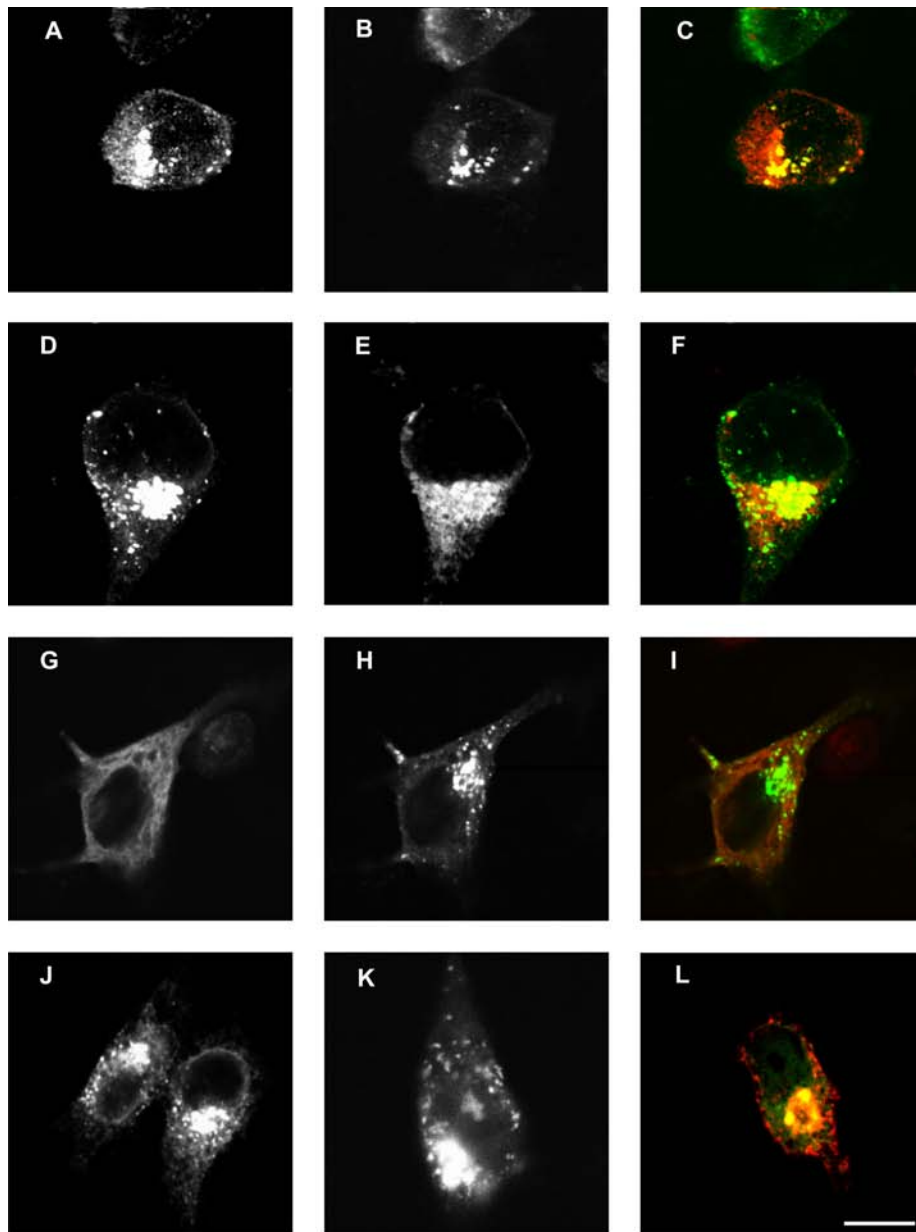
(*These authors contributed equally to this work)

Dilaver, G., van de Vorstenbosch, R., Tárrega, C., Ríos, P., Pulido, R., van Aerde, K., Fransen, J., and Hendriks, W. Proteolytic shedding of the brain-specific receptor-type protein tyrosine phosphatase PTPBR7. *Submitted*

Dilaver, G., de Lange, F., Wijers, M., Croes, H., Kuiper, J., Hendriks, W., and Fransen, J. Differential localization of the protein tyrosine phosphatases PTPBR7 and PTP-SL in early endocytic compartments. *Submitted*

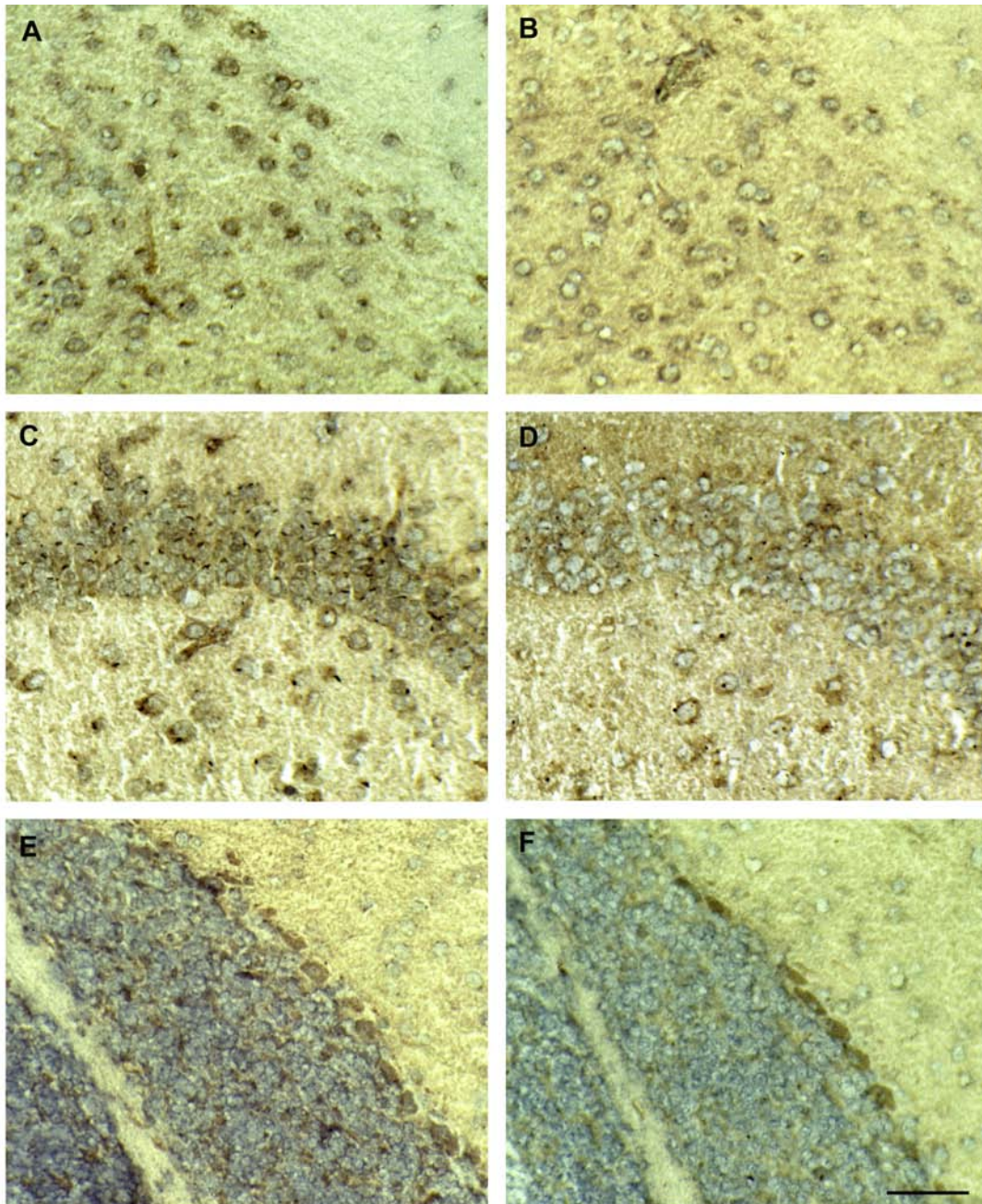


Chapter 2. Fig. 2 PTP-SL containing vesicles partly colocalize with late endosomes but not with MVB and Lysosomes. Neuro-2a cells were transiently transfected with a construct encoding EGFP-tagged PTP-SL (A, D, G, J). Expression of PTP-SL-GFP was found at the Golgi area and at vesicles that are distinct from multi vesicular bodies (B) or lysosomes (E). MVBs were detected immunohistochemically using an antibody directed against LBPA (31). Lysosomes were stained with an antiserum against β -glucocerebrosidase (29). GFP fluorescence was recorded directly. After 5 min of Alexa-549-labeled transferrin uptake (H) no colocalization with PTP-SL-containing vesicles (G) is observed. After 10 min of transferrin uptake (K), suggestive for late endosomes, overlapping structures start to appear (L). Merged images are shown on the right (C, F, I, L), with PTP-SL-GFP fluorescence patterns in green and LBPA (C), β -glucocerebrosidase (F) or transferrin (I, L) signals in red. Experiments using GFP-tagged PTPBR7 essentially led to the same conclusion (data not shown). Confocal sections of the fluorescence signals were collected by CLSM. Bar indicates 10 μ m.

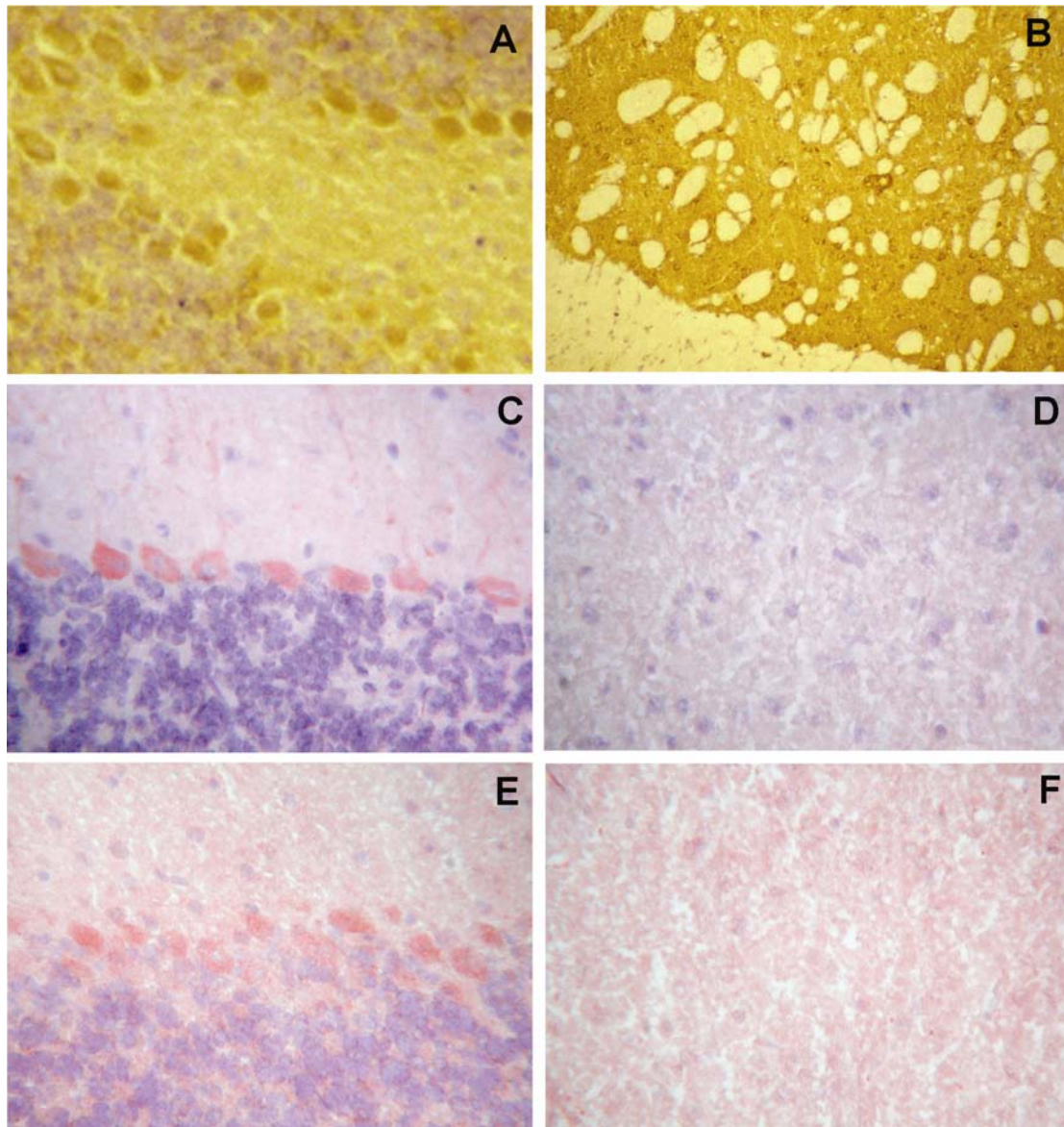


Chapter 2. Fig. 3 Co-transfection of PTP-SL and β 4-adaptin results in an altered localization for PTP-SL.

Analysis of localization patterns in mouse Neuro-2a cells co-transfected with constructs encoding PTP-SL and EGFP-Rab6B (A-C), PTP-SL and EGFP-NAGT (D-F), PTP-SL and EGFP- β 4-adaptin (G-I), and β 4-adaptin and EGFP-Rab6B (L). Panels J and K show single transfectants for PTP-SL and β 4-adaptin, respectively. Untagged PTP-SL and β 4-adaptin proteins were detected immunohistochemically using the antisera anti-SL and anti- β 4-adaptin, respectively. Note the cytoplasmic distribution for PTP-SL (G) upon co-transfection with β 4-adaptin construct (H) as opposed to the vesicle-associated appearance in single transfected cells (J) and in cells co-expressing Rab6B or NAGT (A, D). Merged pictures are shown on the right (C, F, I, L) with PTP-SL (A, D, G) or β 4-adaptin (L) immunofluorescence in red and GFP-fusion protein signals (B, E, H, L) in green. Confocal sections of the fluorescence signals were detected by confocal laser scanning microscopy. Bar indicates 10 μ m.

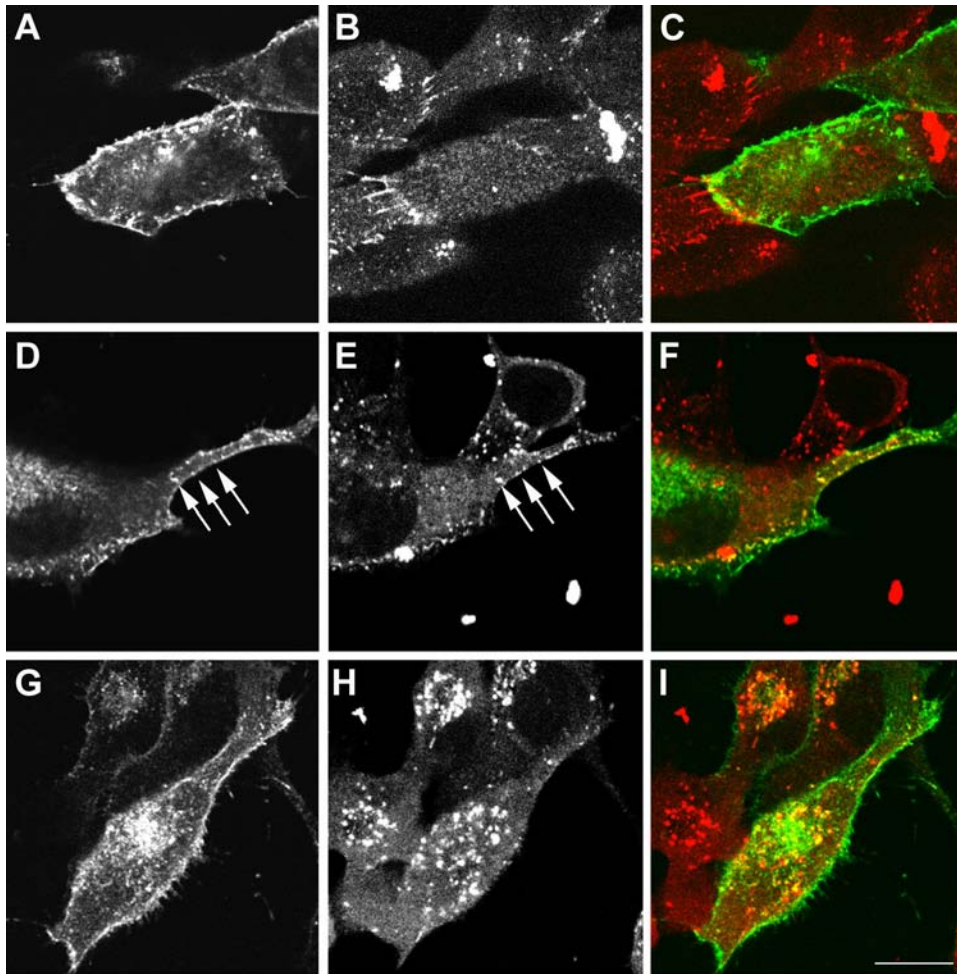


Chapter 2. Fig. 6 $\beta 4$ adaptin and PTP-SL/PTPBR7 immunoreactivity in neurons of several brain regions. Immunohistochemical staining of sequential sections with antibodies against $\beta 4$ -adaptin (A, C, E), and PTP-SL (B, D, F). Colocalization is shown for mouse brain cortex (A, B), pyramidal cells of the hippocampus (C, D), and cerebellum (E, F). Bar indicates 100 μm .



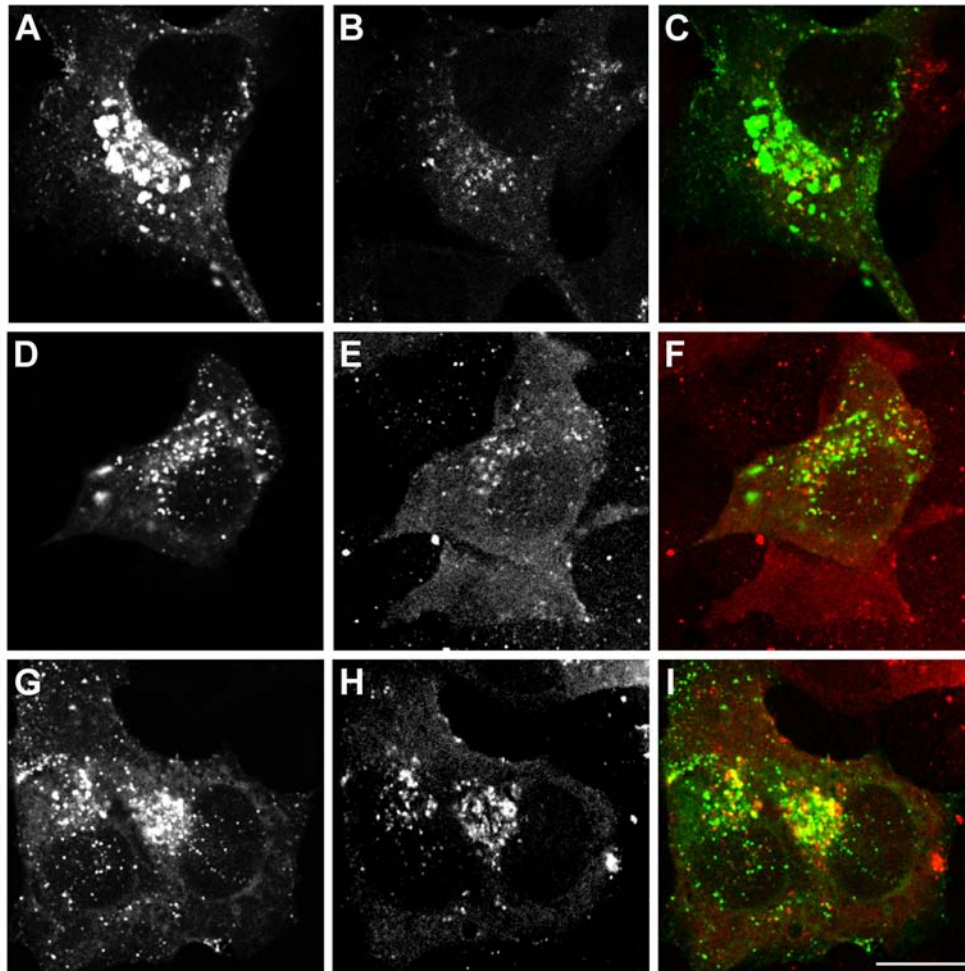
Chapter 3. Fig. 6 Immunolocalization of PTPRR protein in mouse brain.

Brain cryosections were stained using a mixture of three different monoclonal antibodies (1E3, 3E11 and 6A6) immunoreactive towards the common part in PTPRR isoforms and that cross-react with STEP. Positive staining is observed in the Purkinje cells of the cerebellum (A), both the neurons and neuropil of the striatum (B). Similar sections were incubated with monoclonal antibody 5E4, which does not cross-react with STEP. Exclusively Purkinje cell staining was observed (C), and no signal could be detected in the striatum (D). The STEP-absorbed α -SL serum also shows a clear Purkinje cell staining (E) and does not react with striatum (F), suggesting that staining of the striatum (B) reflects STEP immunoreactivity.



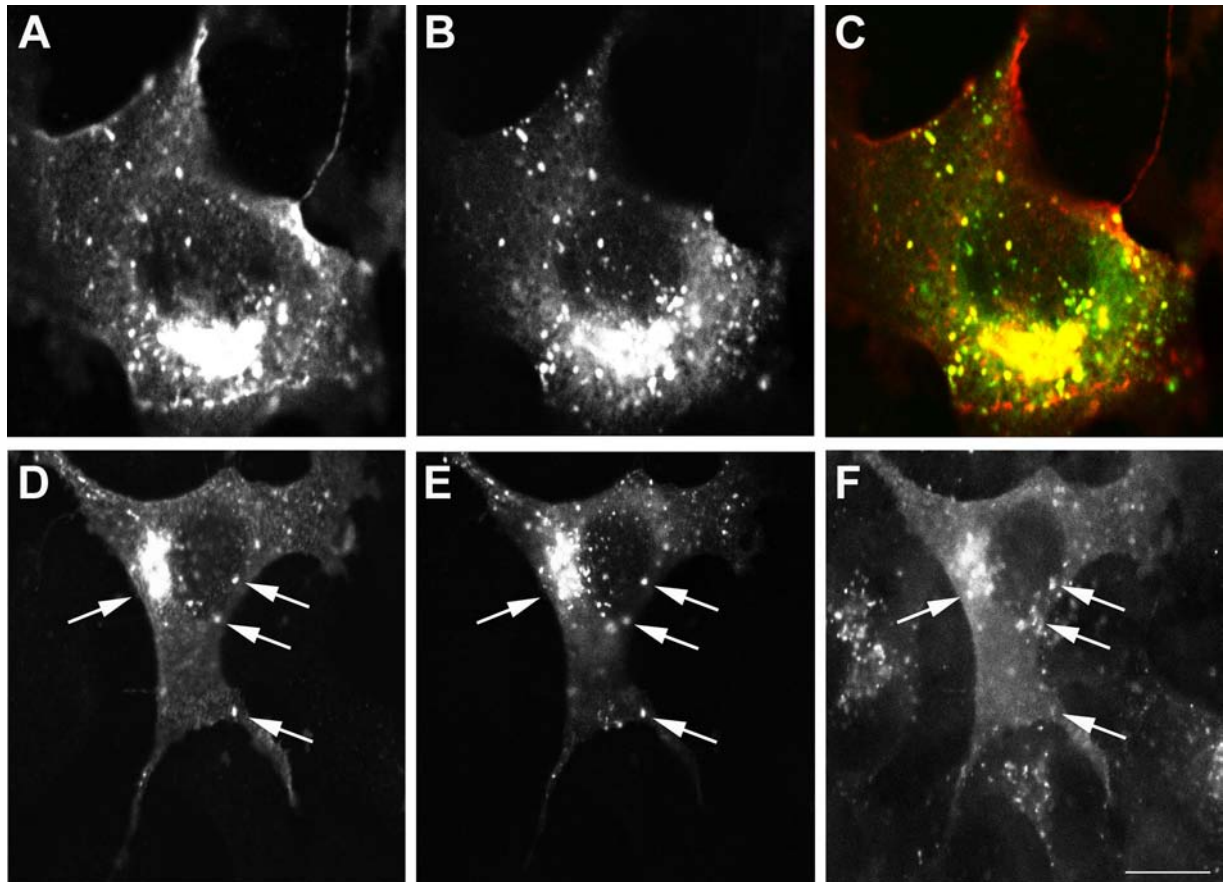
Chapter 5. Fig. 2 PTPBR7 localizes to early and late endosomes.

Neuro-2a cells were transiently transfected with construct pPTPBR7-EGFP. PTPBR7-EGFP fluorescence (A, D, and G) and Alexa549-labeled Dextran uptake (B, E, and H) after 5 min (A-C), 10 min (D-F) and 20 min (G-I) were recorded directly using confocal microscopy. Yellow color in panels C, F and I indicates overlap of PTPBR7-EGFP (green) and Alexa549 Dextran (red) signals. Arrows point to dextran-containing vesicles, which are also positive for PTPBR7 (D and E). Bar indicates 10 μ m.



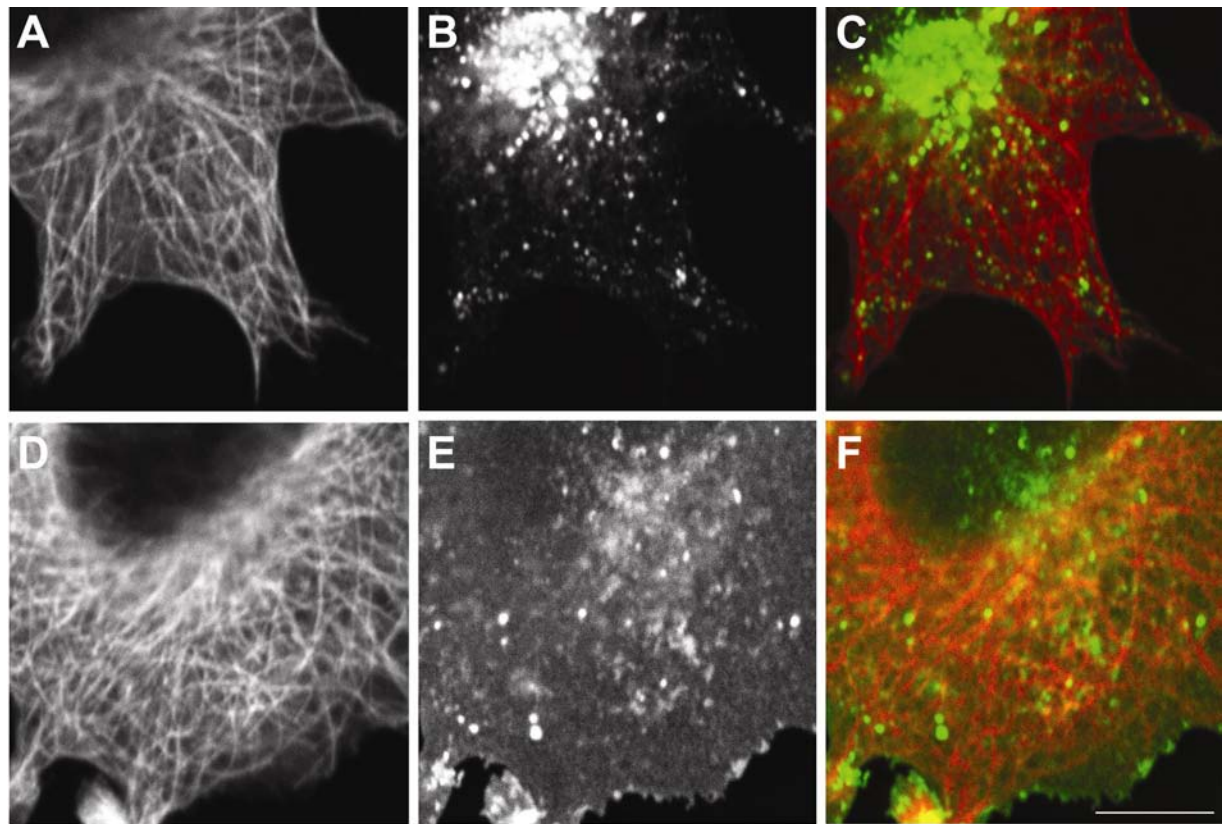
Chapter 5. Fig. 3 PTP-SL localizes to late endosomes.

Neuro-2a cells were transiently transfected with construct pPTP-SL-EGFP. PTP-SL-EGFP fluorescence (A, D, and G) and Alexa549-labeled Dextran uptake (B, E, and H) after 5 min (A-C), 10 min (D-F) and 20 min (G-I) were recorded directly using confocal microscopy. The yellow color in panels C, F and I shows the overlap of PTP-SL-EGFP (green) and Dextran (red) signals. Bar indicates 10 μ m.



Chapter 5. Fig. 5. Some endocytic vesicles contain PTPBR7 as well as PTP-SL.

Neuro-2a cells were co-transfected with pPTP-SL-EGFP and pSG8/PTPBR7-FL-VSV. EGFP fluorescence of PTP-SL-EGFP was recorded directly (B and E) and PTPBR7 proteins were visualized immunohistochemically using the P5D4 antibody against the VSV tag (A and D). Yellow color in panel C indicates overlap of PTP-SL-EGFP (green) and PTPBR7 (red) signals. After 20 min of Alexa-633-labeled Dextran uptake triple-labeled vesicles that are positive for PTPBR7 (D), PTP-SL (E) and Dextran (F) can be detected (arrows). Bar indicates 10 μ m.



Chapter 5. Fig. 7 PTPBR7 and PTP-SL positive vesicles localize along microtubule tracks.

Neuro-2a-SL (A-C) and Neuro-2a-BR7 (D-F) cells were cultured under doxycycline-free conditions for 2 days to induce expression of the EGFP fusion proteins. Fluorescence of PTP-SL-EGFP (B) and PTPBR7-EGFP (E) was recorded directly. Microtubuli (A, D) were stained immunohistochemically using an antibody directed against β -tubulin. Panels C and F display merged images of EGFP-tagged PTPRR autofluorescence (green) and the microtubuli immunostaining (red). Bar indicates 10 μ m.